LOW TEMPERATURE THERMOLUMINESCENCE STUDY OF SOME TERNARY AND QUATERNARY LAYERED STRUCTURED SEMICONDUCTORS

A THESIS SUBMITTED TO
THE GRADUATE SCHOOL OF NATURAL AND APPLIED SCIENCES
OF
MIDDLE EAST TECHNICAL UNIVERSITY

BY

SERDAR DELİCE

IN PARTIAL FULFILLMENT OF THE REQUIREMENTS
FOR
THE DEGREE OF DOCTOR OF PHILOSOPHY
IN
PHYSICS

JULY 2016

Approval of the thesis:

LOW TEMPERATURE THERMOLUMINESCENCE STUDY OF SOME TERNARY AND QUATERNARY LAYERED STRUCTURED SEMICONDUCTORS

submitted by **SERDAR DELİCE** in partial fulfillment of the requirements for the degree of **Doctor of Philosophy in Physics Department, Middle East Technical University** by,

Prof. Dr. Gülbin Dural Ünver
Dean, Graduate School of **Natural and Applied Sciences** _____

Prof. Dr. Mehmet Zeyrek
Head of Department, **Physics** _____

Prof. Dr. Nizami Hasanli
Supervisor, **Physics Dept., METU** _____

Examining Committee Members:

Prof. Dr. Enver Bulur
Physics Dept., METU _____

Prof. Dr. Nizami Hasanli
Physics Dept., METU _____

Assist. Prof. Dr. Mehmet Işık
Electrical and Electronics Dept., Atilim Uni. _____

Prof. Dr. Hatice Kökten
Physics Dept., METU _____

Assoc. Prof. Dr. İpek Güler
Inter-Curricular Cources Dept., Physics Group, Cankaya Uni. _____

Date : ___27.07.2016___

I hereby declare that all information in this document has been obtained and presented in accordance with academic rules and ethical conduct. I also declare that, as required by these rules and conduct, I have fully cited and referenced all materials and results that are not original to this work.

Name, Last Name   :   Serdar Delice

Signature   :

ABSTRACT

LOW TEMPERATURE THERMOLUMINESCENCE STUDY OF SOME TERNARY AND QUATERNARY LAYERED STRUCTURED SEMICONDUCTORS

Delice, Serdar

Ph. D., Department of Physics

Supervisor: Prof. Dr. Nizami Hasanli

July 2016, 116 pages

Thermoluminescence (TL) experiments for ternary and quaternary layered single crystals were carried out in 10−300 K temperature range by employing various heating rates between 0.2 and 1.2 K/s. The TL emissions coming from the trapping centers in the studied samples brought out the TL spectra exhibiting peaks at different temperature regions for each crystals. These peaks were taken under consideration to reveal the TL properties of the associated trap levels.

Characterizations of defect centers existing in the crystals were achieved utilizing the best-known analysis methods (curve fitting, initial rise, peak shape and heating rate methods) of TL theory. Thermal activation energies, capture cross sections and frequency factors of trapping levels were calculated with used TL

analysis methods. Corrections due to temperature lag effect were taken into account for some of the studied crystals to evaluate the activation energy using heating rate method. Order of kinetics exhibited by trap levels were determined through curve fitting and peak shape methods. TL mechanisms of the trap centers in the crystals were studied in depth by investigating the behaviors against different heating rates and stopping temperatures. Although most of the trap levels in the crystals showed the normal heating rate behavior, the traps in Tl_2GaInS_4 and GaS crystals exhibited the properties of anomalous heating rate behavior. Also, thermal quenching was observed for the $Tl_2Ga_2S_3Se$ crystal. In addition, except for the $Tl_4In_3GaS_8$ and GaSe:Mn crystals, which possess the continuous distribution of traps and single trap level, respectively, the quasi-continuous distributions of the trapping levels were exhibited in other studied crystals.

 Keywords: Semiconductors, defects, luminescence, activation energy.

ÖZ

BAZI ÜÇLÜ VE DÖRTLÜ KATMANLI YAPILI YARIİLETKENLERİN DÜŞÜK SICAKLIK TERMOLÜMİNESANS İNCELENMESİ

Delice, Serdar

Doktora, Fizik Bölümü

Tez Yöneticisi: Prof. Dr. Nizami Hasanli

Temmuz 2016, 116 sayfa

Üçlü ve dörtlü katmanlı tek kristalleri için termolüminesans (TL) deneyleri 0.2 ve 1.2 K/s arasındaki ısıtma hızları kullanılarak 10−300 K sıcaklık aralığında gerçekleştirildi. Çalışılan kristallerdeki tuzak merkezlerinden gelen TL salınımları her bir kristal için farklı sıcaklık bölgelerinde pikler sergileyen TL spektrumları ortaya çıkardı. Bu pikler ilgili tuzak seviyelerinin TL özelliklerini göstermek için dikkate alındı.

Kristallerde bulunan kusurların karakterizasyonu TL teorisinin en iyi bilinen metodlarından yararlanılarak yapıldı (eğri fitleme, ilk yükselme, pik şekil ve ısıtma hızı metodları). Tuzak merkezlerinin termal aktivasyon enerjileri, yakalama kesit alanları ve kaçış frekansları bu metodlar ile hesaplandı. Bazı kristallerin aktivasyon enerjisini ısıtma hızı metodu kullanılarak hesaplamak için sıcaklık gecikme

etkisinden kaynaklanan düzeltmeler hesaba katıldı. Eğri fitleme ve pik şekil metodları vasıtasıyla tuzak seviyelerinin sergilediği kinetik sıraları tanımlandı. Kristallerde bulunan tuzak merkezlerinin TL mekanizmaları farklı ısıtma hızları ve aydınlatma sıcaklıklarına karşı davranışları araştırılarak derinlemesine çalışıldı. Kristallerdeki çoğu tuzak merkezlerinin normal ısıtma hızı davranışı göstermesine rağmen, Tl_2GaInS_4 ve GaS kristallerindeki tuzaklar anormal ısıtma hızı davranışının özelliklerini göstermiştir. Ayrıca, $Tl_2Ga_2S_3Se$ kristali için termal sönüm gözlendi. Ek olarak, sırasıyla devamlı tuzak dağılımı ve tek tuzak seviyesine sahip olan $Tl_4In_3GaS_8$ ve GaSe:Mn kristallerinin dışındaki kristallerde devamlı tuzak dağılımı gibi davranış sergilenmiştir.

Anahtar kelimeler: Yarıiletkenler, kusurlar, lüminesans, aktivasyon enerjisi.

ACKNOWLEDGEMENTS

Firstly, I would like to utter my profound thanks to my supervisor Prof. Dr. Nizami Hasanli. He has been supportive and encouraging during my Ph.D study. His magnificent working discipline and vast experience have guided to me to improve myself in terms of working ethics and my research fields. I have been very grateful to him owing to his valuable contributions to my acedemic carrier and my personal life.

I would like to thank the members of my thesis committee: Prof. Dr. Enver Bulur, Prof. Dr. Hatice Kökten, Assist. Prof. Dr. Mehmet Işık and Assoc. Prof. Dr. İpek Güler for their valuable comments and assistances.

I would like to express my very special thanks to Prof. Dr. Enver Bulur for his valuable supports and discussions on this study. He has been very supportive whenever I need an assistance for experimental setup. His suggestions, scientific knowledges and experiences have guided to me in order to complete my Ph.D study.

I would like to express my sincere thanks to Assist. Prof. Dr. Mehmet Işık for his assistance, support and collaboration. I have learned experimental and theoretical basis of my studying field by his experience.

This work has been also supported by TUBİTAK-BİDEP 2211-A scholarship.

Finally, I would like to express my most profound thank, gratitude and appreciation to my family. They have been very supportive and encouraging in every sense for all my life. I know my eternal thanks are insufficient for their labors on me.

To my mother

TABLE OF CONTENTS

xiii

LIST OF TABLES

xv

FIGURES

CHAPTER 1

INTRODUCTION

Semiconductor materials have been getting more and more important subjects in human life with their tremendously expanding usage area in the technology. Researchers and producers have paid great deal of attention for investigation of electrical and optical properties of them and for improvement of the devices fabricated by semiconductor components. They have been used for various purposes for years. Due to their controllable electrical conductivity, they have taken significant roles in a large scale in the electronic devices covering humanity life. They are also optically sensitive materials so that they are chosen for fabrication of light responsive and producing devices. Lately, different compositions of III-VI groups semiconducting elements have been attracted remarkable attention for the production of related devices. Thus, determining the optical and electrical properties of these compounds will be contributor for the development of this technology.

Various binary, ternary and quaternary layered-structured semiconducting materials have been considered as promising materials due to their conformity to semiconductor application areas such as nonlinear optical transducers, emission modulators and memory switching elements in optoelectronics and nonlinear optics [1-3]. Binary and ternary semiconductor crystals have been studied widely by researchers in terms of their electrical and optical properties [4-13]. Since the quaternary compounds of these crystals show similar optical and electrical behaviors

and they allow adjusting the band gap according to intended uses, these types of structured crystals possess great potential for improvement of the semiconductor technology. In this study, we focused to characterize the some binary, ternary and quaternary semiconducting layered single crystals that are composed of GaS-GaSe, $TlGaS_2$-$TlGaSe_2$ and $TlGaS_2$-$TlInS_2$ systems.

Defects or impurities are dominant phenomena for performance of the devices fabricated with semiconductor materials. The efficiency of the devices can be strongly influenced by defects due to interaction of the unintentionally existed energy levels with the charge carriers contributing to the conduction or luminescence process. If it is necessary to exemplify the detrimental effect of the defects, non-radiative transitions can occur due to the presence of the defect centers such that it causes diminishing of the internal quantum efficiency or completely hinder the generation of light in LEDs and lasers. Likewise, carrier mobility can decrease in the electronic devices, if the defect centers act as a scattering centers. Thus, high-frequency operation can become impossible. Further, the effect of the impurities on the electrical and optical properties of the semiconductor materials is the well-known subject. Hence, having information about the existence of the defect levels in the studied crystals will be advantageous for the production of the devices using such materials. The utilized techniques for determination of the defect centers can also be contributory for researchers studying in the same area.

The introduction part is going to continue with the explanation of the known structural and optical properties of the studied crystals. Then, the results of the previous studies on the same crystals will be discussed. Finally, the explanations what we have done in the present study will be mentioned.

1.1. The optical and structural properties of the studied crystals

The ternary layered $TlGaS_2$ and $TlGaSe_2$ single crystals exhibit high photosensitivity for visible light source and they possess transparency in a large scale range between 0.5 and 14.0 μm [12]. These properties make the ternary crystals applicable for optoelectronic devices. These crystals were studied in terms of optical

and electrical properties in Refs. [10-17]. The indirect (E_{gi}) and direct (E_{gd}) band gaps of $TlGaS_2$ and $TlGaSe_2$ crystals were found to be E_{gi} = 2.45 eV, E_{gd} = 2.63 eV and E_{gi} = 1.97 eV, E_{gd} = 2.26 eV, respectively [18]. The quaternary compounds formed from the combination of these crystals bring flexibility for variation of the lattice constant and band gap to obtain desired materials. The lattice constant is significant parameter that can increase the efficiency of light generation at large range of wavelength. Therefore, quaternary crystals carry great potential for optoelectronic applications. The quaternary $Tl_2Ga_2S_3Se$, $TlGaSSe$ and $Tl_2Ga_2Se_3S$ crystals, exhibiting the properties of semiconductors, can be formed from ternary $TlGaS_2$ and $TlGaSe_2$ crystals through the replacement of a quarter, half and three quarter of S (Se) atoms with Se (S) atoms, respectively [1,19]. Two-dimensional layers form the lattice structure by stacking as parallel to the (001) plane. Sequentially created layers make 90 degree with former layer. In these crystals, Tl and S(Se) atoms create interlayer bond while Ga and Se(S) atoms form intralayer bond. The band gap energies of $Tl_2Ga_2S_3Se$, $TlGaSSe$ and $Tl_2Ga_2Se_3S$ crystals were found as E_{gi} = 2.38 eV, E_{gd} = 2.62 eV [20], E_{gi} = 2.27 eV, E_{gd} = 2.58 eV [21], and E_{gi} = 2.15 eV, E_{gd} = 2.54 eV [22], respectively, from the analyses of transmission and reflection data obtained at room temperature.

The ternary $TlInS_2$ crystals were studied previously in point of photoelectrical and optical properties [23-27]. Indirect and direct energy band gaps were established in the crystal with energies of E_{gi} = 2.27 eV and E_{gd} = 2.47 eV, respectively [18]. $Tl_4Ga_3InS_8$, Tl_2GaInS_4 and $Tl_4GaIn_3S_8$ quaternary layered single crystals are constituted from $TlGaS_2$ ($TlInS_2$) crystal by adding a quarter (three quarter), half (half) and three quarter (a quarter) of In (Ga) atoms in replacement of Ga (In) atoms, respectively [1,19]. The lattices of the crystals comprise two-dimensional layers that are parallel to (001) plane. Intra- and interlayer bonds occur between gallium (indium) and sulfur atoms and, between thallium and sulfur atoms, respectively. Coexistence of indirect and direct band gaps were revealed using transmission and reflection measurements for $Tl_4Ga_3InS_8$, Tl_2GaInS_4 and $Tl_4In_3GaS_8$ crystals with

3

energies of E_{gi} = 2.40 eV, E_{gd} = 2.61 eV [28], E_{gi} = 2.35 eV, E_{gd} = 2.54 eV [29], E_{gi} = 2.32 eV, E_{gd} = 2.52 eV [30], respectively.

The binary GaS and GaSe crystals are the $A^{III}B^{VI}$-type semiconductors with layered structure. These crystals possess encouraging optical properties with sensitivities in red and blue visible range for fabrication of devices in optoelectronic area [4-6]. Interlayer bonding interactions occur due to the weak forces (Van der Waals). Conversely, intralayer interactions are governed by strong ionic-covalent bonds [31]. The layers that have stacking sequence S(Se) - Ga - Ga - S(Se) consist of four atoms (two gallium and two sulfur (selenium)) [32]. GaS has wide band gap with indirect and direct energies of 2.59 and 3.04 eV, respectively, which make it as an applicable material to be used in fabrication of near-blue LEDs [33-35].   In addition, this crystal was shown to be responsive in the green-blue region of the spectra due to its electro- and photoluminescence properties [5,36,37]. On the other hand, GaSe crystals were studied widely to investigate the electrical and optical properties. It has a band gap interval with energy about 2.0 eV [38,39]. It is thought as a convenient material for terahertz and infrared generation since it has high birefringence and second order nonlinear optical susceptibility [40-44].

The ternary mixed crystals of GaS_xSe_{1-x} crystals can be obtained using GaS and GaSe crystals by changing the constituent compounds' concentration without any restriction ($0 < x < 1$) [32,45,46]. As being in the GaS and GaSe crystals, GaS_xSe_{1-x} crystals have also layered structure. The intra- and interlayer bonding types are dominated by strong ionic-covalent and weak Van der Waals interactions, respectively. Energy band gap of this system can be easily varied thanks to their flexibility in tunable compositions. Therefore, taking under consideration the usage areas of GaS and GaSe crystals, GaS_xSe_{1-x} mixed crystals can be thought as prominent materials for development of relevant areas like production of long-pass filters, optical switching and light emitting devices [47], and photodetectors [40]. The indirect and direct energy band gaps of GaS_xSe_{1-x} mixed crystals were reported as E_{gi} = 2.08 eV, E_{gd} = 2.16 eV, E_{gi} = 2.28 eV, E_{gd} = 2.38 eV and E_{gi} = 2.39 eV, E_{gd} = 2.53

eV for values of the composition $x = 0.25$, $x = 0.50$ and $x = 0.75$, respectively [48-50].

1.2. Previous studies

Formerly, thermally stimulated currents (TSC) and photoluminescence (PL) measurements have been completed for $Tl_2Ga_2S_3Se$ crystals [51-53]. The TSC experiments were executed at low temperatures in the ranges of 10-60 K [51] and 200-320 K [52] employing various heating rates in the ranges of 0.6−1.5 K/s, and 0.6−1.2 K/s, respectively. The studies indicated that two trapping centers with thermal activation energies of 11 meV [51] and 498 meV [52] exist in the crystal. The PL measurements achieved in the region 10-60 K presented a broad PL band having maximum at 550 nm (2.25 eV) at $T = 10$ K. It was suggested that the observed PL spectrum is owing to the radiative transitions between donor and acceptor levels with energies of $E_d = 10$ meV and $E_a = 160$ meV, respectively [53].

TSC measurements were accomplished for as-grown TlGaSSe crystal in the temperature region of 10−100 K [54]. Analyses of TSC spectra gave one trapping center possessing thermal activation energy of 12 meV. The PL experiments performed in the wavelength interval of 695-1010 nm at low temperatures (20-56 K) exhibited two PL band centered at 1.605 and 1.254 eV [55]. These bands are thought to be raised owing to the transitions between deep donor levels ($E_d = 0.721$ and $E_d = 1.069$ eV) and shallow acceptor levels ($E_a = 0.008$ and $E_a = 0.011$ eV). Hall mobility, temperature-dependent electrical resistivity and photoconductivity (PC) experiments were carried out previously [56]. The analysis of resistivity measurements demonstrated the existence of acceptor levels having energies of 230 and 450 meV. The recombination centers at 10, 181 and 363 meV were revealed by PC measurements.

$Tl_2Ga_2Se_3S$ crystals were investigated to determine the defect centers with the aid of TSC measurements accomplished at low temperatures (10-260 K) [57]. It was observed that three trapping levels centered at 12, 76 and 177 meV occur in the crystal. Moreover, the crystal was studied by means of PL measurements at varying

temperatures from 10 to 50 K [58]. One PL band arising in the wavelength interval of 540-700 nm was recorded. According to the study, one donor and one acceptor level with $E_d = 270$ and $E_a = 10$ meV were ascribed to the transition to be responsible for obtained PL band.

Tl$_4$Ga$_3$InS$_8$ crystals were previously studied in terms of PL measurements. The experiments were done with below ($\lambda_{exc} = 532$ nm) and above ($\lambda_{exc} = 325$ nm) band gap excitations in the wavelength (550-710 and 420-600 nm) and in the temperature (80-300 K and 30-300 K) region [59]. Two PL bands centralized at 580 and 496 nm appeared in the PL spectra. The transitions between donor levels (at 20 and 370 meV) and acceptor level (at 200 meV) were assigned to these PL bands.

TSC experiments on Tl$_2$GaInS$_4$ crystals were achieved in the temperature region 10-60 K [60]. The successive analysis of the obtained TSC spectra revealed two trapping levels that have energies of 4 and 10 meV. The low temperature PL spectrum recorded in the temperature region of 15-150 K exhibited three emission bands [61]. The maxima of these bands were 542, 607 and 707 nm. Tl$_2$GaInS$_4$ crystals were also governed through dark electrical conductivity, PC and space charge limited conductivity measurements in different temperature regions of 220-350 K, 200-350 K and 300-400 K, respectively [62]. Two energy levels with 320 and 600 meV were revealed by dark electrical conductivity. Also, analysis of the PC measurements resulted with two levels having energies of 190 and 280 meV. Single trap level centered at 440 meV was established by space charge limited current measurements.

TSC experiments on Tl$_4$In$_3$GaS$_8$ crystals were achieved between 10 and 90 K [63]. The TSC spectrum presented one peak associated with one trap level which has activation energy of 12 meV. PL measurements of the same crystal carried out in the range 26-130 K displayed two emission bands in the PL spectrum recorded between 500-780 nm wavelength ranges [64]. The donor (30 and 10 meV) and acceptor levels (810 and 190 meV) lead to radiative transitions which are related to observed PL bands.

Previously, TSC experiments on GaS single crystals were carried out below room temperature (10-300 K) [65]. Analysis of the TSC spectra being recorded at a

constant heating rate of 0.1 K/s indicated six trap levels having activation energies of 50, 60, 120, 630, 710, and 750 meV. Also, PL measurements performed at low temperatures produced three bands centered at 2.22, 2.02 and 1.59 eV [66]. Analysis of these emission bands allowed determining the three donor levels at energies of 13, 17 and 151 meV.

Ga$_4$S$_3$Se single crystals were studied in terms of TSC measurements between 10 and 150 K [67]. Three trap levels were demonstrated in the crystal with energies of 70, 210 and 357 meV. Low temperature (10-200 K) PL studies on Ga$_4$S$_3$Se crystals were achieved by recording the PL spectrum having two bands in the wavelength range 500-850 nm [68]. These emission bands had maxima at 527 and 658 nm. The analyses resulted in two shallow donor levels at 43 and 64 meV and two acceptor levels at 88 and 536 meV that were assigned to origin of PL emission bands. Further, temperature-dependent conductivity investigations revealed the existence of two donor levels below the conduction band located at 755 and 465 meV [69].

Ga$_2$SSe single crystals were investigated by means of TSC, PL, electrical and PC measurements [70-72]. Outcome of the analysis for TSC measurements indicated three trap levels which have activation energies of 0.072, 0.100 and 0.150 eV [70]. PL spectrum detected in the wavelength region 565-860 nm exhibited two PL bands originating from the radiative transitions taking place between donor (29 and 40 meV) and acceptor (185 and 356 meV) levels [71]. Dark electrical conductivity and space charge limited current investigations brought out a single trap level at 310 meV [72]. Temperature-dependent PC experiments on Ga$_2$SSe crystals were also successful to determine two additional defect levels having energies of 140 and 100 meV [72].

Ga$_4$Se$_3$S single crystals were previously investigated through TSC measurements at low temperatures (10-300 K) [73]. Activation energy of revealed one trap level was found as 23 meV. PL measurements executed for temperatures from 16 to 200 K in the wavelength interval of 535-855 nm indicated two PL bands having maxima at 572 and 652 nm at 16 K [74]. The first band is ascribed to transition from donor levels at 125 meV to acceptor levels at 11 meV. PC and dark electrical

conductivity experiments were carried out in the temperature region of 100-350 K [75]. Two energy levels located at 310 and 60 meV were revealed by the dark electrical conductivity. Two new energy levels obtained at 209 and 91 meV were also attributed to trap levels existing in the crystal.

In literature, there are many papers presenting the optical and electrical properties of undoped and doped GaSe single crystals. Previously, TSC investigations on undoped GaSe were accomplished in the temperature range of 10-300 K. Three trapping centers located at 20, 100 and 260 meV were reported [76]. Undoped GaSe crystals were studied by virtue of PL measurements with varying temperature from 10 to 300 K in the wavelength interval of 635-750 nm [77]. Thermoluminescence (TL) measurements on undoped GaSe crystals were also achieved below room temperature (10-300 K) [78]. As-grown GaSe crystal was revealed to possess four trapping levels with energies of 140, 180, 240 and 370 meV. Annealing effect on the established defects was also investigated. The annealing up to 500 ºC was not sufficient for eradication of the levels. As a result, four energy levels centered at 110, 160, 180 and 330 meV were obtained [78]. However, the TL peaks related to these energy levels were prominently weak about 100 times in their intensity as compared to intensity of peaks observed for as-grown crystal. Additionally, some doped GaSe crystals were studied by many authors. GaSe:Er crystal was investigated by means of PL, deep-level transient spectroscopy and Hall measurements [79]. Two acceptor levels at 65 and 158 meV were reported by the authors. Shigetomi et al. [80] reported the results of PL, photocurrent and Hall-effect measurements on GaSe:Te crystals. They assigned the acceptor levels located at 20 and 80 meV to the interstitial Te atoms. The same authors studied the GaSe: As, Bi, Sb crystals by virtue of Hall and PL measurements [81]. They found that one donor and one acceptor level at energies of 80 and 600 meV, respectively, exist in the crystals.

1.3. Present study

In this study, the results of TL investigations for binary GaS and Mn doped GaSe, the ternary Ga_4S_3Se, Ga_2SSe and Ga_4Se_3S, and the quaternary $Tl_2Ga_2S_3Se$, $TlGaSSe$, $Tl_2Ga_2Se_3S$, $Tl_4Ga_3InS_8$, Tl_2GaInS_4 and $Tl_4In_3GaS_8$ layered single crystals were reported. Thermoluminescence experiments were carried out below room temperatures using various heating rates ranging from 0.2 to 1.2 K/s to expand the previously realized studies and to give new valuable knowledge about the characteristics of defects and impurities in the studied crystals. The analyses were accomplished through the bases of TL theory which is in accordance with the experimental observations for the crystals.

In chapter 2, some theoretical information related to the semiconductor materials such as band structure of a semiconductor, type of semiconductors, type of defects in semiconductors, have been mentioned for the readers. Moreover, the transitions in or through the band gap which are quite significant for TL process have been demonstrated by exemplifying the possible cases. Theoretical approach for the TL experimental methods and analysis techniques were mentioned in the chapter.

Experimental setup and procedures for TL measurements performed to obtain TL spectra arising due to the existence of defects in the crystals have been explained in chapter 3. TL measurements were explained for each methods used to investigate the characteristics of the trapping levels in the crystals. Simple explanations for EDSA measurements and experimental setup were also given in the chapter.

In chapter 4, the results of the experimental observations have been given using different analysis methods known from the TL theory. Experimentally obtained TL spectra for each studied crystals have been indicated separately in the figures. The activation energies of trapping levels corresponding to obtained TL peaks were calculated using different methods. For this purpose, theoretical curve fit to these TL curves have been achieved successfully by the help of theoretical knowledge given in chapter 2. Moreover, initial rise and peak shape methods were applied to the TL peaks for evaluation of the activation energies. Frequency factors and capture cross sections of the revealed trap levels were calculated using the found activation

energies. TL curves of various heating rates were demonstrated for studied crystals. Distribution of determined traps was studied to get detailed information about the defects.

In chapter 5, the conclusion and physical interpretations of the obtained results for defect levels have been presented clearly. The comments on demonstrated activation energy values and other kinetic parameters, heating rate behavior and distribution of trap levels, the origin of existed defects in the studied crystals have been given by taking into account the theoretical bases and crystals' structures.

CHAPTER 2

THEORETICAL APPROACH

2.1. Introduction

Semiconductor materials possess large application areas in today's technology thanks to their structural, electrical and optical flexibility of application for the devices. Their properties and structures have been studied and improved by many researchers and they are still open for development of devices. The theory of the semiconductors have been studied for decades. They are special materials placing between metals and insulators with regard to their band gap. They can show the properties of metals or insulators when were interfered to them externally. Moreover, they can have defects naturally during the growth process or intentionally doped of different elements. Thus, getting knowledge about these defects gain importance to have high quality devices. In this chapter, we mention the band structure, type of semiconductors, defect types, possible transitions between energy levels, theoretical approach to TL mechanism and analysis methods.

2.2. Band structure of a semiconductor

Discussing the band structure of a semiconductor material is crucial for better comprehension of the electronic properties of semiconductor materials. Simply approaching to subject, band structure of diamond crystal which is completely composed of carbon atoms were shown in Fig. 2.1. Carbon atom has six electrons

occupying the discrete energy levels of 1s, 2s and 2p. The first energy state (1s) is fully filled by electrons with opposite spins. Assuming the diamond crystal consists of N atoms, 1s state has 2N quantum states. By the help of the same assumption, 2s and 2p states have also 2N and 6N quantum states, respectively (see Fig. 2.2).

(a)

(b)

2p

2s

1s

Energy

CB

E_g

VB

Capacity 4N, empty

Capacity 4N, filled

1s band
Capacity 2N, filled
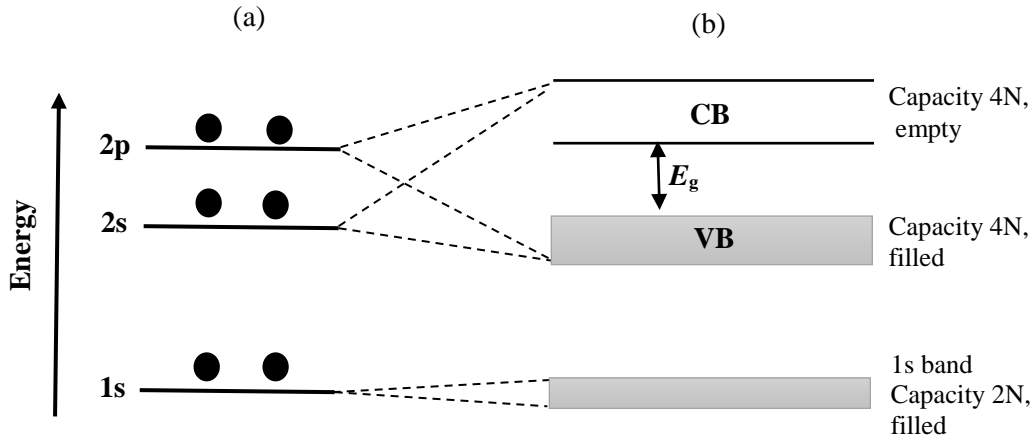
Figure 2.1. (a) Occupancy of quantum states in carbon atom. (b) Configuration of band structure of diamond [82].

Creation of the band structure is due to the interaction of the 2s and 2p states with each other as illustrated in Fig. 2.2. Particularly, as the separation of the states gets equilibrium, two bands called as valence and conduction bands occur. The valence band and conduction band have totally 8N quantum states. 4N states of them are responsible for valence electrons, while the rest of them generates conduction band. In diamond crystal, since four electrons related to $n = 2$ state occupy the valence band, the conduction band is empty at absolute zero. The energy level, denominated as band gap, remaining between valence and conduction bands is forbidden level (E_g) and plays an important role for electronic properties of materials such as metals, semiconductors and insulators. For example, in metals, since the valence and conduction bands overlap each other and the valence band is partially occupied by

electrons, small amount of electric field is sufficient for electrons to gain kinetic energy and to contribute to the electrical conductivity. However, in insulators, forbidden level blocks the electrons in the highest occupied level. Therefore, these materials are electrically insulated. For the case of semiconductors, the band gap can be small enough for electrons to be reached to unoccupied states. Consequently, these type of materials become more of an issue due to their useful electrical properties.
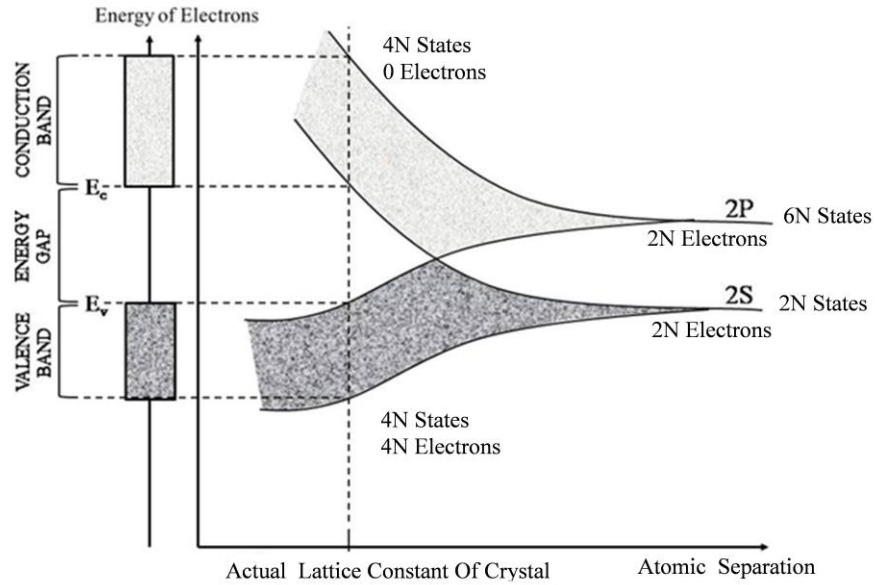
Figure 2.2. Energy levels of n = 2 quantum states in a diamond crystal with *N* carbon atoms versus atomic separation.

The position of the conduction band in *k*-space differs for semiconductor materials. If the minimum energy state of the conduction band and maximum energy state of the valence band are in the same *k*-vector, it is called as *direct gap*. For such a material, interaction with photon that has enough energy is adequate for excitation. On the other hand, some semiconductors has *indirect gap* arising from the differences of *k*-vector between conduction band minima and valence band maxima

(see Fig. 2.3). In this case, not only photon is needed, but also lattice vibration is required for charge carriers to gain momentum for transition.
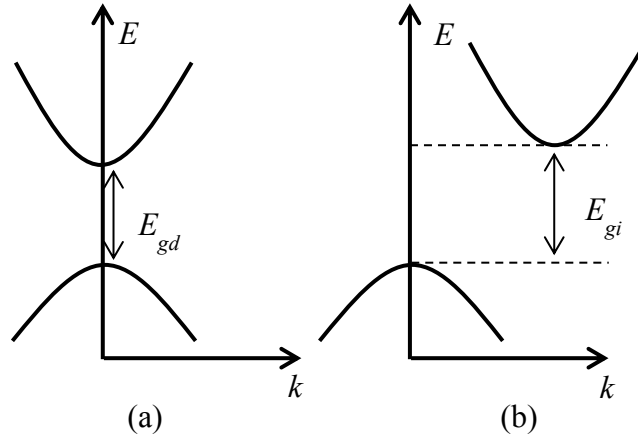
Figure 2.3. Presentation of (a) direct and (b) indirect band structures.

2.3. Semiconductor types

2.3.1. Intrinsic semiconductors

Intrinsic semiconductors can be thought as an ideal crystals since they have no impurities or defects in the lattice structure. The conductivity of the intrinsic semiconductors are dominated by the interband transitions of the electrons. At absolute zero, all of the electrons in the intrinsic semiconductors occupy the valence band and the probability function F(E) for electron to be found in valence band is equal to 1 (see Fig. 2.4). İncreasing temperature leads to some electrons which are near the top of the valence band to be stimulated into conduction band. Therefore, the probability of electrons close to top of the valence band reduces for $T > 0$. In the conduction band there is no electron at $T = 0$ K, and F(E) must be zero for $E > E_c$. For $T > 0$, some electrons can be excited into conduction band and *holes* are created in the valence band. While the excited electrons into the conduction bands contribute to the conductivity, the created holes in the valence band are also employed for conduction. For an intrinsic semiconductor, Fermi energy corresponding to the probability function F(E) = ½ is in the middle of the band gap (E_g / 2). Since the

14

excitation of electrons from valence band causes the same amount of holes to be created, the Fermi energy level must be halfway.
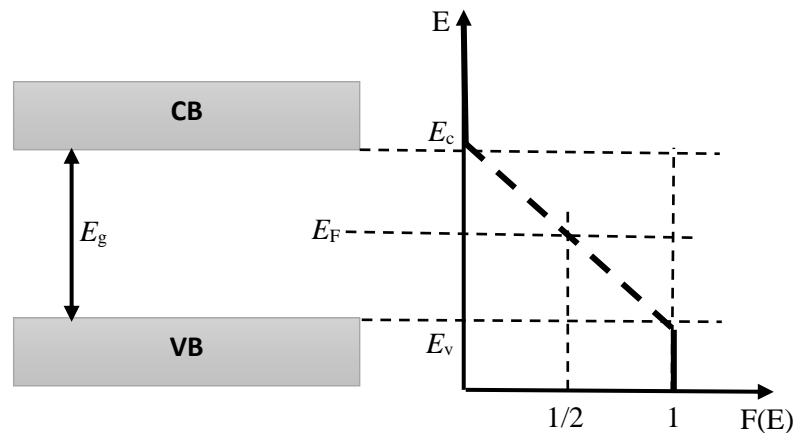
Figure 2.4. Diagram for Fermi distribution function and Fermi energy for an intrinsic semiconductor [83]

2.3.2. Extrinsic semiconductors

In the previous section, we discussed the intrinsic semiconductors that have small amount of electrons (approximately 10^9 per cubic cm) for contribution to conductivity. However, most of the semiconductor devices have capability of better
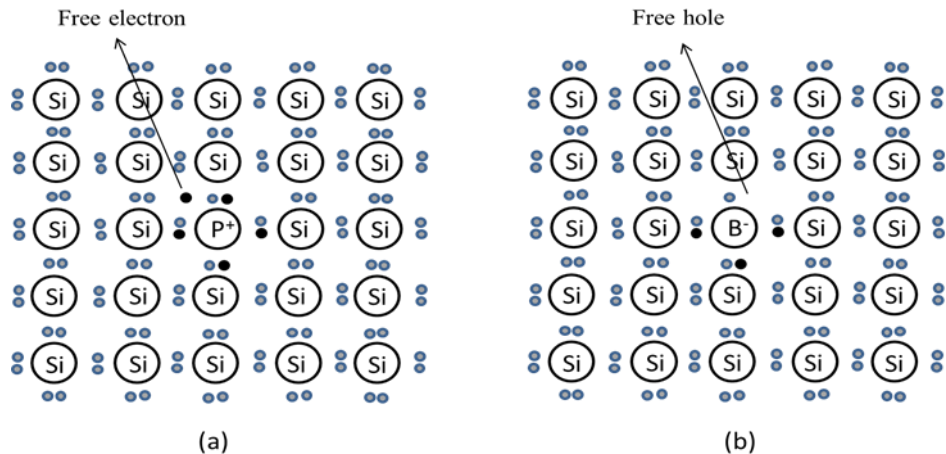
Figure 2.5. (a) Phosphor and (b) Boron atom doping of silicon.

15

conduction due to the existence of impurities by doping or unintentionally created defects. These types of semiconductors are known as extrinsic materials. Two types of extrinsic semiconductor can be obtained by doping to intrinsic one appropriate atom. Generally, elements of the groups III and V in periodic table can be utilized to obtain *p-* and *n-types* semiconductors, respectively. Figure 2.5 illustrates the doping of silicon (Si), which has four valence electrons, with phosphorus (P) and boron (B). Since the P atoms contain 5 valence electrons, four of them creates electron-pair bonds with the Si atom. The last electron can be easily disassociated from the atom with small increase of temperature. By virtue of an extra electron the doped P is called as *donor* (see Fig. 2.5a). The obtained material is *n-type* semiconductor. Similarly, if the Si atom is doped with B atom which has three valence electrons, instead of creating electron-pair bonds for all states, one positive charge is introduced around the B atom that is known as *acceptor*. This type of materials is *p-type* semiconductor (see Fig. 2.5b).
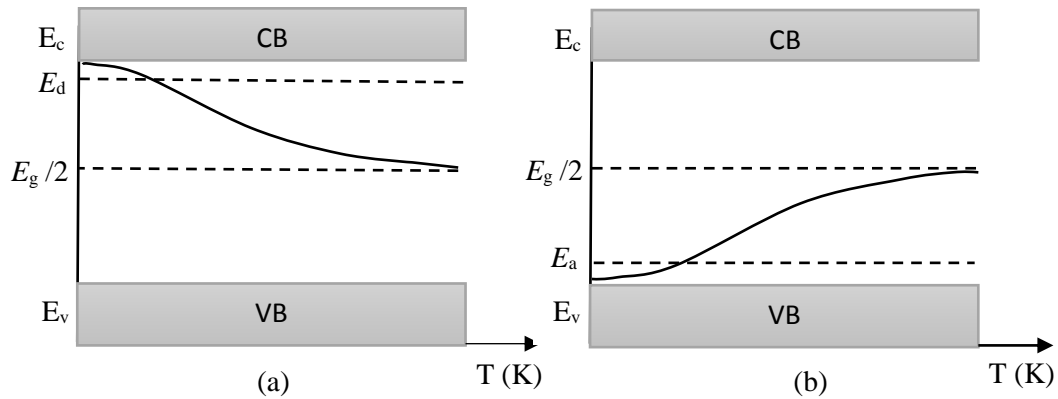
Figure 2.6. Fermi energy level of (a) *n-* and (b) *p*-type semiconductors as a function of temperature [83].

For *n-type* semiconductor, the Fermi energy decreases with increasing temperature as seen in Fig. 2.6a. At low temperatures, Fermi energy level is between the donor energy level and conduction band. By rising the temperature, extrinsic

16

semiconductor starts to behave as intrinsic and the E_F goes to $E_g / 2$. Similarly, p-type semiconductors act as an intrinsic with elevated temperature. The Fermi energy increases to $E_g / 2$ from below the acceptor level (see Fig. 2.6b).

2.4. Defects

Even though the perfectly grown crystals exhibit regular, periodic structure, most of the crystal shows disordered lattices occurring intentionally by doping or unintentionally during the growth process. This imperfection is called as defect. Four types of defects which are point defects, line defects, planar or surface defects, and volume defects were discussed in the following section.

2.4.1. Point defects

These defects arise owing to absence of a host atom (vacancy) or misplacing of an atom and create only single lattice point (not extended). There are four types of point defects. One of them occur due to the existence of the same but an extra atom. The extra atom places anywhere between the bulk atoms and called as *self interstitial atoms*. The other defect type is again created by the same atom with host lattice but the atom is smaller than the bulk atoms. This defect is named as
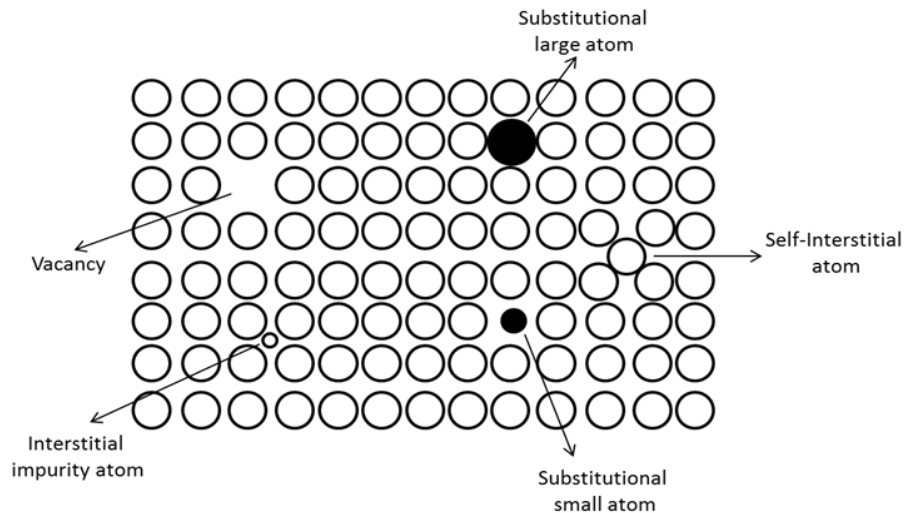
Figure 2.7. Demonstration of various point defects existing in semiconductors.

17

interstitial impurity atom. Moreover, different kind of atoms in the lattice also create the disordered structure by replacing into the bulk atoms. *Substitutional impurity atoms* are classified as this kind of point defects. *Vacancies* are also a point defect types originating from the lacking atom in the crystal structure. Figure 2.7 exemplifies the types of the point defects.

2.4.2. Line defects

Absence of a group of atoms in the crystal structure or locating in a wrong position creates the line defects. Generally, they are called as dislocations. Two types of dislocations can occur in the lattice. *Edge dislocations* are raised due to either removal or replacement of a plane from (to) the crystal. *Screw dislocations* are line defects so that the atomic planes created by atoms trace the dislocation line helically (see Fig. 2.8).

(a)   (b)
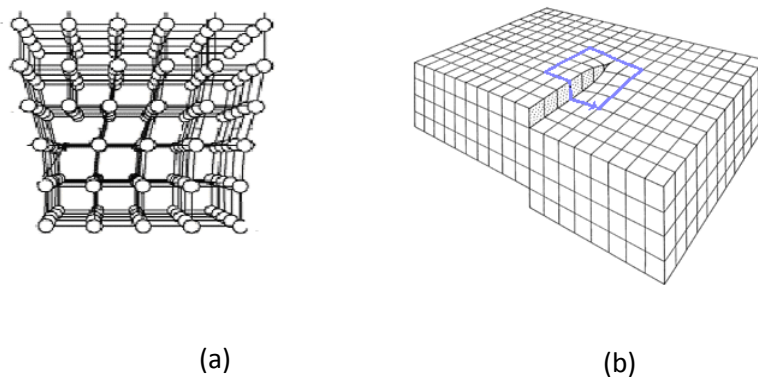
Figure 2.8. Demonstration of (a) edge dislocation and (b) screw dislocation [84].

2.4.3. Planar defects

In this kind of defect type, interfaces occur among homogeneous regions of the structure. *Stacking faults, twin boundaries* and *grain boundaries* are the best known planar defects existing in the semiconductor crystals. If the atom planes

stacked as sequentially as perfect crystals are interrupted by one or two layer, it is called as *stacking faults*. If the stacking fault continues over many atomic spacing, then *twin boundaries* are generated. Stacking fault and twin boundaries are planar defects arising in the single crystals. However, grain boundaries occur in the solid materials composed of different number of grains or crystals.

These grains can have various size ranging between nanometers and millimeters. Orientations of them differ from the neighboring one by some rotation angle. Such an arrangement creates the *grain boundaries*.

2.4.4. Volume or bulk defects

The main three dimensional defect type is known as *void*. This defect is defined as the big regions, which has bigger scale as compared with other type of defects mentioned before, arising owing to missing of atom groups in the lattice. Creation of voids depends on some reasons. If air bubbles is trapped into the atom planes during the growth process of the crystal, the void is generally termed as *porosity*. Shrinking of the material as the growing is performed leads also a kind of void known as *cavitation*. The *precipitates* occur when the impurity atoms form a homogeneous assemblage.

2.5. Transitions between energy states in thermoluminescence

In order to understand the thermoluminescence emission mechanism, possible transitions of charge carriers between allowed energy states should be taken account. Simple model for a semiconductor material is shown in Fig. 2.9. The best-known transitions in a semiconductor occur between the valence and conduction bands explained as following: transition (a) in Fig. 2.9 takes place as electrons in valence band are excited by light which energy is bigger than band gap ($hv > E_g$). This transition is known as band-to-band transition and the process leads to creation of free electrons in conduction band and free holes in valence band. The created free electrons pass back to the valence band and they recombine with the free holes (transition h). This transition is known as direct recombination.
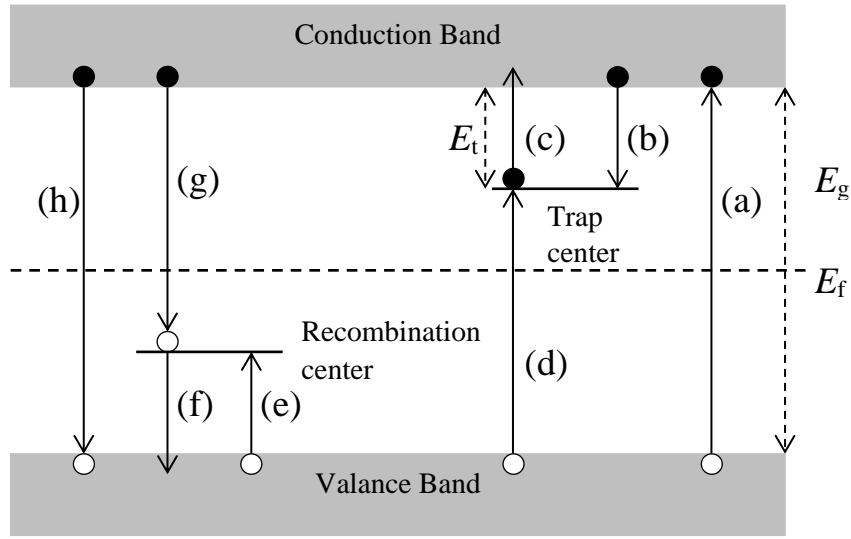
Figure 2.9. Demonstration of electronic transitions between energy levels in TL [85].

In a semiconductor material, other possible transitions can take place between the energy states arising due to the defects and/or impurities. Transitions (b) and (e) exemplify the trapped electrons through the trap center and holes through the recombination center. The transitions (c) and (f) are realized when the trapped electrons and holes are stimulated from the trap and recombination centers, respectively. In order to excite these charge carriers from the trapping centers, thermal energy (kT) plays role in TL experimental technique. The excited charge carriers from trapping centers (released to delocalized states) recombine with each other as shown in the figure (transitions d and g).

If necessary to talk about modeling the simple TL mechanism, electrons in the valence band are excited by light having energy bigger than the band gap and transition (a) takes place. Either these excited electrons in conduction band recombine with holes in the valence band (transition (h)) or they are trapped by energy levels existing in the forbidden energy gap (transition (b)). Opposite charge carriers trapped into the recombination center (transition (e)) recombine with trapped electrons in two way. Thermally stimulated electrons (holes) into the conduction (valence) band

recombine with holes (electrons) at the recombination (trap) center. Therefore, luminescence is produced. The other way of recombination is explained by the electrons (holes) recombining with holes (electrons) through an intermediate localized state instead conduction (valence) band. This transition is non-radiative and no luminescence can be produced.

2.6. Theoretical approach to thermoluminescence

Thermoluminescence intensity (I_{TL}) is the most important parameter for luminescent materials to have knowledge about the trapping centers' characteristics. Obtaining the TL intensity as a function of temperature, one can determine the properties of the defect centers using the theoretical relations between the trapping parameters and TL intensity. Therefore, in this section of the chapter, we decided to give simple explanations and theoretical formulas related to TL intensity for different cases. The physical subject determining the magnitude of TL intensity is the concentration of the trapping levels in luminescent materials. The more the number of charge carriers are trapped, the more the released charge carriers contribute to the TL intensity at a certain temperature. Figure 2.10 shows the simple diagram for one electron-one hole model.
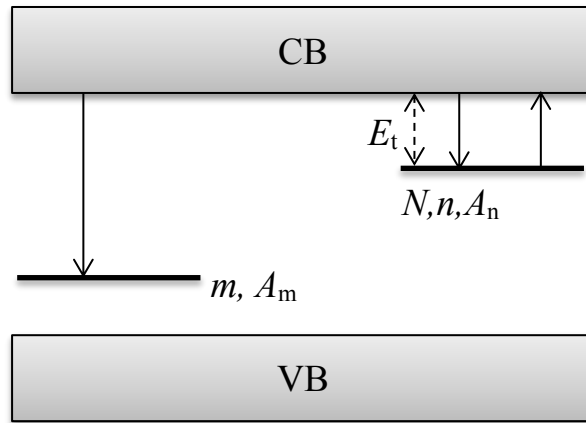
Figure 2.10. Simple diagram for one electron and one hole traps.

The probability (P) of an electron to be released from trap level to the conduction band at a temperature T is given as the following

$$P = s \exp(-E/kT),$$ (2.1)

here, s and k present the frequency factor and Boltzmann constant, respectively. For a semiconductor, s is known as

$$s = N_c A_n = N_c \upsilon_e S_t \quad,$$ (2.2)

where N_c is the effective density of states in conduction band, υ_e is the thermal velocity of electrons released to conduction band, S_t is the capture cross section and A_n is the retrapping probability, N_c and υ_e are defined as

$$N_c(T) = 2(\frac{kTm_e^*}{2\pi\hbar^2})^{2/3}$$ (2.3)

and

$$\upsilon_e(T) = \sqrt{\frac{3kT}{m_e^*}} \quad,$$ (2.4)

In which the m_e^* is effective mass for electron.

The number of charge carriers occupying the traps alters with the transitions among the localized (trap and recombination centers) and delocalized (conduction and valence bands) states. These transitions are explained in theoretically as [86];

Stimulation: The transition of electrons from trap level to conduction band is decisive factor for the concentration of trap levels. The variation of number of charge carriers as a function of time is given as [87]

$$\frac{dn}{dt} \propto -ns \exp(-E/kT) \quad.$$ (2.5)

Retrapping: the event takes places for the electrons (holes) released to conduction (valence) band from trap level. Some of the stimulated electrons (holes) recombine with opposite charges, the others can be retrapped by the defect center. Free electron concentration (n_c) and unfilled traps' concentration ($N-n$) are two important things for the excited charge carriers to be retrapped by the traps. N implies the concentration of fully empty traps. Therefore, the relation between the parameter n and the retrapping event is written as

$$\frac{dn}{dt} \propto n_c (N-n) S_t \upsilon_e \ . \tag{2.6}$$

As the Eqs. (2.5) and (2.6) are rearranged together, the following relation can be obtained

$$\frac{dn}{dt} = n_c (N-n) S_t \upsilon_e - ns \exp(-E/kT). \tag{2.7}$$

Recombination: If the recombination of opposite charge carriers occurs, hole concentration in the recombination center (m) becomes dominant. Therefore, variation of electron concentration in the conduction band is managed by the event of recombination. The relation is given as

$$\frac{dn_e}{dt} \propto \frac{dm}{dt} = -n_c m A_m \ , \tag{2.8}$$

where A_m is the probability of recombination. Eq. (2.8) can be rearranged by using the relation between m and lifetime (τ) as

$$\frac{dn_c}{dt} \propto -n_c m A_m = \frac{n_c}{\tau} \ . \tag{2.9}$$

Taking account the three events and equations obtained above, the following relations can be written

$$n_c = m - n \quad \Rightarrow \quad \frac{dn_c}{dt} = \frac{dm}{dt} - \frac{dn}{dt} \quad \Rightarrow \quad \frac{dn_c}{dt} = -\frac{n_c}{\tau} - \frac{dn}{dt} \quad . \tag{2.10}$$

$$\frac{dn_c}{dt} = -\frac{n_c}{\tau} - n_c(N-n)S_t \upsilon_e - ns\exp(-E/kT)$$

The ultimate result of Eq. (2.7) is achieved for two different cases of trapping process. The third case is taking into account by an empirical formula.

I. **Slow retrapping (first order kinetic)**

The slow retrapping case occurs as the recombination of stimulated electrons in the conduction band with the holes in the recombination center takes place without trapping again by the trap level. The probability of recombination regardless of retrapping dominates the TL process. The theoretical relations determining this case are [87]

$$\frac{n_c}{\tau} \gg n_c(N-n)S_t \upsilon_e \tag{2.11}$$

and

$$\left|\frac{dn_c}{dt}\right| \ll \left|\frac{dn}{dt}\right|, \left|\frac{dm}{dt}\right| \quad . \tag{2.12}$$

With the help of Eqs. (2.11) and (2.12), Eq. (2.7) forms

$$\frac{dn}{dt} \approx -ns\exp(-E/kT) \tag{2.13}$$

and

$$\frac{dn}{dt} \approx -\frac{n_c}{\tau} \quad . \tag{2.14}$$

The equation (2.13) results with the following equation by using the dependence of temperature on the heating rate $T = T_0 + \beta t$

$$n = n_0 \exp\left\{-\int_{T_0}^{T} \frac{s}{\beta} \exp(-E/kT)\, dT\right\}.$$ (2.15)

The TL intensity of luminescent materials is directly related to the emitted photons created by recombination of opposite charge carriers. Thus, the expression defining the TL intensity is given as the alteration in concentration of trapped electrons by time [85]

$$I_{TL} = -\frac{dn}{dt}.$$ (2.16)

Using Eqs. (2.13) and (2.15), TL intensity is obtained as

$$I_{TL} = n_0 s \exp\left\{-\frac{E}{kT} - \int_{T_0}^{T} \frac{s}{\beta} \exp(-E/kT)\, dT\right\}.$$ (2.17)

In the equation, n_0 is the initial concentration of trapped charge carriers, β is the heating rate, T_0 is the starting temperature of heating process.

II. **Fast retrapping (second order kinetic)**

In fast retrapping, retrapping of released electrons dominates the recombination of opposite charge carriers. According to study of Garlick and Gibson on fast retrapping [88], much shorter time is needed for stimulated and trapped electrons to have equilibrium thermally as compared with the recombination lifetime. Taking under consideration these circumstances, for second order kinetics, following relations are given,

$N \gg n$ and $n = m$

Then, the variation rate of electrons is

$$\frac{dm}{dt} \approx \frac{dn}{dt} = -\frac{n_c}{\tau} = -n_c m A_m = -n_c m \upsilon_e S_t \; . \tag{2.18}$$

Combining Eqs. (2.7) and (2.18), one can obtain

$$\frac{dn}{dt} = -\frac{1}{N} n^2 s \exp\left[-\frac{E_t}{kT}\right] \quad . \tag{2.19}$$

Integration of the Eq. (2.19) result with the expression giving TL intensity as

$$I_{TL} = -\frac{dn}{dt} = \left(\frac{n_0^2}{N}\right) s \exp\left[-\frac{E}{kT}\right]\left[1 + \frac{n_0 s}{\beta N}\int_{T_0}^{T}\exp(-E/kT)\,dT\right]^{-2} . \tag{2.20}$$

III. **General order kinetic**

May and Partrige [89] improved a formula for the intensity of TL emission empirically to determine the TL mechanism of the trap states not to obeying the properties of the first and second order kinetics. The expression is given as the following

$$I_{TL} = -\frac{dn}{dt} = -n^b s' exp\left[-\frac{E_t}{kT}\right] , \quad \text{where } s' = \frac{s}{N^{b-1}} . \tag{2.21}$$

In the equation, b is kinetic order and s' is pre-exponential factor. From the solution of the above differential equation one can write a formula as

$$n = n_0 \left[1 + (b-1)\frac{s'}{\beta}n_0^{b-1}\int_{T_0}^{T}\exp\left(-\frac{E_t}{kT}\right)dT\right]^{-\frac{1}{b-1}} \tag{2.22}$$

Inserting the Eq. (2.22) to (2.21), the TL intensity for the traps exhibiting the properties of general order kinetic can be found as

$$I_{TL} = n_0 s'' \exp(-\frac{E_t}{kT}) \left[1 + (b-1)\frac{s''}{\beta} \int_{T_0}^{T} \exp\left(-\frac{E_t}{kT}\right) dT \right]^{-\frac{b}{b-1}} \, , \qquad (2.23)$$

where $s'' = s' n_0^{b-1}$ and it possesses a dimension s^{-1} like the frequency factor. As understood, the Eq. (2.23) corresponds to the second order kinetics as the b is equal to 2 and it reduces to the first order kinetics when the parameter b goes to 1.

2.7. Theoretical approach to thermoluminescence analysis methods

In literature, there are many analysis methods that can be applied to the experimentally obtained TL curves. In this part of the study, we intended to clarify those of the most important and successful analysis techniques which we employed to achieve the analysis results. Application of curve fitting, initial rise, peak shape and heating rate methods were explained in detail in this section.

2.7.1. Curve fitting method

Curve fitting (CF) method is used to evaluate the activation energies of traps existing in the forbidden energy state of semiconductors and insulators. This method is also beneficial to determine the order of kinetics. In this manner, the Eqs. (2.17), (2.20) and (2.23) are applied to the experimental TL glow curve using a software [90]. Eq. (2.17) gives the TL intensity for first order kinetics while the Eqs. (2.20) and (2.23) are responsible for second and general order kinetics, respectively. Depending on geometry of the TL curves, one of these equations is used to get the best fitting curve suitable with the experimental TL curve and activation energy and the kinetics order for the traps can be obtained.

2.7.2. Initial rise method

Initial rise (IR) method is one of the most significant and most chosen method to determine the activation energy of trapping levels due to its undeniable advantage in analysis of the TL peaks. This method is completely independent of the trapping process and can be utilized for all of the peaks regardless of dominant order of kinetics of the traps. Therefore, application of this method creates a chance to compare the activation energy value with other techniques dependent on order of kinetics. Since the trapped charge carriers related to the initial tail of the TL glow curve are assumed to be constant and they should be proportional to $\exp(-E_t / kT)$ as the excitation of the trapped charge carriers to the non-localized states takes place, initial tail of the TL curve is taken under consideration for analysis [90]. By this way, plotting a graph of $\ln(I_{TL})$ versus $1/T$ results with a straight line and the slope of this graph gives the activation energy ($-E_t / k$) of the trapping levels.

2.7.3. Peak shape method

Shape of the TL glow peaks shows geometrical differences depending on the trapping process of the charge carriers stimulated from trap levels. In the case of recombination of trapped charge carriers with opposite ones without retrapping, descending part of the TL curves seems narrower than the ascending part. On the other hand, if the charge carriers are retrapped before recombination, ascending part of the TL curve starts to be narrower by increasing number of retrapped carriers. This variation of the TL peak directly affects the trapping parameters of the energy levels. Peak shape (PS) method is very successful one for analysis of the TL peaks and gives reliable results. Using the geometric structure of the single glow peak, activation energy and geometry factor (μ_g) can be found. According to this method, low (T_l) and high (T_h) temperatures sides at half maximum intensity and the peak maximum temperature (T_m) values of the glow curve help us to compute the activation energies of the charge carrier released from trap using the parameters: $\tau = T_m - T_l$, $\delta = T_h - T_m$, $w = T_h - T_l$ and $\mu_g = \delta/w$ in the following expressions [90]

$$E_\tau = \frac{[1.51+3.0(\mu_g-0.42)]kT_m^2}{\tau} - \left[1.58 + 4.2(\mu_g - 0.42)\right]2kT_m \tag{2.24}$$

$$E_\delta = \frac{[0.976+7.3(\mu_g-0.42)]kT_m^2}{\delta} \tag{2.25}$$

$$E_w = \frac{[2.52+10.2(\mu_g-0.42)]kT_m^2}{w} - 2kT_m\, . \tag{2.26}$$

The average values of above energies gives the activation energy of trap levels. Chen and Kirch claimed that the geometry factor should be approximately 0.42 and 0.52 for first and second order kinetics, respectively [86]. The values that are between 0.42 and 0.52 imply the trap is dominated by mixed order kinetics.

2.7.4. Heating rate method

Variation of heating rate (β) is a significant phenomenon that influences the TL mechanism of the trapping levels. Stimulation of the charge carriers trapped into the energy levels in the band gap of the material is directly related to β which plays dominating role for position of TL peaks. Although the parameter β is decisive for the TL curves of a certain trap, it is independent of activation energy of the trap levels. In other words, whatever the β is used to obtain the TL curve, the activation energy associated with this curve should be constant. In TL theory, there are numerous calculation techniques for activation energy. Among these techniques, we used the best known two calculation methods. One of them can be applied to experimentally obtained TL glow peak by the following equation using several heating rates [90]

$$\ln\left(\frac{T_m^2}{\beta}\right) = \frac{E_t}{kT_m} + \ln\left(\frac{E_t}{sk}\right) \tag{2.27}$$

Plotting $\ln(T_m^2/\beta)$ versus $1000/T_m$ graph should give a straight line with a slope that allows us to evaluate E_t. The other method is also based on the same equation by

taking into consideration the idea as the following: Eq. (2.27) can be rearranged and rewritten in the form as below [90]

$$\beta = (sk/E_t)T_m^2 \exp(-E_t/kT_m) \, . \tag{2.28}$$

In this equation, T_m in exponential term contributes to the variation of luminescence process predominantly more than the T_m which is out of the exponent. Taking this under consideration, logarithmic plot of β as a function of reciprocal of T_m value presents a straight line which has a theoretical slope of $-E_t/k$.

2.7.5. Calculation of frequency factors and capture cross section

The frequency factor and capture cross section are important parameters that characterize the trapping properties of the defects. Frequency factor can be defined as the transition rates of the charge carriers from trap levels to free energy levels (conduction band) by the help of the enough external energy. Capture cross section shows the traps effectiveness to capture the untrapped charge carriers and related to effective area of the traps. These parameters can be determined by knowing the activation energy and T_m of the TL peak corresponding to trap levels. For this purpose, s value of the trapped charge carriers can be calculated according to the following expression [90]

$$s = \frac{\exp(t_m) \, t_m^3 \, \beta k}{(2b + t_m) \, E_t} \, , \quad \text{where} \quad t_m = \frac{E_t}{kT_m} \, . \tag{2.29}$$

Knowing the value of s, the capture cross section of the revealed traps can be determined using the expression [90]

$$S_t = \frac{s}{N_c \upsilon_{th}} \, . \tag{2.30}$$

30

CHAPTER 3

EXPERIMENTAL

3.1. Introduction

Characterization of defects existed in quaternary $Tl_2Ga_2S_3Se$, $TlGaSSe$, $Tl_2Ga_2Se_3S$, $Tl_4Ga_3InS_8$, Tl_2GaInS_4, $Tl_4In_3GaS_8$, ternary Ga_4S_3Se, Ga_2SSe and Ga_4Se_3S, and binary GaS and GaSe:Mn layered single crystals were studied through thermoluminescence measurements that are effective and mostly used experimental method to reveal the trap levels and determine the trapping parameters. Since defects in semiconductors cause the charge carriers excited into conduction band to be captured before recombination, they can be thought as luminescence centers. The trapped charge carriers due to defects need an external energy to be released from the traps. This can be achieved in different ways. One of them is the stimulation of trapped charge carriers by thermal energy (kT). If the given thermal energy is enough for charge carriers to escape from the traps, they are released to delocalized states and then recombine with opposite charges. Therefore, some luminescence is emitted related to concentration of released carriers. TL method is used for this purpose. The temperature of the studied material is increased systematically and emitted luminescence is recorded by a system. The experimental setup which is a building system for TL measurements and applied experimental TL methods are discussed in this chapter in detail.

3.2. Experimental setup for TL measurements

TL measurements were performed by increasing the temperature from 10 to 300 K to reveal the trap levels in the studied crystals using closed cycle helium gas cryostat which is enable to decrease the temperature of the environment approximately 9 K practically in laboratory conditions. The required experimental setup for TL measurements were assembled around the cryostat. The sample used for experiments was prepared properly (it was cleaned and attached to contact material which is suitable to place in the cryostat) to prevent the undesirable results that can influence the luminescence efficiency of the sample. After positioning the studied crystal in the cryostat, the pressure of the environment was diminished nearly to 10^{-3} Torr. Then, the temperature of the sample was decreased to starting temperature $T_0 = 10$ K from room temperature by managing the variation regularly by the help of the Lakeshore 331 temperature controller. The temperature of the sample was measured with a small semiconductor detector placed in the cryostat. The crystals were exposed to blue light (~470 nm) at 10 K to stimulate the charge carriers from valence band to conduction band for sufficient time for trap levels to be filled completely. Following the stopping, the crystals were heated up to 300 K with a definite heating rate, which can be adjusted up to 1.2 K/s using the temperature controller, to release the trapped charge carriers. Luminescence emitted due to recombination was directed to a photomultiplier (PM) tube (Hamamatsu R928; spectral response: 185 to 900 nm) by the aid of mirror and lenses connected to the quartz window of the cryostat. The PM tube delivered the pulses thanks to emitted luminescence to the Hamamatsu Photon Counting Unit C3866 (fast amplifier/discriminator) which was employed for converting the pulses from PM tube into transistor-transistor logic (TTL) pulses. Data acquisition module counter (National Instruments, NI-USB 6211) was operated for the purpose of counting the coming TTL pulses. The counted pulses were transferred to the personal computer which was also exploited to rule the whole experiment system with handled a software written in LabView^{TM} graphical development environment. Simple configuration of the experiment setup was shown in Fig. 3.1.
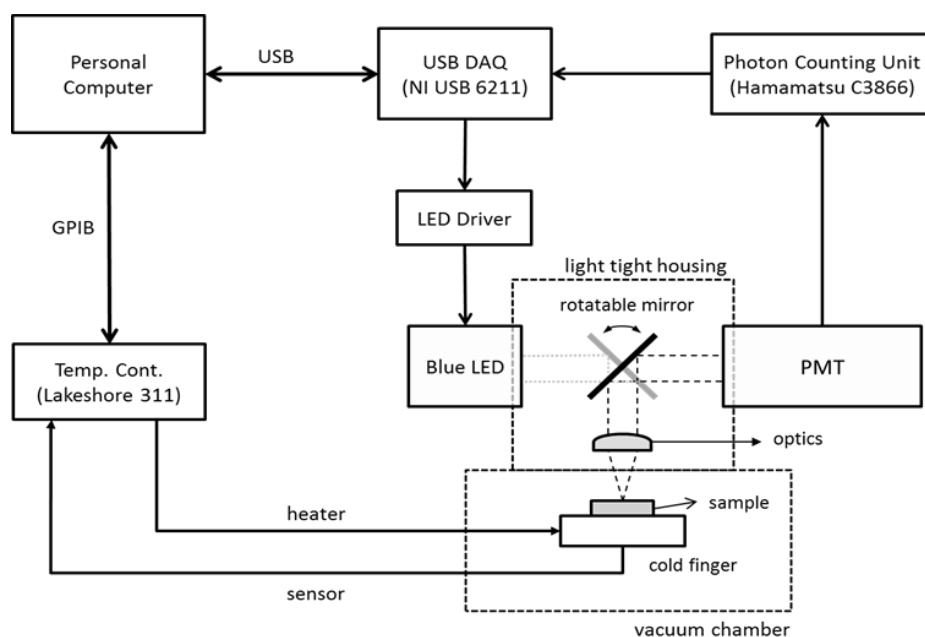
Fig. 3.1. Simple configuration of TL measurement system.

3.2.1. TL experiments for heating rate method

In order for investigation of heating rate dependencies of existed trap levels in the studied crystals, TL experiments have been carried out by taking account the advantage of availability in temperature controller to heat the samples at various rate. Accordingly, the studied samples were kept in an environment which the temperature was reduced to 10 K and they were illuminated with a light that energy is bigger than the band gap. Then, the temperature of the sample was gradually increased by step of the definite heating rate. In the study, each heating treatment for the crystals was completed for rates between the minimum rate of 0.2 K/s and the maximum rate of 1.2 K/s. Therefore, the resulted TL glow curves were recorded in a separate data sheet as a function of temperature variation to analyze and comprehend the behavior of the traps for different heating rates.
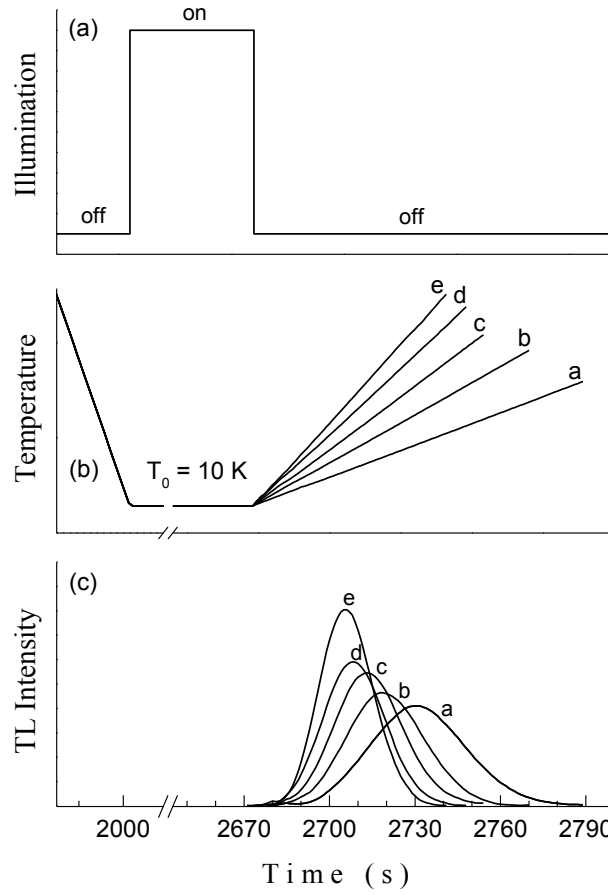
Fig. 3.2. Bases of TL measurements for $Tl_2Ga_2S_3Se$ crystal: (a) time period for stopping; (b) temperature alteration vs time; (c) TL curves observed with various heating rates between 0.4 (curve (a)) and 1.2 (curve (e)) K/s as a function of time [91].

Figure 3.2 illustrates the stopping process, temperature variation and TL intensities of the curves obtained for various heating rates ranging from 0.4 to 1.2 K/s as a function of time. As can be seen from the Fig. 3.2a, the decrease of the temperature to 10 K was taken about 2000 seconds. Then, the sample was illuminated for approximately 600 second that was enough for the studied crystal to fill the total concentration of the traps. Following the switching of the light, the sample was heated for rates between 0.4 and 1.2 K/s. Fig. 3.2b shows the temperature variation vs time

34

graph. As can be understood, higher heating rates (1.2 K/s, corresponding to (e)) leads to trapped charge carriers to be released from the trap levels faster. Therefore, for a definite time more charge carriers contributes to the TL emission as the stimulation of the traps was realized at higher heating rates (see Fig. 3.2c).

3.2.2. TL experiments for traps distributions

Characterization of revealed traps was continued with the investigation of the traps distribution. Understanding the exhibited traps' characteristics which is discrete, single level or the existence of overlapping many levels is important phenomenon for the semiconductor material. For this purpose, an experimental technique was implemented for the demonstrated trap levels in the crystals. As explained in the previous section, TL measurements were being carried out by decreasing the temperature to $T_0 = 10$ K and heating the sample up to room temperature with a constant rate. In this case, the sample being kept at $T_0 = 10$ K is heated up to a definite temperature called as stopping temperature (T_{stop}) using the temperature controller. Then, the temperature is kept constant at T_{stop} value until the measurement system and the sample get equilibrium. The stopping of the sample is followed out at this temperature for the same time (600 sec.) with the previous experiments. After the light is switched off, the temperature is diminished again to starting value. Thus, TL spectra is recorded with a constant heating rate in the temperature range of 10-300 K. By this way, since the stopping is performed at T_{stop} value, shallower levels cannot be allowed capturing the free charge carriers and the contribution to TL spectra comes from the deeper levels. The same process is maintained with higher T_{stop} values until the trap levels is fully emptied. As a result of this successive method, one can experience with two different cases for TL curves recorded with different cleaning temperatures. One of them is that the ascending part of the TL peak shifts to higher temperatures whereas the descending part of the TL peak keep its position except for decreasing intensity. This situation is generally observed for continuum case of traps. The other situation is encountered for single trap and the initial and latest tails do not change in position. Only alteration seems in

TL intensity. As the T_{stop} value is increased, intensity of the TL peak tends to decrease prominently while the peak maxima keep constant.

3.3 Energy dispersive spectral analysis

Energy dispersive spectroscopic analysis (EDSA) experiment is used to determine the chemical composition of the materials by differentiating the abundance of individual elements in the materials. We used this experimental method to find the concentrations of each constituent elements in Ga_4S_3Se, Ga_2SSe and Ga_4Se_3S single crystals. JSM-6400 scanning electron microscope (SEM) was employed for EDSA measurements. "Noran System6 X-ray microanalysis system" and "Semafore Digitizer" were integrated to the microscope to be utilized for the analysis of experimental data. Figure 3.3 depicts the simple diagram for EDSA system building around the SEM.
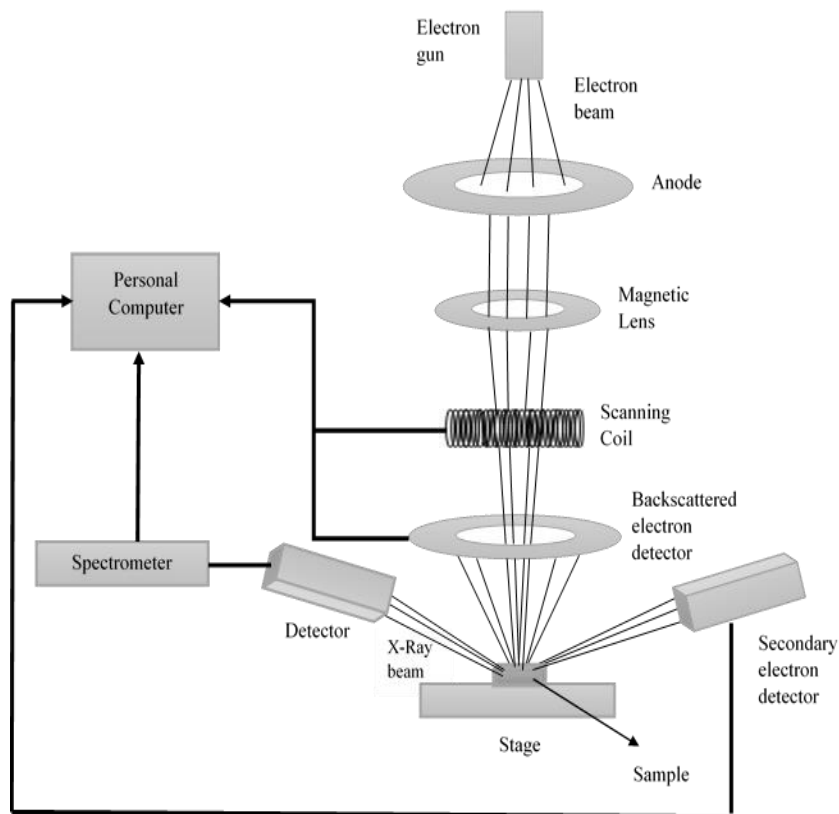
Fig. 3.3. Schematic configuration of EDSA experiment system.

Typically, the SEM is used to get knowledge about either the surface characterization or the elemental composition of the samples. As the electron beam hit the sample, one can observe three different signals coming from backscattered electrons, secondary electrons and X-ray beam. EDSA experiment is related to X-ray beam emitted from the sample due to the interaction between primary electrons with the atomic shells. The created characteristic X-ray beams of the elements are directed to the EDS detector that converts the individual beam into the electrical pulses. These pulses are converted to voltage pulses which correspond to energies of the elemental X-ray beams.

CHAPTER 4

RESULTS AND DISCUSSIONS

4.1. Introduction

Thermoluminescence is effective experimental method consistent with the known theoretical information to determine and characterize the defects in the semiconductor lattice structure. The TL experimental observations and the analysis outcomes for the studied crystals are given throughout this chapter. Activation energies, capture cross sections and frequency factors of the trapping levels in the crystals are presented using various analysis techniques. Heating rate behaviors of the trap levels are demonstrated for the studied crystals. Traps distribution is also a subject of this chapter. The discussions about the analysis results are given clearly by taking into account the TL theory.

4.2. Results of TL studies on $Tl_2Ga_2S_3Se$, $TlGaSSe$ and $Tl_2Ga_2Se_3S$ single crystals

4.2.1. Determination of activation energies, frequency factors and capture cross sections

TL peaks of $Tl_2Ga_2S_3Se$, $TlGaSSe$ and $Tl_2Ga_2Se_3S$ single crystals were observed between 10 and 100 K, 10 and 180 K, and 10 and 80 K temperature regions, respectively, by heating the samples with a rate $\beta = 1.0$ K/s. Although the experiments were achieved between 10 and 300 K, rests of the recorded TL spectra of the crystals were not indicated in the presented figures since no peak was observed out of the

shown temperature interval. The CF method applied by means of equations (2.17) and (2.23) was used to compute the activation energies, frequency factors and capture cross sections of $Tl_2Ga_2S_3Se$, TlGaSSe and $Tl_2Ga_2Se_3S$ crystals. Figure 4.1 shows the experimental TL peak with a maximum temperature (T_m) of 47 K and theoretical curve fit applied for $Tl_2Ga_2S_3Se$ crystal. Application of Eq. (2.17) did not give successful fitting result. Therefore, we realized the CF analysis with the help of Eq. (2.23) by gradually altering the parameter b between the ranges 1 and 2. The most prosperous result was attained for $b = 1.2$. This value stated that general order of kinetics dominated the trapping mechanism. Activation energy of trapping center in $Tl_2Ga_2S_3Se$ single crystal was found as 16 meV using this successful method [91].
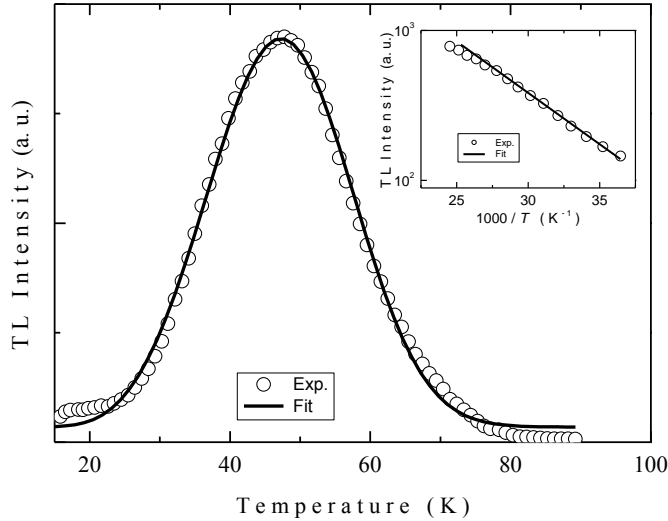
Figure 4.1. Experimentally detected TL peak (circles) of $Tl_2Ga_2S_3Se$ crystal using $\beta = 1.0$ K/s and theoretical curve fit (solid peak). Inset: TL intensity versus $1000/T$. Circles and line exemplify the experimental data and the fitted line, respectively.

Figure 4.2 shows the experimentally observed TL peaks of TlGaSSe crystal labeled as peak A and peak B and their theoretical fits. As shown from the figure, the TL peaks reach maximum intensities at $T_{mA} = 39$ K and $T_{mB} = 131$ K. Since peaks A

and B appeared independently from each other, we had a chance to analyze each peak separately. Implementation of CF method for peak A was achieved using Eq. (2.20) corresponding to parameter $b = 2$. This value was a strong evidence for the trap level to be attributed to the presence of second order of kinetics. Thermal activation energy for trapping level correlated to peak A was evaluated as $E_{tA} = 16$ meV [92]. Eq. (2.23) gave reliable result for peak B as seen in the figure. The parameter b was found as 1.2 that demonstrates the trap level corresponding to peak B exhibits the physical properties of general order kinetics. Further, the existence of trap level was revealed with the value $E_{tB} = 97$ meV (see Table 4.1).
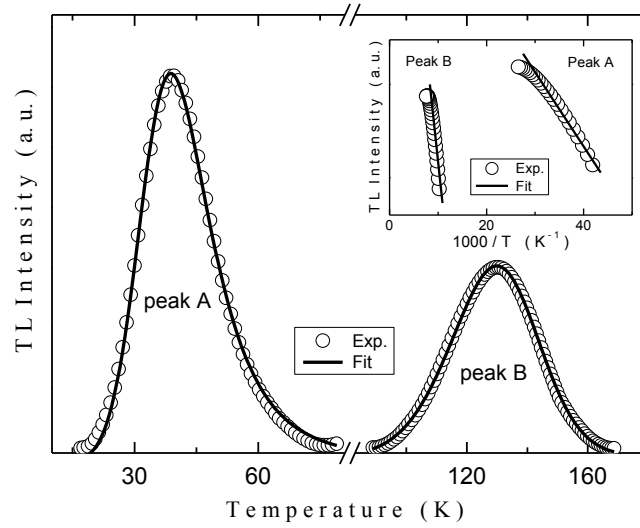
Figure 4.2. Experimentally detected TL peaks (circles) of TlGaSSe crystal using $\beta = 1.0$ K/s and theoretical curve fits (solid peak). Inset: TL intensity versus $1000/T$. Circles and lines exemplify the experimental data and the fitted lines, respectively.

TL experiments of $Tl_2Ga_2Se_3S$ layered single crystals performed at low temperatures and with heating rate 1.0 K/s provided one TL peak appearing around $T_m = 36$ K as seen in Fig. 4.3. The curve fitting analysis of recorded TL peak suggested one trapping center with activation energy of $E_t = 13$ meV found from the application of Eq. (2.23) [93]. Mixed order of kinetics was ascribed to trap level through the calculated parameter of $b = 1.4$.
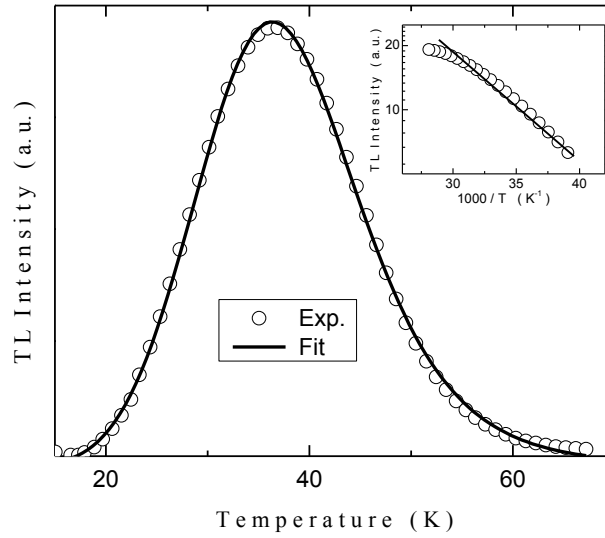
Figure 4.3. Experimentally detected TL peak (circles) of Tl$_2$Ga$_2$Se$_3$S crystal using $\beta = 1.0$ K/s and theoretical curve fit (solid peak). Inset: TL intensity versus 1000/T. Circles and line exemplify the experimental data and the fitted line, respectively.

Table 4.1. The calculated E_t, S_t and s values of established traps in TlGaSSe crystal.

T_m (K)	E_t (meV)			S_t (cm^2)	s (s^{-1})
	Curve fitting method	Initial rise method	Peak shape method		
39	16	16	17	6.6×10^{-24}	14,3
131	97	97	101	1.4×10^{-23}	353,8

The computed activation energies for trap levels obtained in Tl$_2$Ga$_2$S$_3$Se, TlGaSSe and Tl$_2$Ga$_2$Se$_3$S single crystals were utilized to calculate the frequency factors and the capture cross sections of the trapping levels in the crystals using Eqs. (2.29) and (2.30), respectively. As a result of the analyses, The s and S_t values were found as 2.9 s^{-1} and 1.6×10^{-24} cm^2 for Tl$_2$Ga$_2$S$_3$Se, 14.3 and 353.8 s^{-1}, and 6.6×10^{-24} and 1.4×10^{-23} cm^2 for peaks A and B related to traps in TlGaSSe, 8.7 s^{-1} and

4.3×10^{-24} cm^2 for Tl$_2$Ga$_2$Se$_3$S, respectively. The capture cross sections of the trap centers were calculated at the hands of the effective masses of $m_e^* = 0.25m_0$, $m_h^* = 0.44m_0$ and $m_h^* = 0.48m_0$ for Tl$_2$Ga$_2$S$_3$Se, TlGaSSe and Tl$_2$Ga$_2$Se$_3$S, respectively. Since the trap levels observed at shallower energy states activated at low temperatures, s values were found to be too small than the physically expected value. Examples of such a similar behavior were shown in the ternary compounds (TlGaS$_2$, TlGaSe$_2$, and TlInS2) and Zn$_{1-x}$Cd$_x$O alloy films [94, 95].

Secondly, IR method that is independent of kinetics' order was taken under consideration to get the activation energies of revealed traps in Tl$_2$Ga$_2$S$_3$Se, TlGaSSe and Tl$_2$Ga$_2$Se$_3$S single crystals. For this purpose, logarithmic plots of TL intensities versus inverse of recorded temperature were indicated in the insets of Figs. 4.1, 4.2 and 4.3. As seen in the graphs, such a plots of TL intensities result with a straight line that the slopes give a value of $(-E_t/k)$. Insets demonstrate the experimentally obtained straight lines (circles) and linear fits (lines). Consequently, the E_t values of trap levels were obtained as 16 meV for Tl$_2$Ga$_2$S$_3$Se, 16 and 97 meV for TlGaSSe, and 13 meV for Tl$_2$Ga$_2$Se$_3$S, respectively. These values coincide with those found by CF method.

PS method was implemented to experimental TL curves in order to compute the thermal activation energies of trapping levels. Application of this method gave the activation energies as 18 meV for Tl$_2$Ga$_2$S$_3$Se, 17 and 101 meV for TlGaSSe and 14 meV for Tl$_2$Ga$_2$Se$_3$S, respectively. Moreover, in our studies on Tl$_2$Ga$_2$S$_3$Se, TlGaSSe and Tl$_2$Ga$_2$Se$_3$S crystals, the calculated values of μ_g were approximately equal to 0.48 for Tl$_2$Ga$_2$S$_3$Se, 0.52 and 0.44 for TlGaSSe and 0.48 for Tl$_2$Ga$_2$Se$_3$S, respectively. These values indicated that kinetics order for the obtained trap levels differ from the first order. The outcomes of this method conformed to the curve fitting and initial rise analysis results.

Thermal activation energy of defect centers could be calculated through variable heating rate technique. To this end, the Eq. (2.27) was taken into consideration and plotting $\ln(T_m^2/\beta)$ versus $1000/T_m$ graph gave a straight line using different β values and related T_m values of the experimental TL curves of Tl$_2$Ga$_2$Se$_3$S crystals. The activation energy of trap level was found as 6 meV from the slope (see

Fig. 4.4). This energy value was not consistent with those obtained by other analysis techniques. Therefore, we thought that the T_m's of the experimental TL peaks showed some deviation owing to the phenomenon known as temperature lag effect that creates greater deflection at bigger heating rates [96-98].
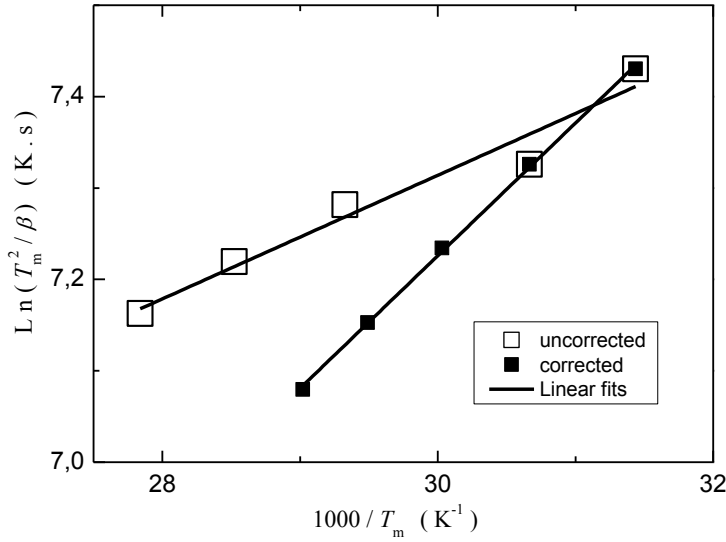
Figure 4.4. $\ln(T_m^2/\beta)$ vs. $1000/T_m$ plot for $Tl_2Ga_2Se_3S$ crystals. Open and black squares are experimental and theoretical data, respectively. Solid lines are the fitted lines.

Since the left hand side of the Eq. (2.27) was strongly affected by T_m, determining the real temperature of the sample is crucial for application of heating rate method to calculate activation energy. Overtly, for TL measurement, the sample is attached to a holder in the cryostat and heated with definite rate by temperature controller, which have an interaction with the sample holder. Therefore, the TL spectra is recorded as a response to the heater temperature. However, sample and recorded temperatures may not simultaneously conform with each other as the heating process is applied due to some reasons such as inappropriate contact of sample to holder, thermal gradient all along the sample, and/or thermal gradient between the heating strip and temperature controller. Those of some expectable cases lead to temperature deviation

44

on detected TL curves. Such a dissonance in temperatures is known as lag effect. In order to prevent incorrect calculations due to temperature difference, a method improved by Kitis and Tuyn [99] can be utilized to compute the activation energy of defect centers accurately by means of the following equation

$$T_{\mathrm{mj}} = T_{\mathrm{mi}} - c \ ln\left(\frac{\beta_{\mathrm{i}}}{\beta_{\mathrm{j}}}\right) \tag{4.1}$$

Here, T_{mi} and T_{mj} are peak maximum temperatures that corresponds to linear heating rates β_{i} and β_{j}, respectively. c presents a constant value. We applied equation (4.1) to compute the constant c using the lower rates $\beta = 0.6$ and $\beta = 0.7$ K/s and it was found as 5.19. The corrected T_{m} values associated with heating rates 0.8, 0.9 and 1.0 K/s were computed with the same equation. Therefore, thermal activation energy was obtained as 13 meV for the trapping center from the slope of $\ln(T_{\mathrm{m}}^2/\beta)$ versus $1000/T_{\mathrm{m}}$ graph depicted by corrected T_{m} values [92]. This energy value was correlated with the found values by other applied methods.

4.2.2. Heating rate dependencies of trap levels in Tl$_2$Ga$_2$S$_3$Se, TlGaSSe and Tl$_2$Ga$_2$Se$_3$S crystals

Heating rate dependencies of TL glow curves obtained for Tl$_2$Ga$_2$S$_3$Se, TlGaSSe and Tl$_2$Ga$_2$Se$_3$S crystals were investigated performing the TL experiments with varied heating rates. Figure 4.5 illustrates the TL peaks of Tl$_2$Ga$_2$S$_3$Se detected by employing the rates of heating varying from 0.4 to 1.2 K/s. On the strength of TL theory, change of heating rates culminate in alteration of location and structure of TL peak [90]. As can be noticed from Fig. 4.5, TL intensity decreases and its T_{m} value moves to higher temperatures with raising heating rate. The integral of the TL spectra is commensurate with initial trap concentration. In the heating rate dependence, it was observed that area (S_0) of the spectra decreases when the heating rate is elevated (see inset of Fig. 4.5). This is an evidence of thermal quenching of luminescence caused by increasing the probability of non-radiative transitions as the temperature

increases [100-102]. Some explanations for shifting tendency of T_m values of TL curve to higher temperatures were stated in a TL study on lithium magnesium borate phosphors by Anishia et al. [103]. Assuming a small heating rate is employed for stimulation of trapped charge carriers, someone detects a TL peak possessing a value of T_{m1}.
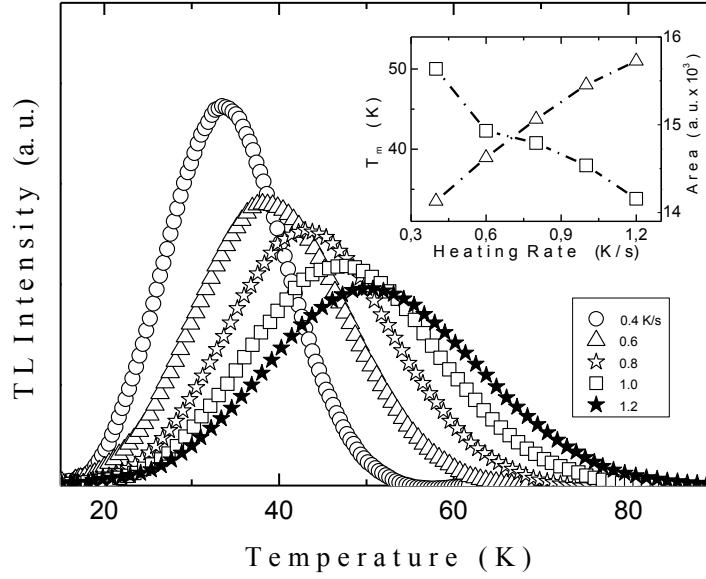
Figure 4.5. Experimentally detected TL peak of Tl$_2$Ga$_2$S$_3$Se crystal with varied β values. Inset: T_m (triangles) and area (squares) dependencies on heating rate.

If charge carriers occupying traps are excited with bigger heating rate β_2, the trapped carriers recombine with opposite ones more quickly. Thus, the number of releasing carriers stimulated at T_1 temperature diminishes as the heating mechanism was operated with β_2. The same number of released carriers can merely be reached at T_2 temperature ($T_2 > T_1$) when the β_2 is applied for stimulation. Therefore, the T_m value of new glow peak (T_{m2}) moves to higher temperatures. Moreover, the full width half maximum (FWHM) of the TL curve expand from 16 to 28 K with varying β from 0.4 to 1.2 K/s (see inset of Fig. 4.5). However, the asymmetry of the TL spectra is nearly

conserved as proved by the calculation of geometry factors for each spectrum around 0.48.

Figure 4.6 depicts the TL curves of TlGaSSe, denominated as peak A and peak B, detected with varied rates of heating ranging from 0.5 to 1.0 K/s. It is clear from the figure that the TL intensities tend to decrease and T_m values have gradual increment with elevating heating rate. Figure 4.7 shows the dependence of T_m, FWHM and integral of the curves to the heating rate. The T_m and FWHM values of the curves alter from 31 to 39 K and 12 to 19 K for peak A and vary from 95 to 131 K and 32 to 37 K for peak B.
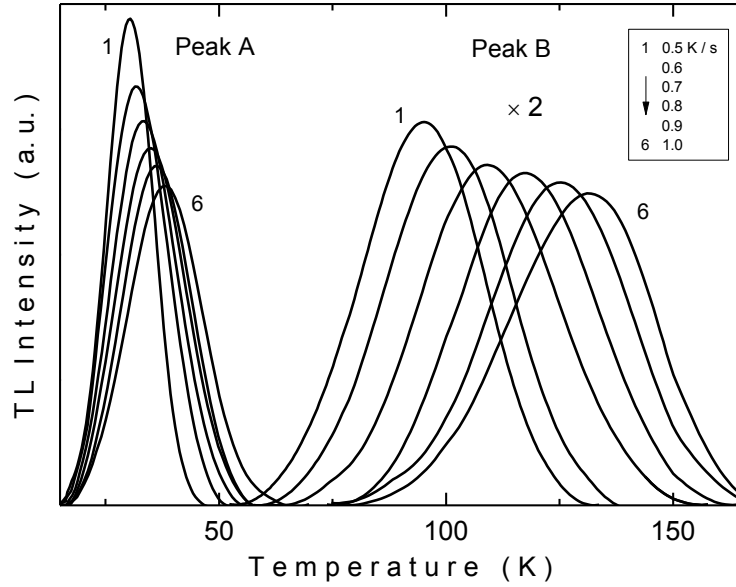
Figure 4.6. Experimentally detected TL peaks of TlGaSSe crystal with varied β values.

The integrals of the peaks stand for the charge carrier liberated from traps during each measurement. Since same amount of charge carriers are released unless the stopping time is changed, the integral of each curve must be constant. Thus, in order to conserve the same area value for the peaks the FWHM value must increase gradually as the peak intensity diminishes. Figure 4.7 illustrates analogous variation of the peak

areas. As seen, the areas are very close to each other with some slight experimental variations.
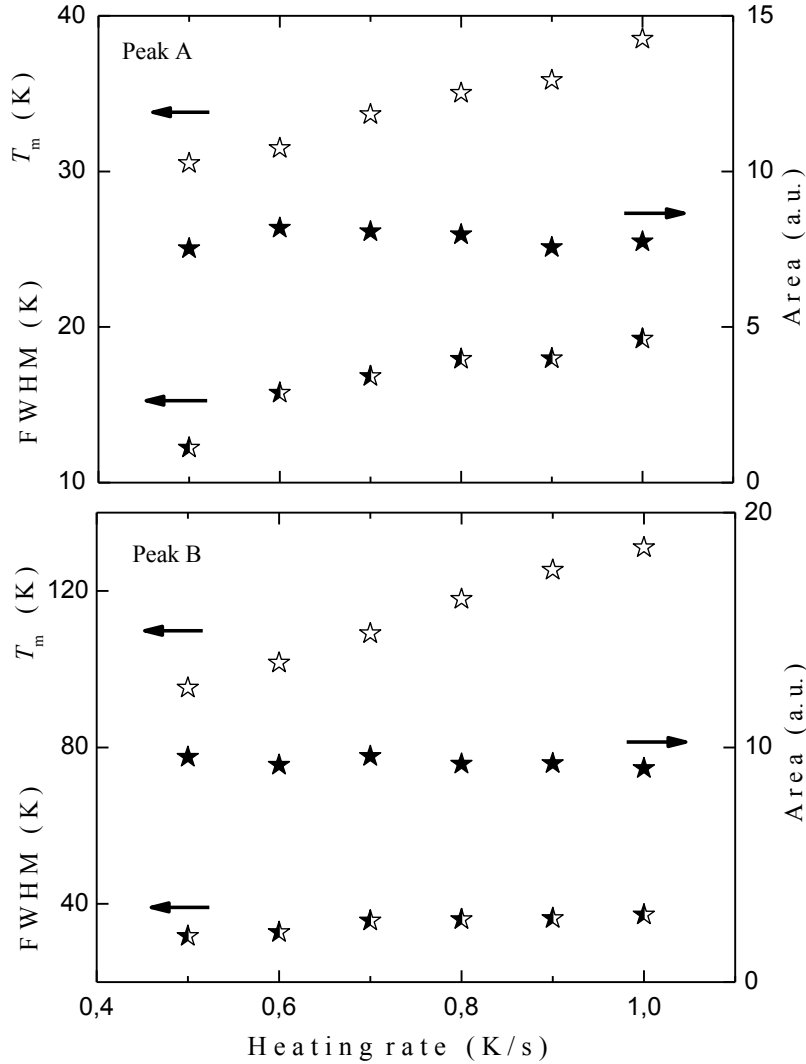
Figure 4.7. T_m, FWHM and area (S_0) dependencies on heating rate for TlGaSSe crystal (peaks A and B).

Figure 4.8 depicts the dependence of heating rate on TL curve of $Tl_2Ga_2Se_3S$ crystals. The exhibited glow curves were observed by heating the sample for different rates changing from 0.6 to 1.0 K/s. Inset of Fig. 4.8 demonstrates the variation of T_m,

FWHM and the area of the curves. Increasing tendency of the T_m and FWHM was noted with the values from 32 to 36 K and 17 to 23 K, respectively. Moreover, S_0 value of the peaks remains nearly same with slight variations.
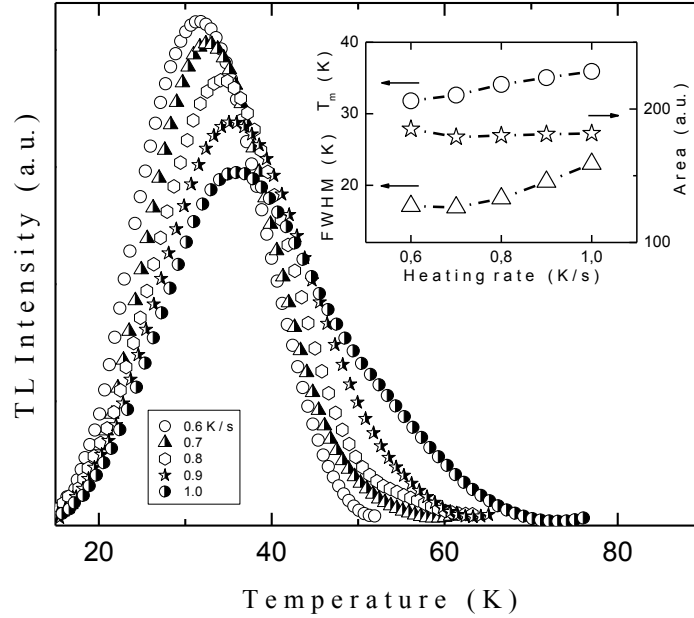
Figure 4.8. Experimentally detected TL peaks of $Tl_2Ga_2Se_3S$ crystal with varied β values. Inset: T_m, FWHM and area (S_0) dependencies on heating rate for TlGaSSe crystal.

4.2.3. Distribution of trap levels in $Tl_2Ga_2S_3Se$, TlGaSSe and $Tl_2Ga_2Se_3S$ crystals

The defect centers revealed in the studied crystals can possess different trap characteristics due to some reasons regarding growth process and/or natural formation of the traps. It is known from the theory that the crystals either exist the single, isolated discrete trap level or they compose of the many trapping levels that are very close to each other. Thermoluminescence mechanisms of such traps show diversity and kinetic parameters of these traps should be dealt with disparately. Thus, understanding the trap mechanism of the studied crystal gain importance. To investigate the trap's distribution of $Tl_2Ga_2S_3Se$, TlGaSSe and $Tl_2Ga_2Se_3S$ crystals, T_{stop} method was applied to the observed glow curves of the crystals with a rate of

49

heating $\beta = 1.0$ K/s. Figure 4.9 shows TL peaks detected at different T_{stop} values (10 to 25 K). As understood from the figure, TL intensity diminishes gradually and T_m of the peaks shifts to higher temperatures. This behavior can be explained with the fact that the concentration of charge carriers diminishes with increasing T_{stop}.
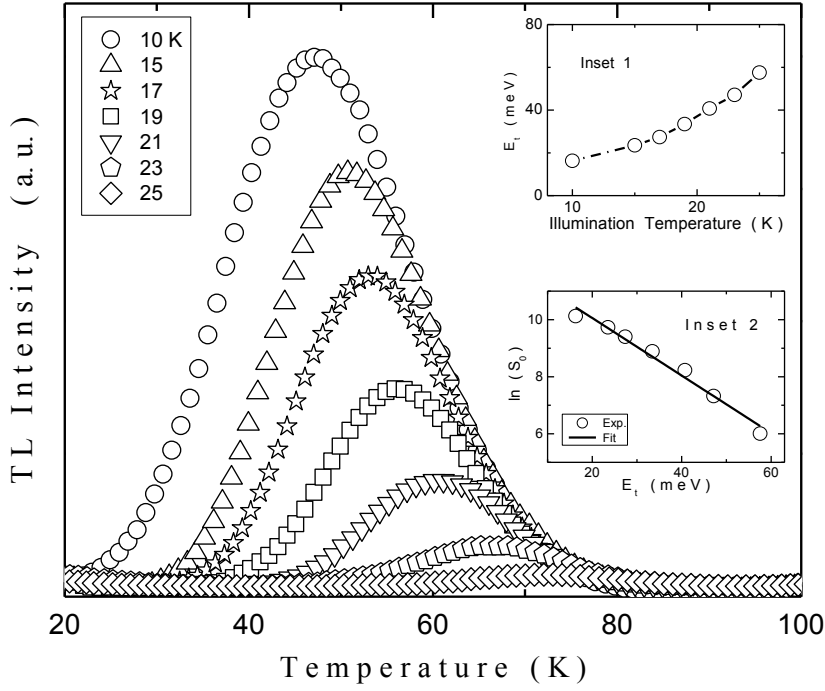
Figure 4.9. Experimentally detected TL peaks of Tl$_2$Ga$_2$S$_3$Se crystal with different T_{stop} values. Inset 1: E_t vs. T_{stop} plot. Inset 2: Logarithmic plot of S_0 as a function of E_t. Solid line is the fitted line.

In other words, shallower trapping levels are emptied and the contribution to luminescence comes from the deeper levels. The E_t values for each glow peak were found to be rising from 16 to 58 meV when the T_{stop} is increased from 10 to 25 K, respectively (inset 1 of Fig. 4.9). The frequency factors for each glow peak were taken into account to understand its dependency of temperature. It was found that shifting T_m to high temperature leads to increase in s values.

Table 4.2. The obtained T_m, S_0, E_t and s values for $Tl_2Ga_2S_3Se$ crystal at different T_{stop}.

Curve	1	2	3	4	5	6	7
T_{stop} (K)	10	15	17	19	21	23	25
T_m (K)	47.8	50.7	53.0	55.9	61.1	65.2	73.0
S_0 (a.u.)	24940	16880	12130	7250	3760	1520	410
E_t (meV)	16	24	27	33	41	47	58
s (s^{-1})	2.9	16.0	32.4	95.4	220	441	931
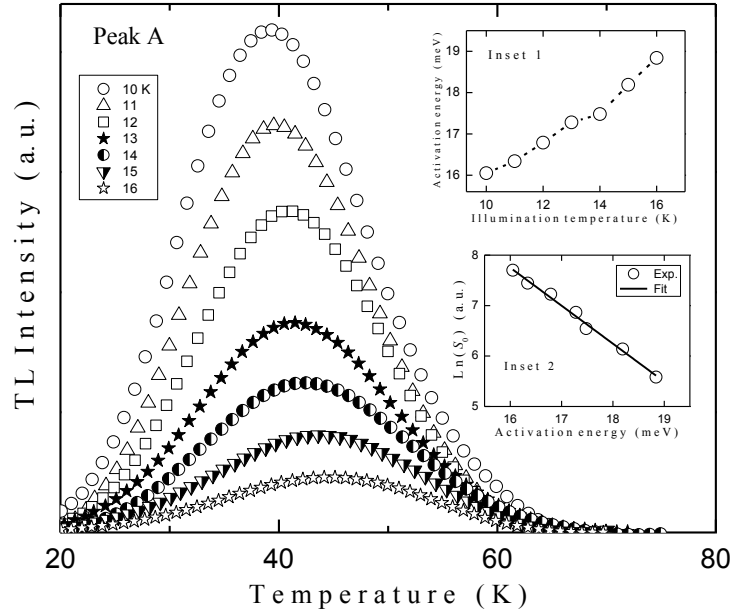
Figure 4.10. Experimentally detected TL peaks of TlGaSSe crystal with different T_{stop} values (peak A). Inset 1: E_t vs. T_{stop} plot. Inset 2: Logarithmic plot of S_0 as a function of E_t.

Figures 4.10 and 4.11 represent the TL glow curves of TlGaSSe crystals (peaks A and B) at different T_{stop} ranging from 10 to 16 K and from 35 to 50 K, respectively. Similar to $Tl_2Ga_2S_3Se$ crystals, intensities of the glow peaks (A and B)

51

decreased proportionally with the emptied concentration of trap center and increment in T_m was experienced by employing varied T_{stop} values (see Table 4.3). Insets 1 of Figs. 4.10 and 4.11 produce the thermal activation energies of liberated carriers corresponding to utilized T_{stop} values. As seen from the inset 1 of the figures, the activation energies increased from 16 to 27 meV and 97 to 146 meV for peaks A and B with increasing T_{stop}, respectively.
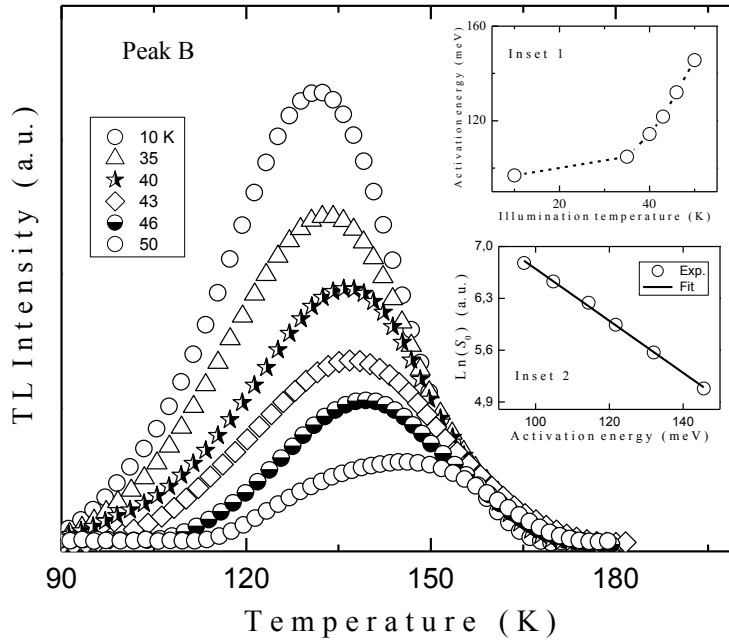
Figure 4.11. Experimentally detected TL peaks of TlGaSSe crystal with different T_{stop} values (peak B). Inset 1: E_t vs. T_{stop} plot. Inset 2: Logarithmic plot of S_0 as a function of E_t.

TL glow curves of $Tl_2Ga_2Se_3S$ crystal detected with different stopping temperatures (10 to 15 K) were shown in Fig. 4.12. It is easily noticed from the figure that increasing T_{stop} ensured the luminescence intensity to be decreased and peak maximum temperature to be shifted gradually. E_t values were shown in the inset 1 of Fig. 4.12. Energy values raised from 13 to 18 meV with increasing T_{stop} from 10 to 15 K (Table 4.4).
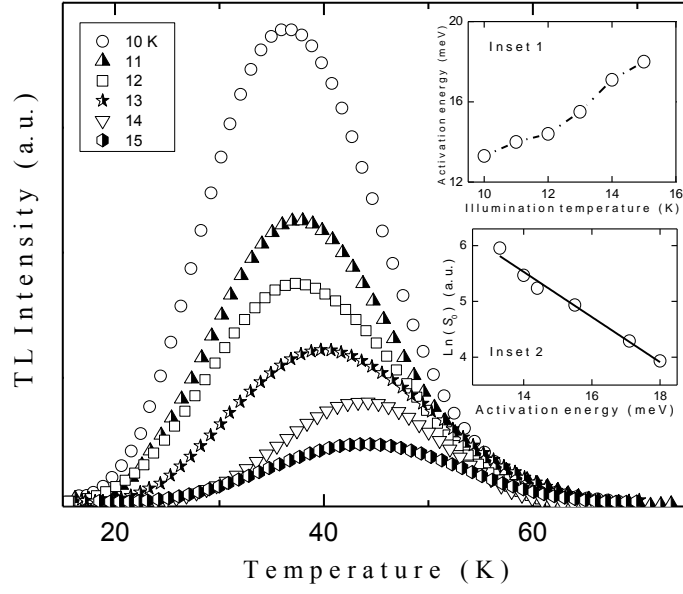
Figure 4.12. Experimentally detected TL peaks of $Tl_2Ga_2Se_3S$ crystal with different T_{stop} values. Inset 1: E_t vs. T_{stop} plot. Inset 2: Logarithmic plot of S_0 as a function of E_t.

Table 4.3. The obtained T_m, S_0, E_t and s values for TlGaSSe crystal at different T_{stop} (peaks A and B).

	Peak A						Peak B				
Curve	1	2	3	4	5	6	1	2	3	4	5
T_{stop} (K)	11	12	13	14	15	16	35	40	43	46	50
T_m (K)	40	41	42	43	44	45	133	136	138	140	145
S_0 (a.u.)	1711	1375	959	696	464	266	685	513	381	262	161
E_t (meV)	17	19	20	22	24	27	105	114	122	132	146
s (s^{-1})	17.1	28.4	33.1	52.3	80.8	165.5	6.6×10^2	1.2×10^3	2.1×10^3	4.4×10^3	9.6×10^3

The reason of increment of activation energy by rising stopping temperature depends on the charge carriers occupying deeper levels. Much more thermal energy is needed for stimulation of the carriers at deeper centers [86,90,104]. The analogous behavior was ascribed to the quasi-continuous traps distribution [105-107].

Table 4.4. The obtained T_m, S_0, E_t and s values for $Tl_2Ga_2Se_3S$ crystal at different T_{stop}.

Curve	1	2	3	4	5	6
T_{stop} (K)	10	11	12	13	14	15
T_m (K)	36	38	38	40	44	45
S_0 (a.u.)	385	240	190	140	75	50
E_t (meV)	13.3	14.0	14.4	15.5	17.1	18.0
s (s^{-1})	8.7	8.1	9.4	10.1	9.3	10.7

The detailed characterization of traps distribution was achieved by assuming exponential distribution for the trap center. By this way, the density of trap is considered as proportional to the E_t values of glow peaks in Figs. 4.9−4.12. Therefore, the density of traps can be presented as

$$N_{ti} = A \exp(- \alpha E_{ti}). \tag{4.2}$$

The area under the peaks are proportional to the density of traps. Then the Eq. (4.2) equation can be rewritten as [105]

$$S_0 \propto A \exp(-\alpha E_{ti}). \tag{4.3}$$

In the Eq. (4.3), α is a parameter related to energy and characterizes the distribution. Logarithmic plot of S_0 as a function of E_t bring out straight line with a slope of α. The insets 2 of Figs. 4.9−4.12 show the analogous graphs. The slopes were found as $\alpha = 0.10$ meV^{-1} for Tl$_2$Ga$_2$S$_3$Se, $\alpha_A = 0.191$ and $\alpha_B = 0.035$ meV^{-1} for TlGaSSe and $\alpha = 0.41$ meV^{-1} for Tl$_2$Ga$_2$Se$_3$S crystals. These values imply that 23 meV for Tl$_2$Ga$_2$S$_3$Se, 12 and 66 meV for peaks A and B of TlGaSSe, and 6 meV for Tl$_2$Ga$_2$Se$_3$S vary with the alteration of one order of magnitude.

4.3. Results of TL studies on Tl$_4$Ga$_3$InS$_8$, Tl$_2$GaInS$_4$ and Tl$_4$In$_3$GaS$_8$ single crystals

4.3.1. Determination of activation energies, frequency factors and capture cross sections

Figure 4.13(a) reproduces TL spectrum of Tl$_4$Ga$_3$InS$_8$ crystal obtained in the temperature range of 10-200 K for $\beta =1.0$ K/s. Since no intensive peak was observed in the range of 200-300 K, the measured spectrum in that range are not displayed in the figure. As can be seen from the Fig. 4.13(a), there exist two distinctive peaks arising nearly at peak maximum temperatures of 60 and 165 K. Moreover, the existence of one faint peak nearly at $T_m = 100$ K can be detected from the spectrum. Before starting the analysis (especially by curve fitting method) of the experimental data, the determination of the number of peaks arising due to different defect centers is first and important way. We have used the thermally cleaning procedure to separate overlapped peaks. The obtained glow curve using this method for $T_{stop} = 42$ K has been shown in Fig. 4.13(b). The existence of the trap level B, which is not clear in the main TL curve (see Figure 4.13(a)), is verified by this method.
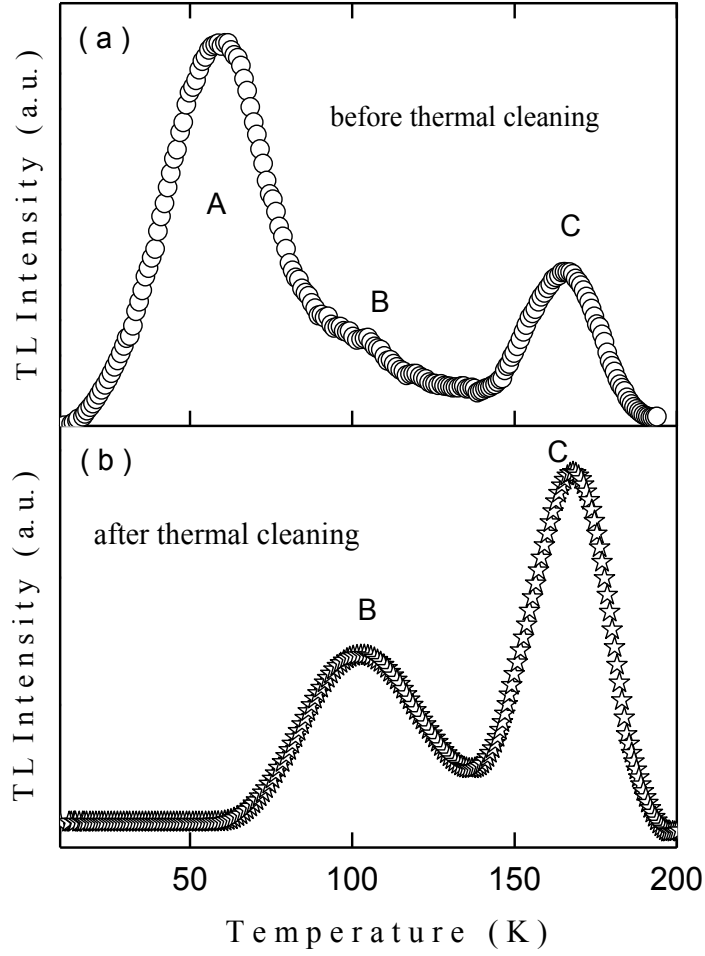
Figure 4.13. Experimentally detected TL curves of Tl$_4$Ga$_3$InS$_8$ crystal using $\beta = 1.0$ K/s. (a) and (b) present the TL curves recorded before and after thermal cleaning, respectively.

In Figure 4.14, solid curve expresses the theoretical fit of the experimental data for Tl$_4$Ga$_3$InS$_8$ obtained from CF method. The curve fitting analysis in accordance with Eq. (2.17) successfully revealed the presence of three trapping centers with energies of $E_{tA} = 13$, $E_{tB} = 44$ and $E_{tC} = 208$ meV (see Table 4.5) [108].

The dashed-dot curves in Fig. 4.14 under the main curve represent the decomposed peaks related with each defect center.

Table 4.5. The calculated E_t, S_t and s values of established traps in $Tl_4Ga_3InS_8$ crystal.

Peak	T_m (K)	E_t (meV)			S_t (cm^2)	s (s^{-1})
		Curve fitting method	Initial rise method	Peak shape method		
A	58	13	13	16	2.9×10^{-25}	0.5
B	103	44	44	--	9.4×10^{-25}	8.4
C	166	208	--	204	9.6×10^{-21}	2.0×10^5
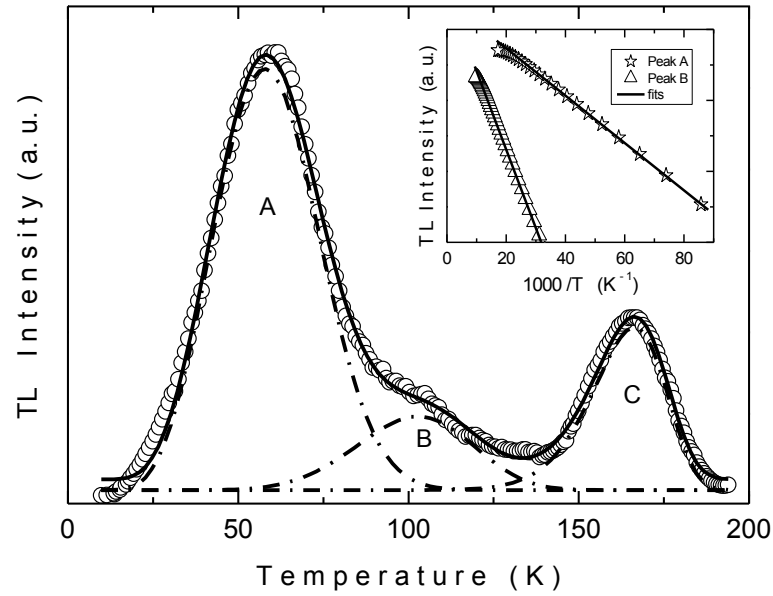
Figure 4.14. Experimentally detected TL curve (circles) of $Tl_4Ga_3InS_8$ crystal using $\beta = 1.0$ K/s and theoretical curve fit (solid curve). Dash-dotted peaks are decomposition of solid curve. Inset: TL intensity versus 1000/T for peaks A and B. Stars (peak A), triangles (peak B) and solid lines exemplify the experimental data and the fitted lines, respectively.

57

TL experiments performed for Tl$_2$GaInS$_4$ with heating rate of 1.0 K/s resulted with two successive peaks (A and B) with T_m values of 34 and 55 K as seen in Fig. 4.15. First order approach to the TL curve by virtue of Eq. (2.17) did not provided the compatible fitted curve with the observed TL curve. Implementation of Eq. (2.23) was necessary to fit the experimental curve well. Thus, the glow curve was subjected to Eq. (2.23) by regularly altering the parameter b until the well describing fitting curve was succeeded. By this way, the presence of two trap centers in the forbidden energy level of Tl$_2$GaInS$_4$ crystal was established with thermal activation energies of $E_{tA} = 12$ and $E_{tB} = 26$ meV as the parameters $b_A = 1.0$ and $b_B = 1.6$ were employed for peaks A and B, respectively (see Table 4.11) [109]. The first and general order kinetics were proved with this successful method for the peaks A and B respectively.
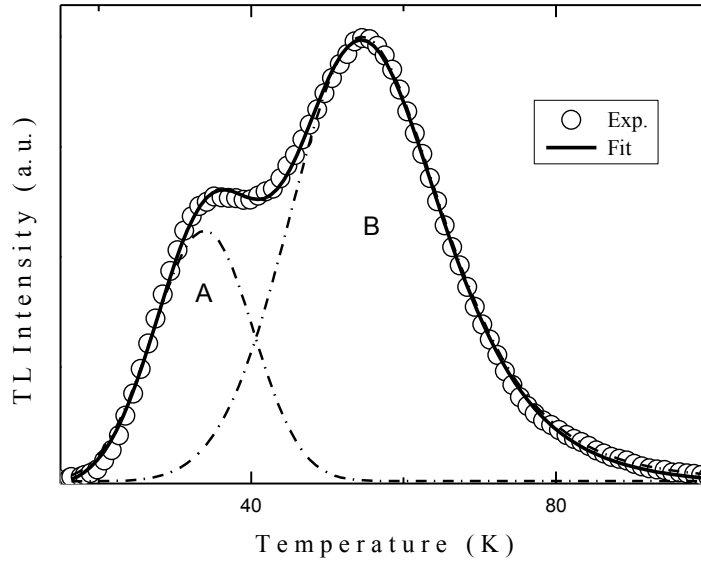
Figure 4.15. Experimentally detected TL curve (circles) of Tl$_2$InGaS$_4$ crystal using $\beta = 1.0$ K/s and theoretical curve fit (solid curve). Dash-dotted peaks are decomposition of solid curve.

Thermally cleaning procedure using T_{stop} = 26 K which was enough to clean the shallower traps related to peak A of Tl$_2$InGaS$_4$ crystal allowed peak B to appear separately from peak A as demonstrated in Fig. 4.16. The small shift of the T_m value of glow curve obtained after thermal cleaning process arises due to the closeness of the two trap levels (related to peaks A and B). This shift can considered as be negligible. After cleaning the initial part of the TL spectra, the successively obtained TL glow peak (peak B) was analyzed using CF method (by equation (2.23) with parameter b = 1.6). Application of the method revealed the existence of the trapping center correlated to peak B with E_{tB} = 27 meV (see inset 1 of Fig. 4.16).
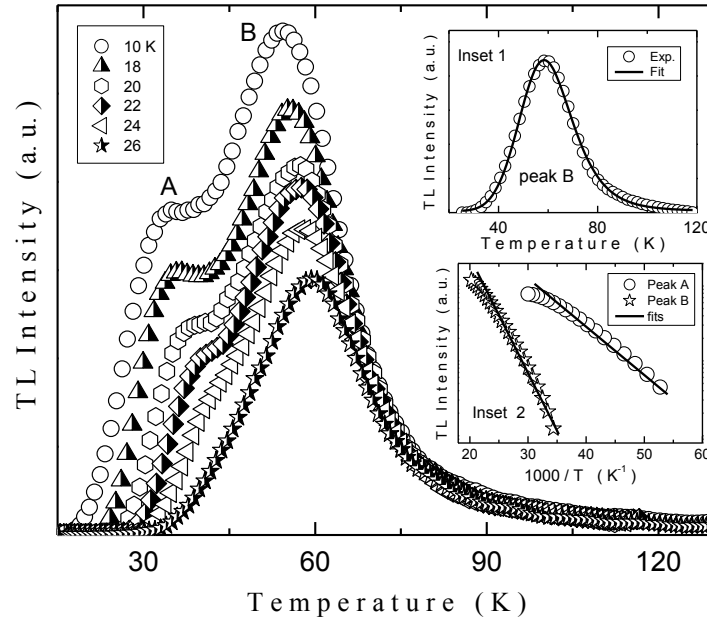
Figure 4.16. Experimentally detected TL curves of Tl$_2$InGaS$_4$ crystal before (circles) and after (stars) thermal cleaning process. Inset 1: TL peak (circles) obtained at T_{stop} = 26 K and curve fit (solid line) to the peak. Inset 2: TL intensity versus 1000/T for peaks A and B. Circles (peak A), stars (peak B) and solid lines exemplify the experimental data and the fitted lines, respectively.

Table 4.6. The calculated E_t, S_t and s values of established traps in Tl_2GaInS_4 crystal.

Peak	T_m (K)	E_t (meV)			S_t (cm^2)	s (s^{-1})
		Curve fitting method	Initial rise method	Peak shape method		
A	34	12	12	--	1.0×10^{-23}	7.2
B	55	26	27	28	1.3×10^{-23}	24.1
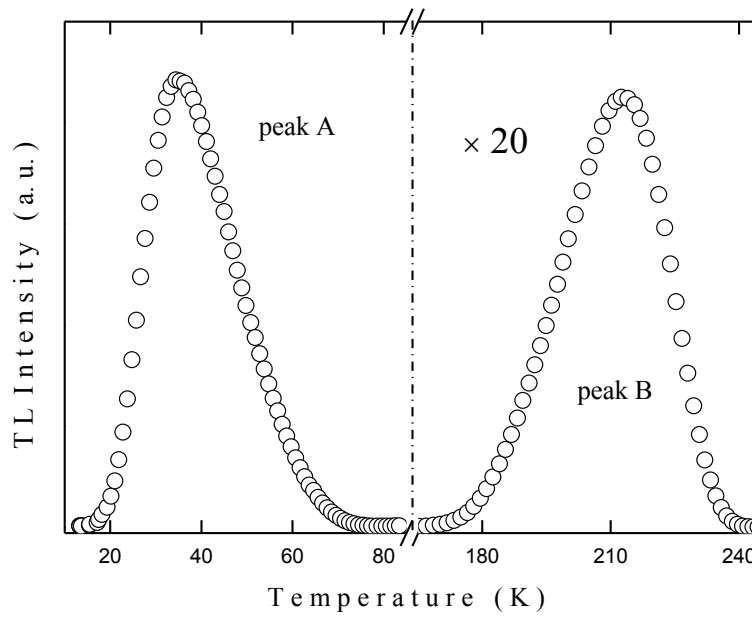
Figure 4.17. Experimentally detected TL peaks of $Tl_4In_3GaS_8$ crystal using $\beta = 1.0$ K/s.

Figure 4.17 presents the observed TL glow curve of $Tl_4In_3GaS_8$ obtained in the 10-240 K temperature range with a constant heating rate of $\beta = 1.0$ K/s. The temperature ranges of 80-170 and 240-300 K were not shown in the figure due to the absence of TL peaks in these ranges. The TL spectra give peaks (called as peak A and B as represented in the figure) arising at the peak temperatures of approximately 36 and 213 K. As can be seen from the figure, A and B peaks show different behavior

in the temperature region of $T > T_\mathrm{m}$. Peak A has a broad descending part (region of $T > T_\mathrm{m}$) compared to the ascending region (region of $T < T_\mathrm{m}$), but peak B shows the opposite behavior of the peak A. Therefore, we have investigated these peaks separately. The broadening of the peak A in the temperature region of $T > T_\mathrm{m}$ can be attributed to the two possible cases; (i) the existence of many peaks corresponding to the various defects, (ii) the existence of one peak related to one defect level. In both cases, first and/or non-first order kinetics may be responsible for TL process. At this point, usage of a parameter value (μ_g) given by Chen and Kirsh will be helpful to get an insight about the number of peaks [86]. The μ_g value for the peak A is found nearly as 0.63 which is very far from the predicted range (0.42−0.52) [110]. This is a powerful indication of the fact that there are many peaks under the main peak A.
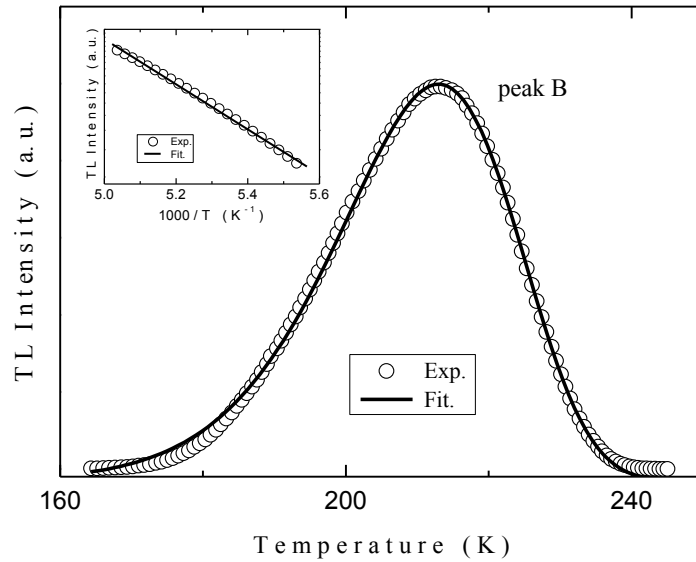
Figure 4.18. Experimentally detected TL peak B (circles) of $Tl_4In_3GaS_8$ crystal using $\beta = 1.0$ K/s and theoretical curve fit (solid curve). Inset: TL intensity versus $1000/T$ for peak B. Circles and solid line exemplify the experimental data and the fitted line, respectively.

Using a fitting program under the light of theoretical expressions giving TL intensity as a function of temperature to reveal these many peaks gives unreliable results. Therefore, we have decided to use thermally cleaning technique and have dealt with

the analysis of this peak in the section 4.3.3. However, the peak B descends more sharply compared to the peak A for the region of $T > T_m$ (see Figure 4.18). This can be strongly due to the dominant mechanism of the first-order kinetics. Moreover, we have calculated the μ_g value to obtain an opinion about the number of peaks. The μ_g value for peak B was found as 0.42 which corresponds to the value of the first order kinetics for one trap level. First order approach to the TL peak B by virtue of Eq. (2.17) provided the fitted curve which described the experimental TL curve successively. Therefore, the presence of one trap centers in the forbidden energy level of $Tl_4In_3GaS_8$ crystal was established with thermal activation energy of $E_{tB} = 292$ meV [110].

The activation energies found by CF method were used to compute the s and S_t values of the trapping levels in $Tl_4Ga_3InS_8$, Tl_2GaInS_4 and $Tl_4In_3GaS_8$ crystals with the help of Eqs. (2.29) and (2.30), respectively. Analyses resulted with the s and S_t values of 0.5, 8.4 and 2.0×10^5 s^{-1} and 2.9×10^{-25}, 9.4×10^{-25} and 9.6×10^{-21} cm^2 for peaks A, B and C of $Tl_4Ga_3InS_8$, 7.2 and 24.1 s^{-1}, and 1.0×10^{-23} and 1.3×10^{-23} cm^2 for peaks A and B of Tl_2GaInS_4, and 6.1×10^5 s^{-1} and 2.6×10^{-20} cm^2 for peak B of Tl_4In_3GaS crystals, respectively. Effective masses $m_e^* = 0.21m_0$, $m_e^* = 0.19m_0$ and $m_e^* = 0.16m_0$ were utilized to obtain the capture cross sections of $Tl_4InGa_3S_8$, Tl_2GaInS_4 and $Tl_4GaIn_3S_8$ crystals, respectively.

The IR method has also been applied to analyze the TL peaks determined for $Tl_4Ga_3InS_8$, Tl_2GaInS_4 and $Tl_4In_3GaS_8$ crystals. The activation energies of trapping levels existing in $Tl_4Ga_3InS_8$ crystal were found as 13 and 44 meV for peaks A and B as seen in the inset of Fig. 4.14. In order to calculate the activation energy of the trap level related to peak B, we used the TL peak obtained after thermal cleaning at T_{stop} = 42 K (see Fig. 4.13b). However, we could not apply this method to peak C since the initial tail of the peak was not obtained experimentally. For Tl_2GaInS_4 crystal, activation energy of observed trap level was successfully evaluated by implementation of the method to the main curve for peak A and to the TL peak arising after thermal cleaning at $T_{stop} = 26$ K for peak B. As a result, E_t values of 12 and 27 meV revealed the existence of trap levels (see inset 2 of Fig. 4.16). The method was

also achieved for peak B of $Tl_4In_3GaS_8$ crystal and $E_{tB} = 293$ meV was established for the corresponding trap level (Inset of Fig. 4.18).

PS method gave the activation energies of trapping levels as 16 and 204 meV for peaks A and C of $Tl_4Ga_3InS_8$ crystal using experimentally observed TL peaks (Table 4.5). Since the T_l and T_h values of peak B was not clear in the observed TL spectra, the method was not achievable for application. The main TL curve of Tl_2GaInS_4 crystal was not also suitable for the analysis of this method. Therefore, we decided to apply this method to only peak B. The activation energy was obtained for the related trap to be $E_{tB} = 28$ meV (Table 4.6). For the $Tl_4In_3GaS_8$ crystal, the activation energy of deeper trap correlated to peak B was computed as $E_{tB} = 290$ meV. The consistency of found energy values with above techniques indicated the reliability of the energy values. The μ_g values have been computed as 0.44 and 0.42 for peaks A and C of $Tl_4Ga_3InS_8$, 0.45 for peak B of Tl_2GaInS_4 and 0.42 for peak B of $Tl_4In_3GaS_8$ crystals, respectively.

4.3.2 Heating rate dependencies of trap levels in $Tl_4Ga_3InS_8$, Tl_2GaInS_4 and $Tl_4In_3GaS_8$ crystals

4.3.2.1 Normal heating rate dependencies of trap levels in $Tl_4Ga_3InS_8$ and $Tl_4In_3GaS_8$ crystals

The studies on $Tl_4Ga_3InS_8$ and $Tl_4In_3GaS_8$ crystals have been expanded by accomplishing the heating rate dependencies of the trap levels. The experiments were achieved with varied rates between 0.2 and 1.2 K/s for $Tl_4Ga_3InS_8$ and between 0.2 and 1.0 K/s for $Tl_4In_3GaS_8$ crystals. In the studies, we merely investigated the heating rate behaviors of trap levels corresponding to peaks A in TL curves $Tl_4Ga_3InS_8$ and $Tl_4In_3GaS_8$ crystals due to the low intensities and complexities of the analysis for other observed peaks of the crystals. Chen and McKeever [90] assumed that T_m shifts to higher values and a decrease in intensity of TL peak occurs with increase of heating rate. The same behavior of the TL curve obeying this rule has been observed in $Tl_4Ga_3InS_8$ and $Tl_4In_3GaS_8$ crystal (see Figs. 4.19 and 4.20).
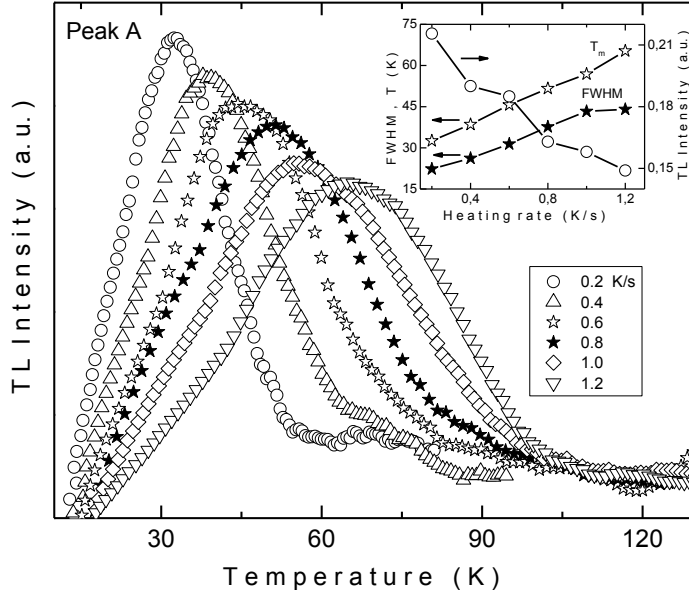
Figure 4.19. Experimentally detected TL peaks of $Tl_4Ga_3InS_8$ crystal with varied β values. Inset: T_m, FWHM and TL intensity dependencies on heating rate (peak A).

Besides the shift of T_m, there occur some changes on the shape of TL glow curve with variation of heating rate β. Inset to Figs. 4.19 and 20 demonstrate the heating rate dependencies of FWHM, TL intensity and T_m values clearly. The FWHM of the TL spectra enlarges from 22 to 44 K for $Tl_4Ga_3InS_8$ and from 11 to 24 K for $Tl_4In_3GaS_8$ crystals as heating rate increases. Moreover, T_m and I_{TL} obey to TL theory with showing increasing and decreasing tendencies, respectively, with heating rate as shown in the insets of Figs. 4.19 and 20.
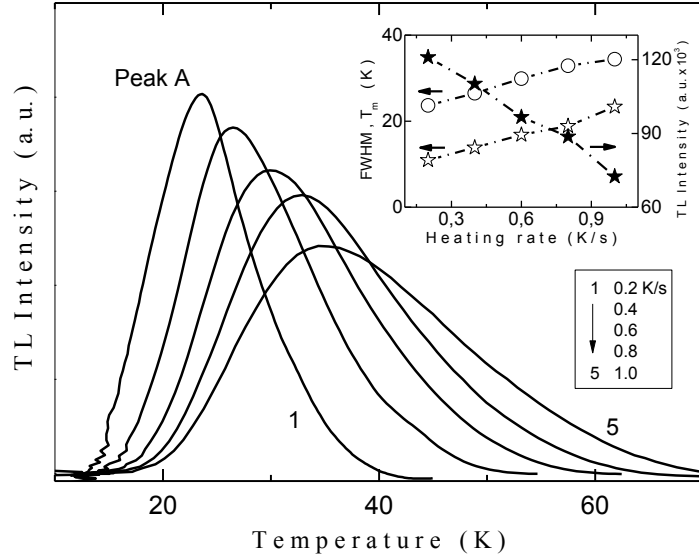
Figure 4.20. Experimentally detected TL peaks of $Tl_4In_3GaS_8$ crystal with varied β values. Inset: T_m, FWHM and TL intensity dependencies on heating rate (peak A).

4.3.2.2 Anomalous heating rate dependence of trap level in Tl_2GaInS_4 single crystals

Until this part of the study, we have come across the normal behavior of trap levels for variation of heating rate. The well-known dependence (normal heating rate) in TL theory was established in the previous sections presenting the various heating rate dependence of the trap levels in above mentioned crystals. However, the trap level (associated with peak B) being observed in Tl_2GaInS_4 crystals acted differently from the well-known phenomenon. Figure 4.21 illustrates such behavior in TL peak B with the variation of the heating rate between 0.2 and 1.2 K/s. As seen from Fig. 4.21, the glow peak's TL intensity increases and the T_m shifts to higher values with ascending heating rate. Moreover, the area under the curves grows from 78 to 181 (a. u.) as the heating rate varies from 0.2 to 1.2 K/s [109]. In this part of the chapter, we try to understand and explain the reason of such an opposite behavior.

65
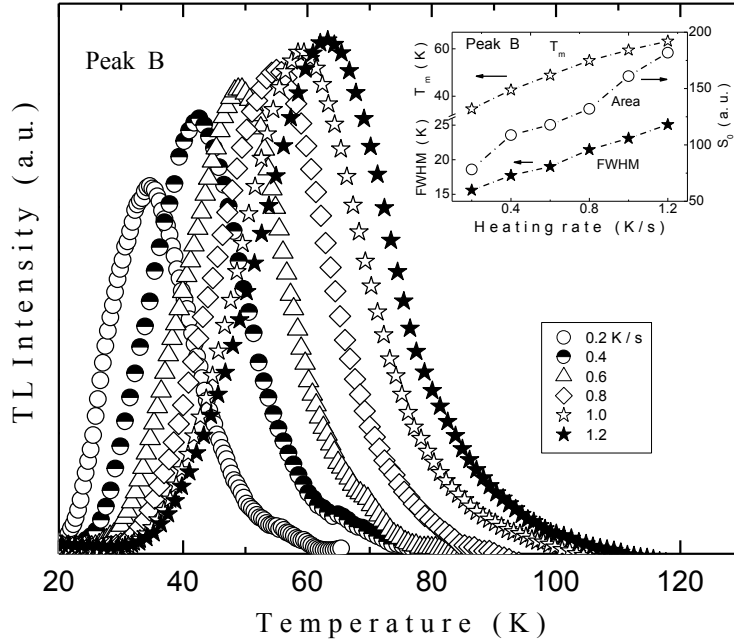
Figure 4.21. Experimentally detected TL peaks of Tl$_2$GaInS$_4$ crystal with varied β values (peak B). Inset: T_m, FWHM and area (S_0) dependencies on heating rate.

Up to this section of the thesis, thermoluminescence mechanisms of the trapping states with regard to varied rates of heating were demonstrated by virtue of the illustrious behaviors. As we mentioned, the unchanging integral of the glow peaks as a response to elevating rate is the expected behavior of TL because of the same number of emitted photons at each heating rate. In case the decrescent area and intensity of luminescence, the mechanism was explained with the phenomenon of thermal quenching [90]. In recent years, the opposite behavior was revealed with the study on YPO$_4$ crystals where the intensity of total luminescence tends to rise with the heating rate [111]. This experience was denominated as anomalous heating rate and approached by aid of a two-stage TL model [112].

66
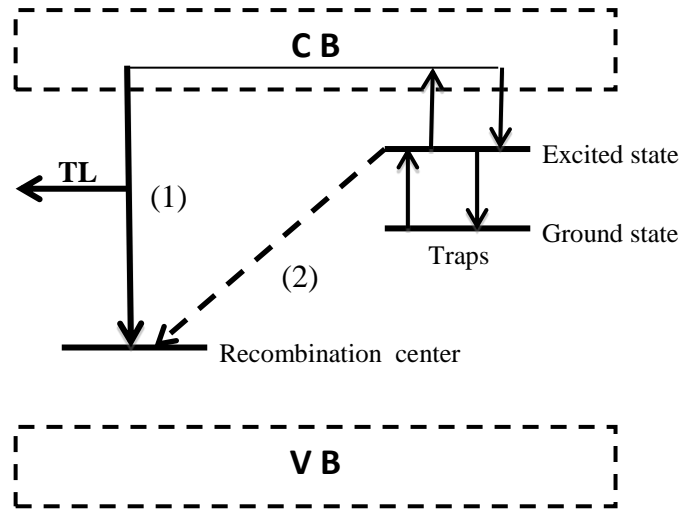
Figure 4.22. Simplified diagram of energy levels for Tl$_2$GaInS$_4$ crystal. Radiative and non-radiative transitions are illustrated by pathway 1 (solid arrow) and pathway 2 (dashed arrow), respectively.

This model takes into account the recombination of electrons producing only radiative transitions. However, in the semi-localized model [113, 114], non-radiative transitions realized between the excited state of the trap and the recombination center are also taken under consideration (see Fig. 4.22). Clearly, the electrons, stimulated from the ground state of the trap into the excited state by thermal energy, are released into the conduction band. Then, two ways are possible for electrons. One of them is the recombination with holes situated in the recombination center. The other is the capturing by trap state. The former event (pathway (1) in the Fig. 4.22) produces the TL emission while the latter (pathway (2) in the Fig. 4.22) results with the non-radiative recombination. Two-stage process of stimulation of electrons from traps suggests the increment of probability of the radiative transitions relative to non-radiative one. The electrons situated at excited state are decisive for the localized transitions. As long as the electrons spent time at the excited state, the probability of non-radiative transitions increases proportionally with that time. The higher heating

67

rates lead to this time to decrease thanks to the increasing stimulation probability of electrons into the conduction band. Thus, one can say that the number of localized transitions diminishes with elevating heating rate causing the increase in the emitted luminescence. The anomalous heating rate phenomenon is physically based on the rivalry among the non-radiative and radiative transitions. This competition between pathways (1) and (2) brings about the TL peak to rise whereas the related non-radiative transitions decrease relatively to conserve the total number of charge carriers [114]. Under the light of these explanations, the increase of the area under the TL curves (230 percent enhancement) that can be affirmed as increase in the probability of radiative transitions over that of the non-radiative transitions revealed the anomalous behavior of the corresponding trap level. Further, the T_m and FWHM values of each peak show increasing tendency from 34 to 63 K and from 16 to 25 K, respectively. Inset to Fig. 4.21 shows the heating rate dependencies of T_m and FWHM of the related glow curves and area enclosed under the curves.

4.3.3. Distribution of trap levels in Tl$_4$Ga$_3$InS$_8$, Tl$_2$GaInS$_4$ and Tl$_4$In$_3$GaS$_8$ crystals

As we mentioned in part 4.3.1, the trap level established in Tl$_4$In$_3$GaS$_8$ crystals (related to peak A) exhibited the behavior of highly defective structures. Therefore, the activation energy depth of the traps was investigated utilizing the thermally cleaning procedure. Figure 4.23 shows the obtained TL glow curves at different stopping temperatures satisfying the emptying of the shallower levels. The activation energies of the trap levels were obtained using initial rise method. Since the initial rise method based on the analysis of the initial part of the curve, the obtained energy corresponds to the firstly emptied trap level if there are many levels in the crystal structure. The activation energies of the revealed trapping centers were observed to be shifted from ~12 to ~125 meV by increasing the stopping temperature from 10 to 36 K (see inset 1 of Figure 4.23 and Table 4.7) [110]. The increase of the activation energy values when T_{stop} increases is consistent with the gradual emptying

of shallowest trapping levels during each preheating treatment [86, 104]. Similar results on the traps distribution were also reported previously in the Refs. [115-117].
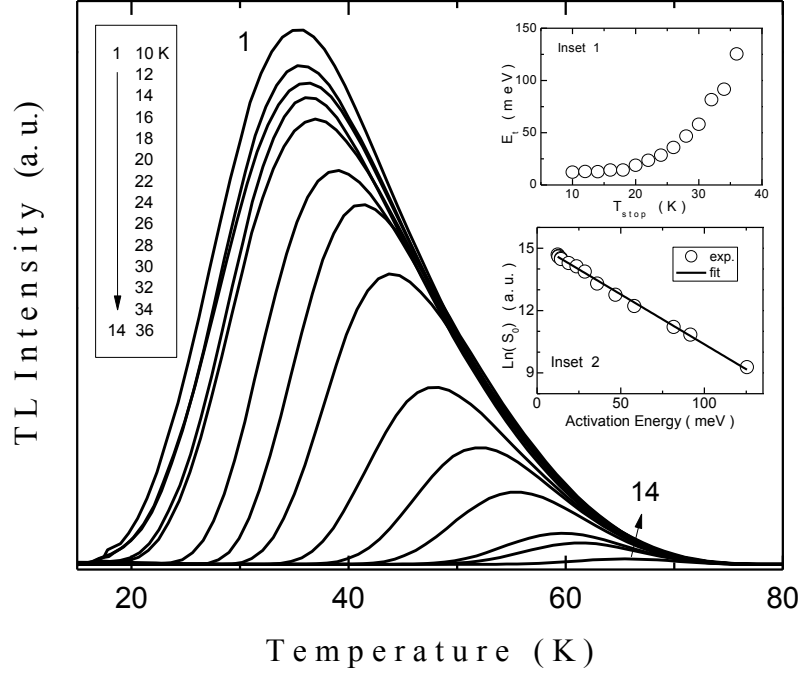
Figure 4.23. Experimentally detected TL curves of $Tl_4In_3GaS_8$ crystal with different T_{stop} values at $\beta = 1.0$ K/s (peak A). Inset 1: E_t vs. T_{stop} plot. Inset 2: Logarithmic plot of S_0 as a function of E_t.

Table 4.7. The obtained T_m, S_0, E_t and s values for $Tl_4In_3GaS_8$ crystal at different T_{stop} (peak A).

Peak A	1	2	3	4	5	6	7	8	9	10	11	12	13	14
T_{stop} (K)	10.0	12.0	14.0	16.0	18.0	20.0	22.0	24.0	26.0	28.0	30.0	32.0	34.0	36.0
T_m (K)	35.8	35.3	36.5	36.0	36.9	39.1	41.5	43.7	48.3	51.7	55.9	59.6	61.8	65.5
S_0 (a.u. $\times 10^6$)	2.41	2.26	2.19	2.03	1.94	1.60	1.37	1.06	0.60	0.35	0.20	0.07	0.05	0.01
E_t (meV)	12.3	12.9	12.7	14.3	14.3	18.9	23.6	28.5	35.9	46.8	58.1	81.6	91.6	125.4
s (s^{-1})	3.0	4.3	3.2	6.9	5.8	23	73	218	681	5.4×10^3	2.8×10^4	1.7×10^6	6.7×10^6	1.3×10^9
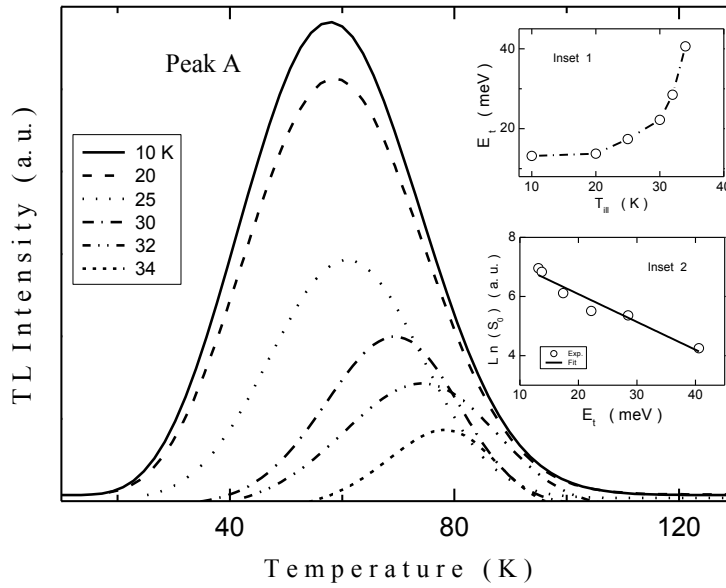
Figure 4.24. Experimentally detected TL curves of $Tl_4Ga_3InS_8$ crystal with different T_{stop} values at $\beta = 1.0$ K/s (peak A). Inset 1: E_t vs. T_{stop} plot. Inset 2: Logarithmic plot of S_0 as a function of E_t.

Figures 4.24 and 4.25 show the measured TL curves for $Tl_4Ga_3InS_8$ (peak A) and Tl_2GaInS_4 (peak B) crystals obtained after illuminating the sample at various stopping temperatures between 10 and 34 K, and 26 and 36 K, respectively. As can be seen from the figures, The TL intensities of peaks gradually decreased and T_m values shifted to higher temperatures with increasing the T_{stop} values. This behavior can be explained with the assumption of a quasi-continuous traps distribution [104-106]. The activation energies of released charge carriers were found by using the CF method (see inset 1 of Figs. 4.24 and 4.25). The increase of the activation energy values from 13 to 41 meV for $Tl_4Ga_3InS_8$ and from 27 to 67 meV for Tl_2GaInS_4, with the rising stopping temperatures, respectively, was obtained (Tables 4.8 and 4.9) [108,109].
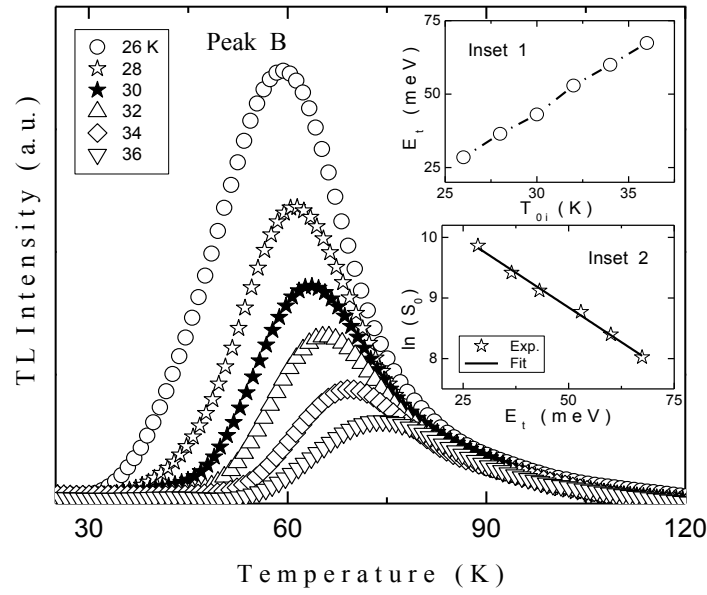
Figure 4.25. Experimentally detected TL curves of Tl_2GaInS_4 crystal with different T_{stop} values at $\beta = 1.0$ K/s (peak B). Inset 1: E_t vs. T_{stop} plot. Inset 2: Logarithmic plot of S_0 as a function of E_t.

Using Eq. (4.3), we plotted $\ln(S_0)$ versus E_t graphs for each crystals as seen in the inset 2 of the Figs. 4.23−4.25. The slopes of the experimental data were found as $\alpha = 0.048$ meV^{-1} for Tl$_4$In$_3$GaS$_8$ (peak A), $\alpha = 0.046$ meV^{-1} for Tl$_2$GaInS$_4$ (peak B) and $\alpha = 0.096$ meV^{-1} for Tl$_4$Ga$_3$InS$_8$ (peak A) crystals. These values correspond to the variation of one order of magnitude in traps density for every 48, 50 and 24 meV, respectively.

Table 4.8. The obtained T_m, S_0, E_t and s values for Tl$_4$Ga$_3$InS$_8$ crystal at different T_{stop} (peak A).

Curve	1	2	3	4	5	6
T_{stop} (K)	10.0	20.0	25.0	30.0	32.0	34.0
T_m (K)	57.8	58.6	60.4	68.9	74.0	78.0
S_0 (a.u.)	1049	929	452	247	213	70
E_t (meV)	13.2	13.7	17.4	22.2	28.5	40.6
s (s^{-1})	0.7	0.8	1.6	2.3	5.3	32.5

Table 4.9. The obtained T_m, S_0, E_t and s values for Tl$_2$GaInS$_4$ crystal at different T_{stop} (peak B).

Curve	1	2	3	4	5	6
T_{stop} (K)	26	28	30	32	34	36
T_m (K)	59	61	64	66	70	74
S_0 (a.u.)	19225	12300	9155	6440	4440	3050
E_t (meV)	27	37	43	53	60	67
s (s^{-1})	18.2	131.6	296.4	1.6×10^3	3.0×10^3	5.2×10^3

4.4. Results of EDSA for Ga$_4$S$_3$Se, Ga$_2$SSe, Ga$_4$Se$_3$S crystals

Chemical composition of Ga$_4$S$_3$Se single crystal was determined utilizing the EDS analysis method in the energy range of 0−10 keV. The characteristics x-rays arising from the constituent elements revealed the EDSA spectrum exhibiting distinctive peaks as shown from the Fig. 4.26. The background in the spectra originates from the interaction of atomic nuclei with the incident electrons. The apparent peaks symbolize the contribution of each elements in the spectrum. The ratio of constituent elements in the crystal was determined by counting the detected x-rays relatively. The composition rates Ga : S : Se were obtained as 51.0 : 36.8 : 12.2, respectively.
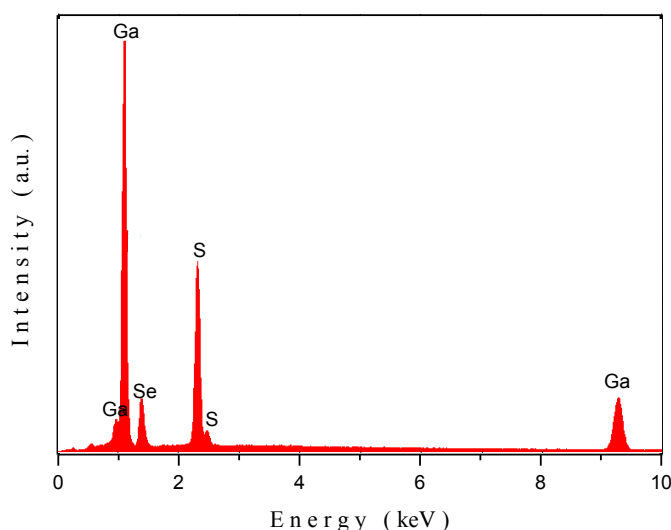
Figure 4.26. Energy dispersive spectrum for Ga$_4$S$_3$Se crystal.

Figure 4.27 depicts the EDSA spectrum of Ga$_2$SSe crystal between the energy ranges of 0−10 keV. The observed peaks were denominated by the constituent elements using the characteristics X-ray emissions from each element in the mixed crystal. EDS measurements established the chemical composition ratio of the elements (Ga: S: Se) to be 49.8 : 24.8 : 25.4, respectively.

73
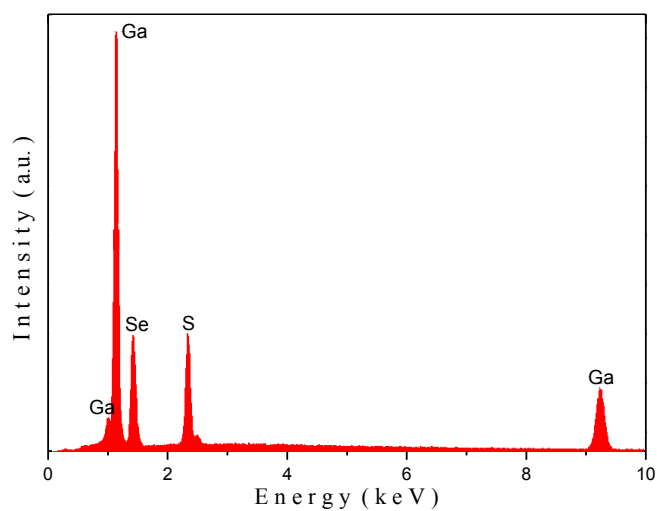
Figure 4.27. Energy dispersive spectrum for Ga_2SSe crystal.
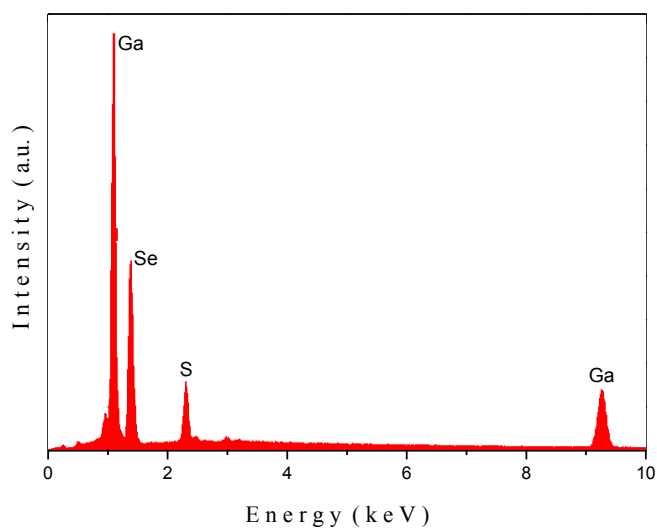
Figure 4.28. Energy dispersive spectrum for Ga_4Se_3S crystal.

EDSA spectrum of Ga_4Se_3S crystal was demonstrated in the $0-10$ keV energy range in Fig. 4.28. Characteristics emission energies of each element in the mixed

crystal were taken account to determine which peak in the spectrum belongs to its own element. Therefore, the ratio of the atomic compositions was found as 50.6 : 37.2 : 12.2 for Ga : Se : S, respectively. The slight deficiency of selenium and sulfur in the growth crystals can be explained with the higher volatility of them as compared to the gallium.

4.5. Results of TL studies on GaS, Ga_4S_3Se, Ga_2SSe, Ga_4Se_3S and GaSe:Mn single crystals

4.5.1. Determination of activation energies, frequency factors and capture cross sections

An example of a TL glow curve of GaS obtained by heating the sample from 10 to 225 K at a rate of 1.0 K/s is shown in Fig. 4.29. As seen in the figure, the TL curve exhibited two strong overlapping peaks with maxima around 91 and 146 K

Figure 4.29. Experimentally detected TL curve (circles) of GaS crystal using $\beta = 1.0$ K/s and theoretical curve fit (solid curve). Dash-dotted peaks are decomposition of solid curve. Inset: TL intensity versus 1000/T for peak A. Circles and solid line exemplify the experimental data and the fitted line, respectively.

labeled as "peak A" and "peak B", respectively. In addition, a weak third peak C (shoulder) is observed around 170 K. The TL curve did not exhibit any peak beyond 200 K. The intensity of the high-temperature peak C around 170 K (see Fig. 4.29) is too low as can be understood by comparison with its neighboring peak at around 146 K. Therefore, we decided to exclude this peak for curve-fitting analysis. Figure 4.29 shows the two underlying components (peaks A and B) of the TL glow curve of GaS obtained by deconvolution using curve fitting. A first-order kinetic approach was not successful in describing the TL glow peaks. However, the glow curve could be deconvoluted into its components using a model function based on non-first order approach. The curve was fitted to Eq. (2.23) by gradually varying the kinetic order parameter b between 1 and 2 separately for peaks A and B. The best fitting was obtained with parameters $b_A = 1.6$ and $b_B = 1.2$ for peaks A and B, respectively. This outcome implies that mixed order kinetics dominates the excitation process from the traps. Using CF, the thermal activation energies of peaks A and B were determined as 52 and 200 meV, respectively. (see Table 4.10) [118].

Table 4.10. The calculated E_t, S_t and s values of established traps in GaS crystal.

Peak	T_m (K)	E_t (meV)		S_t (cm^2)	s (s^{-1})
		Curve fitting method	Initial rise method		
A	91	52	51	4.4×10^{-24}	55.3
B	146	200	--	2.7×10^{-20}	8.7×10^5
C	170	304	--	2.9×10^{-18}	1.3×10^8

Fig. 4.30 shows the observed TL glow curve of the Ga$_4$S$_3$Se crystals accomplished by heating the sample at a constant rate of 0.4 K/s between the temperatures 140 and 200 K. As seen from the figure, one TL peak appearing at T_m = 168 K was obtained. Application of Eq. (2.23) was achieved to obtain the best fit

by varying the parameter b in the fitting program. The most reliable result was obtained with $b = 1.5$ which is responsible for general order of kinetics [86]. The activation energy of the trap level was found as $E_t = 495$ meV [50].
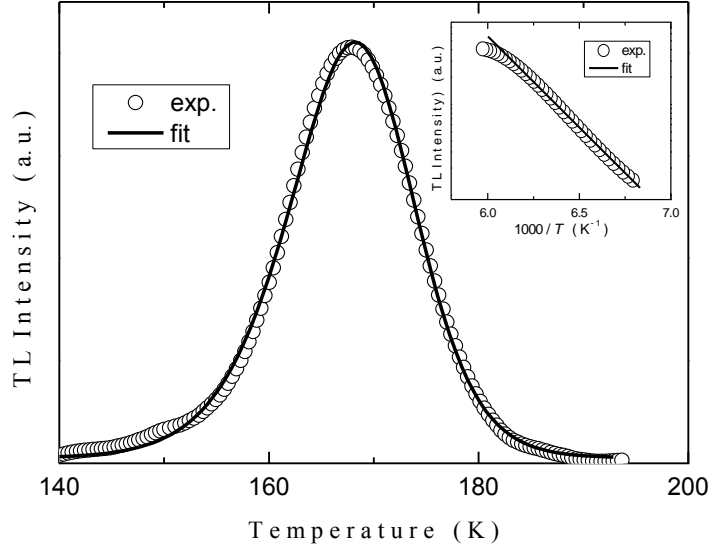
Figure 4.30. Experimentally detected TL peak (circles) of Ga$_4$S$_3$Se crystal using $\beta = 0.4$ K/s and theoretical curve fit (solid curve). Inset: TL intensity versus 1000/T. Circles and solid line exemplify the experimental data and the fitted line, respectively.

Fig. 4.31 shows the TL spectra of Ga$_2$SSe crystal obtained at $\beta = 0.4$ K/s heating rate. The fitting process was successfully resulted with the presence of three trapping centers located at $E_{tA} = 6$, $E_{tB} = 30$ and $E_{tC} = 72$ meV under the light of Eq. (2.17) (solid curve in Fig. 4.31). The good agreement between the experimental glow curve and fitted curve obtained using Eq. (2.17) confirms that the parameter b which is responsible for order of kinetics is equal to 1 corresponding to slow retrapping process. The reliability of the CF method is thought as decreasing with increasing fitting parameters which is proportional to the number of peaks. Therefore, we have also performed the analysis on the glow curve in which shallowest trapping center was emptied using thermally cleaning procedure. The fitting (dash-dot line) of the thermally cleaned TL glow curve (triangles in Fig. 4.31) was resulted for remaining

77

peaks with $E_{tB} = 30$ and $E_{tC} = 74$ meV which can be thought as a powerful indication of accuracy of results [119].
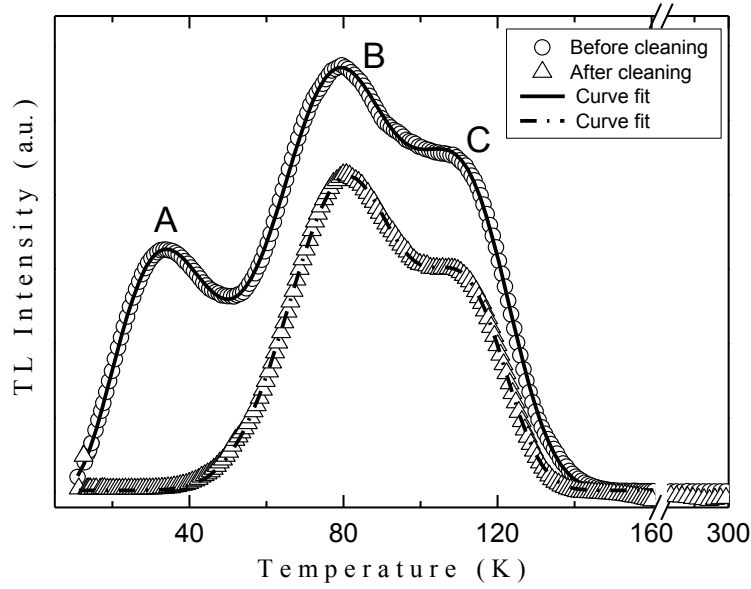
Figure 4.31. Experimentally detected TL curves of Ga₂SSe crystal before (circles) and after (triangles) thermal cleaning process at $\beta = 0.4$ K/s. Solid and dash-dotted curves depict the curve fits to the TL curves.

Figure 4.32 presents the TL glow curve of Ga₄Se₃S crystal for heating rate of 0.4 K/s. In the figure, temperature range in which TL peak was observed is presented although measurements were carried out in the 15-300 K temperature range. TL spectra exhibit only one peak with T_m of nearly 74 K. CF analysis done using both Eqs. (2.17) and (2.23) gave successful results for general order kinetics with parameter $b = 1.2$. Solid line in Fig. 4.32 is the fitted curve giving activation energy of the trap center as 27 meV [120].
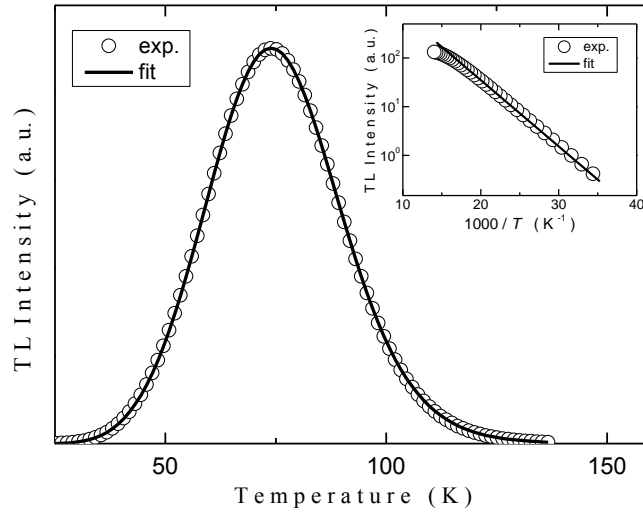
Figure 4. 32. Experimentally detected TL peak (circles) of Ga_4Se_3S crystal using $\beta = 0.4$ K/s and theoretical curve fit (solid curve). Inset: TL intensity versus $1000/T$. Circles and solid line exemplify the experimental data and the fitted line, respectively.

Figure 4.33 shows a typical TL curve for GaSe:Mn crystal in the temperature range 10–225 K with heating rate of $\beta = 1.0$ K/s. Three overlapping peaks (A, B and C) and one isolated peak D were observed with maximum temperatures (T_m) nearly at 47, 102 and 139 K, and 191 K, respectively. For the first three peaks (A, B and C), Eq. (2.17) gave the best-fit result with the activation energy values of $E_{tA} = 8$ meV, $E_{tB} = 34$ meV and $E_{tC} = 130$ meV [121]. This is an evidence for the trap levels that characteristics of the first order kinetics are exhibited. Since the last peak (labeled as D in Fig. 4.33) was distinctively independent of the others, we analyzed it separately. Application of Eq. (2.17) was unsuccessful for fitting of the peak D. Therefore, Eq. (2.23) was utilized several times by varying the parameter b between 1 and 2. The best fit was accomplished with the value of $b = 1.2$, which indicates the mixed-order of kinetics dominates the trap level corresponding to the TL peak D [90]. At the end of fitting process, activation energy of trapping center was calculated as $E_{tD} = 388$ meV.
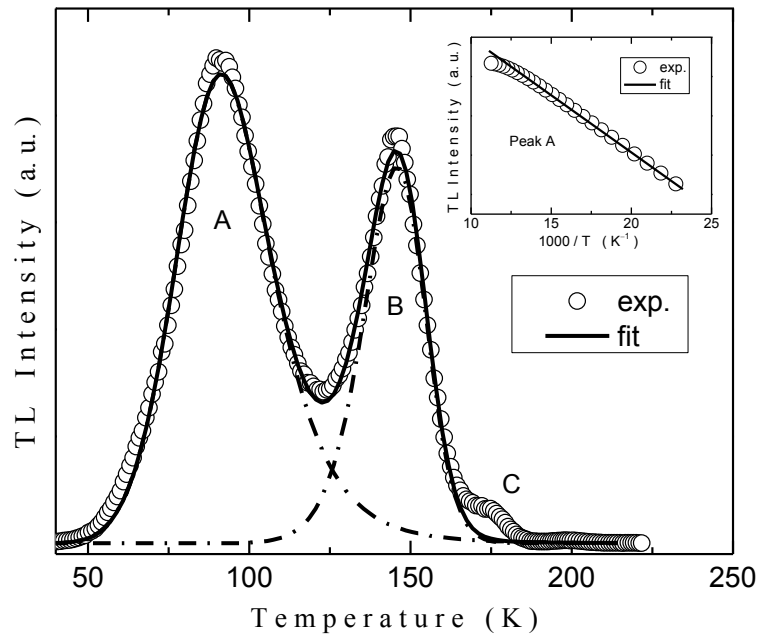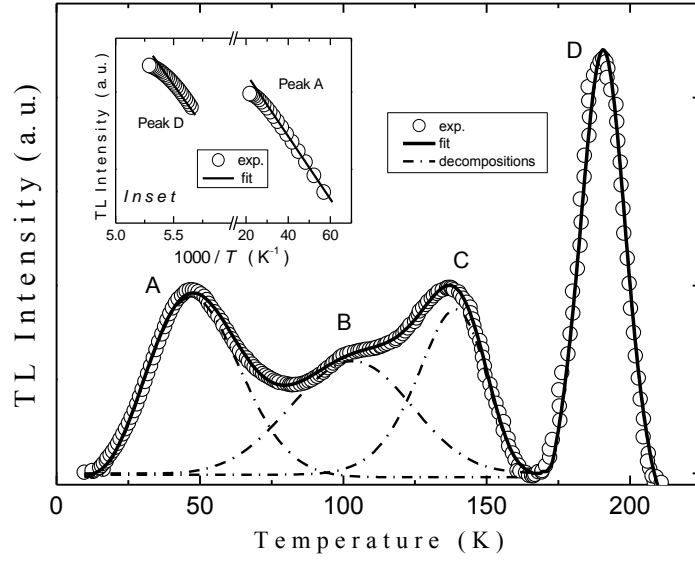
Figure 4.33. Experimentally detected TL curve (circles) of GaSe:Mn crystal using $\beta = 1.0$ K/s and theoretical curve fit (solid curve). Dash-dotted peaks are decomposition of solid curve. Inset: TL intensity versus $1000/T$ for peaks A and D. Circles and solid lines exemplify the experimental data and the fitted lines, respectively.

At this point, we focused to compare found energy values with previous studies on related crystals reported by several authors [78,122,123]. The acceptor levels with activation energies of 130 and 388 meV are close to those observed in undoped GaSe crystals (140 and 370 meV) [78]. These levels may be associated with native defects or defect complexes [122]. In our experiments on GaSe:Mn crystals, we have not observed the acceptor levels with energy of 180 and 240 meV reported in undoped GaSe crystals by TL measurements [78]. It is generally adopted that the major acceptors in undoped GaSe are gallium vacancies V_{Ga} [123]. Doped with mangan, most of the gallium vacancies are occupied by mangan atoms, and the Mn_{Ga} defects may be nonradative centers. Thus, the absent in the TL spectra of GaSe:Mn crystals of bands with activation energies of 180 and 240 meV may probably be associated with recovering of these defect levels by Mn atoms doping.

Table 4.11. The calculated E_t, S_t and s values of established traps in Ga$_2$SSe crystal.

Peak	T_m (K)	E_t (meV)		Heating rate method	S_t (cm^2)	s (s^{-1})
		Curve fitting method				
		Before cleaning	After cleaning			
A	34	6	--	7	1.3×10^{-25}	1.2
B	79	30	30	32	2.2×10^{-25}	2.8
C	108	72	74	--	4.2×10^{-24}	65.6

The shallow acceptor level of 34 meV observed in our study of GaSe:Mn crystal by low-temperature TL experiments may be attributed to the Mn atoms by analogy with the results of work on GaSe:Cu crystals [122], where shallow acceptor level of 40 meV was assigned to the Cu atoms. As for the extremely shallow level of 8 meV, which was not previously observed in any GaSe crystals doped with various atoms, this level probably may be attributed also to the Mn atoms.

Using the energy values found by CF method, we calculated the frequency factors and capture cross sections of the determined trapping levels obtained in GaS, Ga$_4$S$_3$Se, Ga$_2$SSe, Ga$_4$Se$_3$S, and GaSe:Mn single crystals. The Eqs. (2.29) and (2.30) were employed for evaluation of these two trapping parameters. Eventually, 55.3, 8.7 $\times$ 10^5 and 1.3 $\times$ 10^8 s^{-1} of frequency factors and 4.4 $\times$ 10^{-24}, 2.7 $\times$ 10^{-20} and 2.9 $\times$ 10^{-18} cm^2 of capture cross sections for the traps associated with peaks A, B and C, respectively, were obtained for GaS crystals. The single peak related to trap level in Ga$_4$S$_3$Se crystal gave the s and S_t values as 5.8 $\times$ 10^{13} s^{-1} and 1.5 $\times$ 10^{-12} cm^2, respectively. Analysis for Ga$_2$SSe crystals resulted with 1.2, 2.8 and 65.6 s^{-1}, and 1.3 $\times$ 10^{-25}, 2.2 $\times$ 10^{-25} and 4.2 $\times$ 10^{-24} cm^2 for trapping centers corresponding to peaks A, B and C, respectively. In addition, the s and S_t values were computed as 1.6 s^{-1} and 2.4 $\times$ 10^{-25} cm^2 for Ga$_4$Se$_3$S crystals. The four trapping levels in GaSe:Mn crystal were also investigated by means of frequency factor and capture cross section that

found as 0.3, 1.8, 4.1×10^3 and 4.6×10^9 s^{-1} and 2.6×10^{-26}, 4.4×10^{-26}, 6.8×10^{-23} and 2.2×10^{-17} cm^2 for peaks A, B, C and D, respectively. The S_t values of the trap levels were obtained by the effective masses $m_e^* = 0.47m_0$, $m_e^* = 0.44m_0$, $m_e^* = 0.41m_0$, $m_e^* = 0.38m_0$ and $m_h^* = 0.8m_0$ for GaS, Ga$_4$S$_3$Se, Ga$_2$SSe, Ga$_4$Se$_3$S, and GaSe:Mn single crystals.

IR method was accomplished for the trap levels observed in GaS, Ga$_4$S$_3$Se, Ga$_2$SSe, Ga$_4$Se$_3$S, and GaSe:Mn crystals to corroborate and improve the reliability of the results getting in curve fitting method. For this purpose, logarithmic variations of the TL intensities as a function of reciprocal of the respective temperature were presented in the insets of Figs. 4.29, 4.30, 4.32 and 4.33. Linear fit of such a plot was resulted with thermal activation energy of 51 meV for peak A of GaS single crystal (see inset of Fig. 4.29 and Table 10). Due to the closeness of peaks to each other, we could not separate the peaks B and C in the main TL curve to their individual peaks so that we were not allowed applying IR method to these peaks. The TL peak of Ga$_4$S$_3$Se crystal was achievable for implementation of IR method since it exhibits the properties of one trap level. Therefore, compatible result with CF technique was achieved with $E_t = 493$ meV (see inset of Fig. 4.30). The same convenience for application of IR method to the TL single peak of Ga$_4$Se$_3$S gave a chance to determine the E_t value of the associated trap level (inset of Fig. 4.32). The logarithmic plot gave successful outcome ($E_t = 26$ meV) enough to rely on the result of CF method. We could only analyze the peaks A and D in the TL spectra of GaSe:Mn crystal since the peaks B and C overlap with peak A and each other as can be seen in Fig. 4.33. Obtained activation energies of trap levels were reported as $E_{tA} = 7$ meV and $E_{tD} = 386$ meV (see inset of Fig. 4.33).

PS method was used to evaluate the E_t values of trap levels in Ga$_4$S$_3$Se, Ga$_4$Se$_3$S and the E_t value of trap level corresponding to peak D of GaSe:Mn crystal. The obtained value of 495 meV for Ga$_4$S$_3$Se was in good agreement with the values found by above mentioned techniques. Analysis of TL peak observed for Ga$_4$Se$_3$S crystal by means of this method established the presence of the trap level with $E_t = 28$ meV. The peak D of GaSe:Mn crystal gave consistent result ($E_{tD} = 400$ meV) with

the above techniques by the help of peak shape method. On the other hand, The TL peaks of GaS, the TL peaks of Ga_2SeS and the TL peaks of GaSe:Mn (A, B and C) were not suitable for application of the method due to their overlapping tails. The μ_g values were calculated as 0.48, 0.47 and 0.44 which are strong evidences implying the trap levels related to peaks of Ga_4S_3Se, Ga_4Se_3S and peak D of GaSe:Mn crystals, respectively, are dominated by mixed order of kinetics.

Table 4.12. The calculated E_t, S_t and s values of established traps in GaSe:Mn crystal.

Peak	T_m (K)	E_t (meV)			S_t (cm^2)	s (s^{-1})
		Curve fitting method	Initial rise method	Peak shape method		
A	47	8	7	--	2.6×10^{-26}	0.3
B	102	34	--	--	4.4×10^{-26}	1.8
C	139	130	--	--	6.8×10^{-23}	4.1×10^3
D	191	388	386	400	2.2×10^{-17}	4.6×10^9

The activation energies of trapping centers determined in Ga_2SSe and Ga_4Se_3S crystals were also calculated taking the advantage of β dependence of TL glow curves according to the Eq (2.28). Therefore, the plots of $ln\ (\beta)$ vs. $1/T_m$ were achieved using various heating rates of 0.4−1.0 K/s for Ga_2SSe and 0.4−1.2 K/s for Ga_4Se_3S crystals. Figures 4.34 and 4.35 show these plots and their linear fits for peaks A and B of Ga_2SSe and TL peak of Ga_4Se_3S crystals. Since the T_m value of the peak C of Ga_2SSe is not clearly determined from the glow curve, we have left this peak out of heating rate dependence analysis. The activation energy values were obtained from the slope as $E_{tA} = 7$ meV and $E_{tB} = 32$ meV for Ga_2SSe crystal (see Fig. 4.34 and Table 4.11) [119].
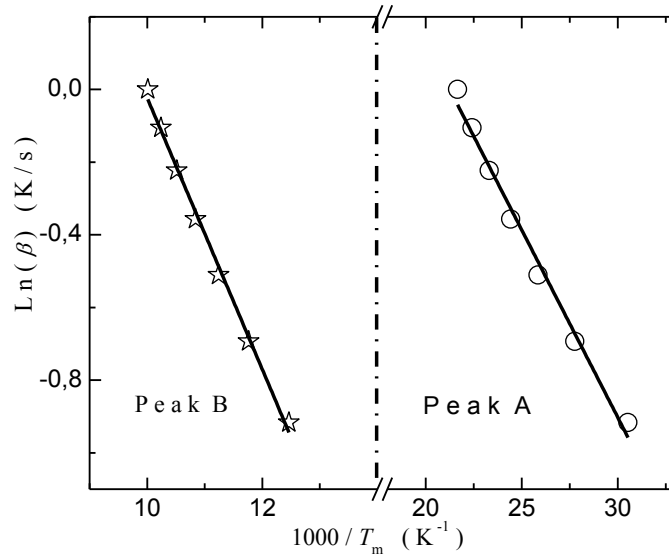
Figure 4.34. ln(β) vs. 1000/T_m plot for Ga$_2$SSe crystals. Circles, stars and solid lines demonstrate the experimental data and fitted lines, respectively.

However, experimental T_m values of the peak being observed for Ga$_4$Se$_3$S crystals were not applicable for the analysis. Thus, we decided to correct these values using the phenomenon which is temperature lag effect. We used the Eq. (4.1) that are prosperous for the corrections. The constant c in the equation was equal to 31.1 found by the help of the smallest β values of 0.4 and 0.6 K/s. Utilizing the corrected T_m values, ln (β) vs. 1/T_m graph was replotted and E_t was obtained as 23 meV from the slope of the plot (see Fig. 4.35) [120].
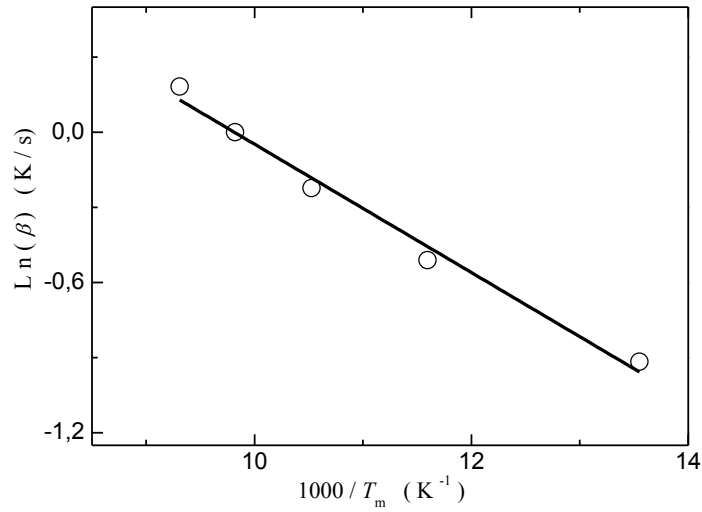
Figure 4.35. ln(β) vs. 1000/T_m plot for Ga$_4$Se$_3$S crystals. Circles and solid line demonstrate the experimental data and fitted line, respectively. Temperature lag effect corrections are used for the data.

4.5.2 Heating rate dependencies of trap levels in GaS, Ga$_4$S$_3$Se, Ga$_2$SSe, Ga$_4$Se$_3$S, and GaSe:Mn crystals

4.5.2.1 Anomalous heating rate dependence of trap level in GaS single crystals

TL glow curves of the GaS crystal, measured at various heating rates ranging between 0.2 and 1.0 K/s, were given in Fig. 4.36. As can be seen from the figure, a shift of the peak temperatures was observed for both peaks A and B. It was interesting to observe that the intensities of the peaks behave differently. The intensity of the low-temperature peak (peak A) behaved in an expected manner, i.e. the intensity decreased on increasing the heating rate. However, the intensity of peak B was observed to increase with increasing heating rate. A close inspection of the figure showed that the intensity of peak B increases seven fold as the heating rate varies from 0.2 to 1.0 K/s. Such an increase can be ascribed to an increase in the probability of radiative transitions over that of the non-radiative transitions. The details of the anomalous behavior of the TL peaks were discussed in section 4.3.2.2 (see also Fig. 4.21).
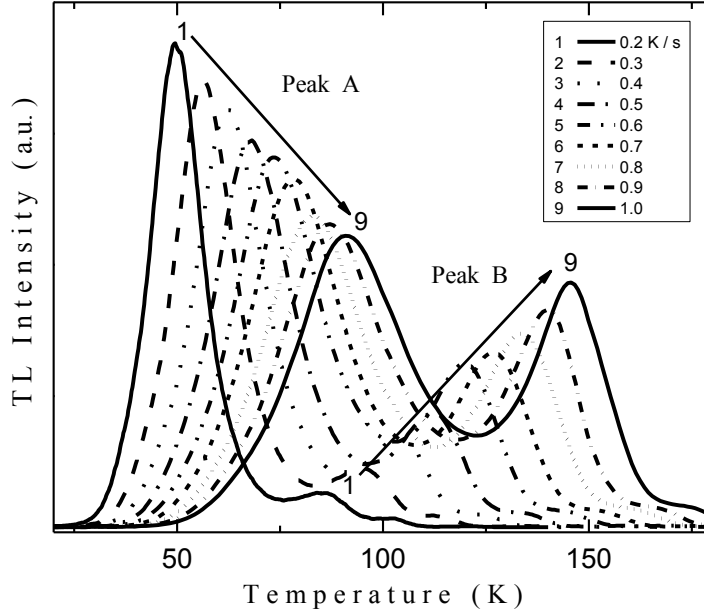
Figure 4.36. Experimentally detected TL curves of GaS crystal with varied β values.

Our current observation of an increase in intensity of peak B of the GaS TL glow curve can be explained using the same approach. It should be noted that the coexistence of normal (peak A) and anomalous heating rate (peak B) dependences is reported here for the first time. In addition to the above-mentioned observation of heating rate dependencies of the peak intensities, the heating rate dependencies of the two peak temperatures and the FWHM values were also analyzed. Figures 4.37a and 4.37b present the heating rate dependencies of the FWHM, T_m and intensities of peaks A and B. As can be seen from the figures, for peak A both the peak temperature and FWHM increase from 49.5 to 91.2 K and from 14.5 to 35.0 K respectively. For peak B, these values increase from 85.3 to 145.6 K and from 16.9 to 22.9 K, respectively [118].
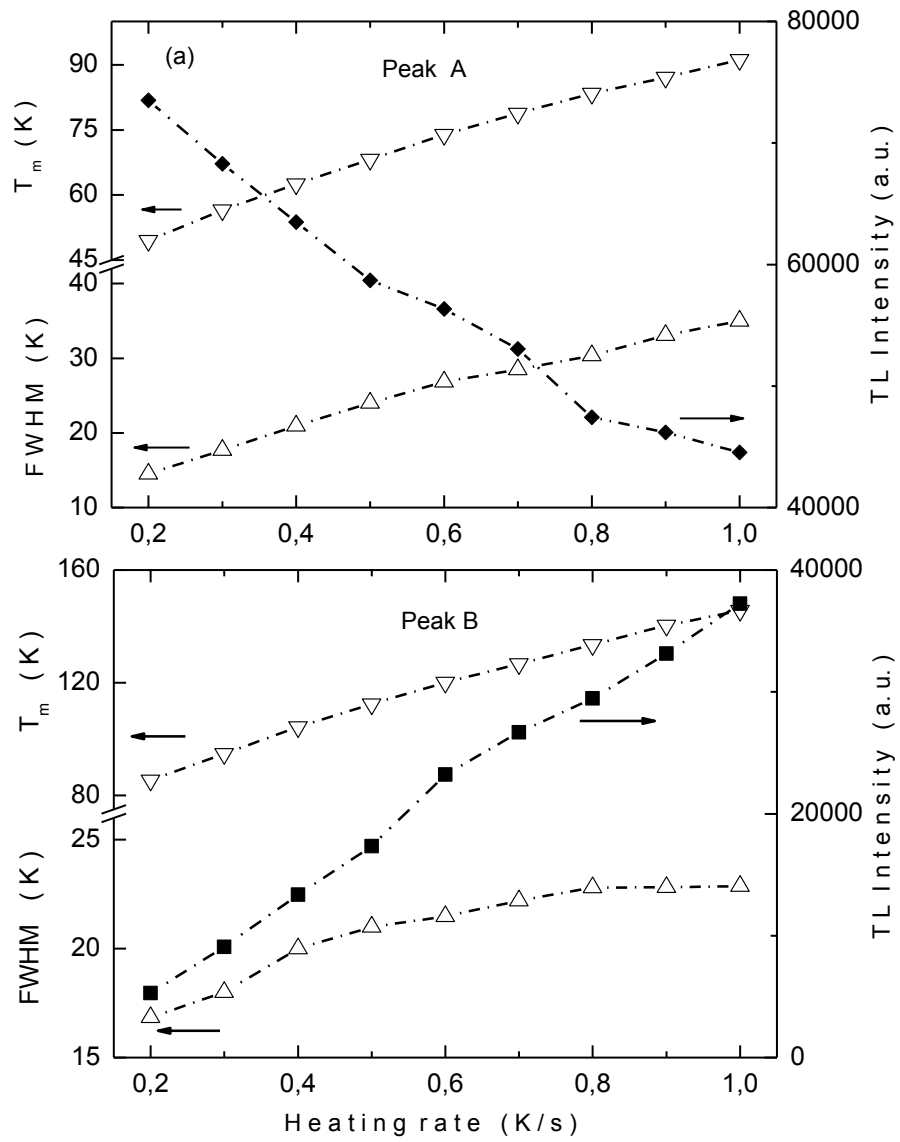
Figure 4.37(a) and (b). T_m, FWHM and TL intensity dependencies on heating rate for GaS crystal (peaks A and B).

4.5.2.2 Normal heating rate dependence of trap level in Ga$_4$S$_3$Se, Ga$_2$SSe, Ga$_4$Se$_3$S, and GaSe:Mn single crystals

Fig. 4.38 illustrates the heating rate dependency of the TL curve of Ga$_4$S$_3$Se crystals obtained for rates between 0.4 and 0.8 K/s with step of 0.1 K/s. As can be seen from the figure, the T_m of the glow curves tends to shift to higher values with increasing heating rate.
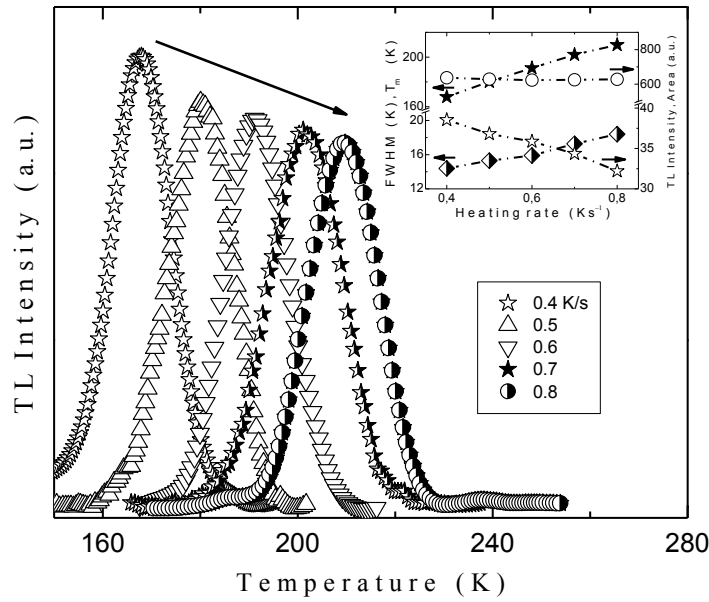
Figure 4.38. Experimentally detected TL curves of Ga$_4$S$_3$Se crystal with varied β values. Inset: T_m, FWHM, TL intensity and area (S_0) dependencies on heating rate.

The variation of the TL intensities, the peak maximum temperatures, the full-width-half-maximums (FWHM) and the areas enclosed under the obtained curves were represented in the inset of Fig. 4.38. As can be seen from the figure, the T_m and FWHM values raised from 168 to 210 K and from 14.4 to 18.4 K, respectively [50]. Moreover, the TL intensity decreased whereas the area enclosed under the curves did not change with temperature since the experiments were performed for the case of fully filled traps.

The dependency of the TL glow curve on the rate of heating was investigated for Ga_2SSe crystal with rates between 0.4 and 1.0 K/s (see Fig. 4.39). Peak maximum temperatures of the peaks shifted to higher temperatures in accordance with theoretical approach given by Chen and McKeever (Inset of Fig. 4.39) [90]. We could not determine the T_m values of peak C truly, so we left this peak out of our analysis. Moreover, the TL intensities of each peaks (A, B and C) decreased as a response to increasing heating rates as expected from the TL theory. Since the observed peaks overlap each other, we were also unable to determine the FWHM values and individual areas of the peaks.
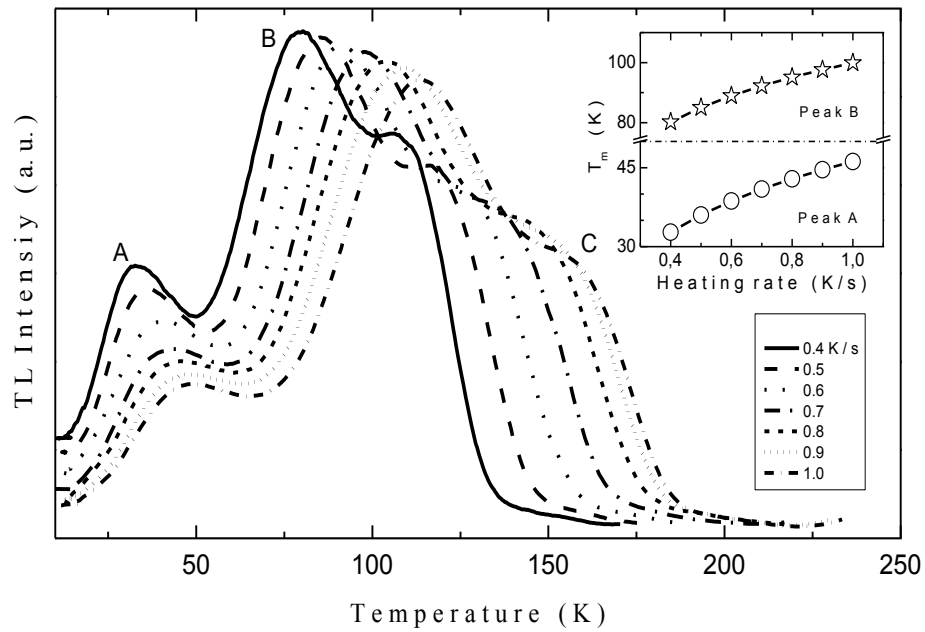
Figure 4.39. Experimentally detected TL curves of Ga_2SSe crystal with varied β values. Inset: T_m dependencies on heating rate for peaks A and B.

Heating rate dependence of the observed TL peak for Ga_4Se_3S crystals was investigated for rates between 0.4 and 1.0 K/s (see Fig. 4.40).. As can be seen from figure presenting the variation of T_m, FWHM and intensity with heating rate,

theoretical evidences are satisfied in our experimental data. The T_m values shifted from 74 to 113 K, FWHM increased from 39 to 45 K, and the TL intensity decreased from 190 to 169 (a.u.) with increased heating rates between 0.4 and 1.0 K/s [120].
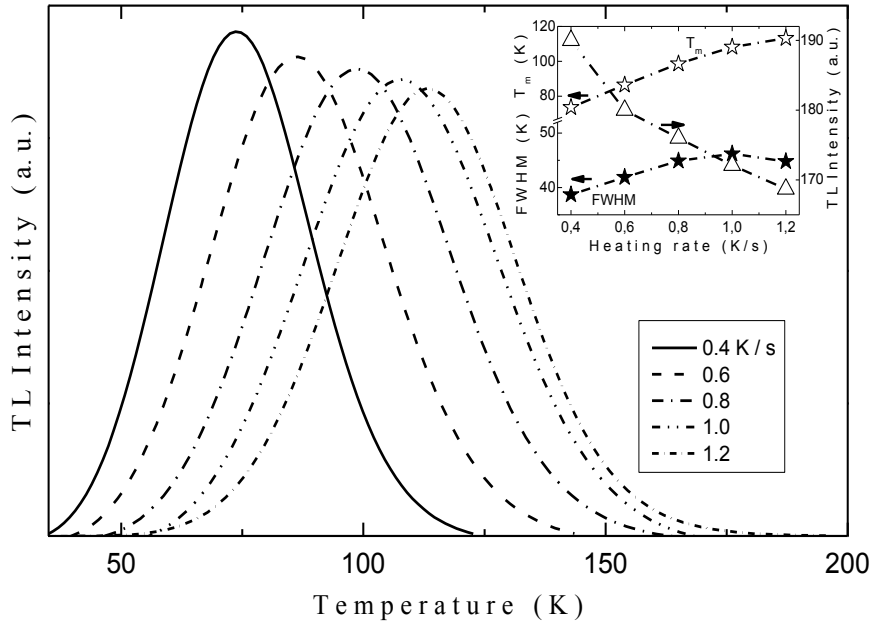
Figure 4.40. Experimentally detected TL curves of Ga$_4$Se$_3$S crystal with varied β values. Inset: T_m, FWHM and TL intensity dependencies on heating rate.

In order to better comprehend the TL mechanism of the indicated trap levels in GaSe:Mn crystals, heating rate dependencies of the glow curves were investigated. Figure 4.41 shows the detected TL glow curves of Mn doped GaSe crystals obtained by heating the sample with various β values ranging from 0.4 to 1.0 K/s with step of 0.2 K/s. One can easily observe the alteration of the position and shape of the TL curves as a response to variation of heating rate in the graph. Clearly, T_m value of each glow curves shifts to higher temperatures and TL intensity decreases with increase of heating rates in accordance with the TL theory.

90
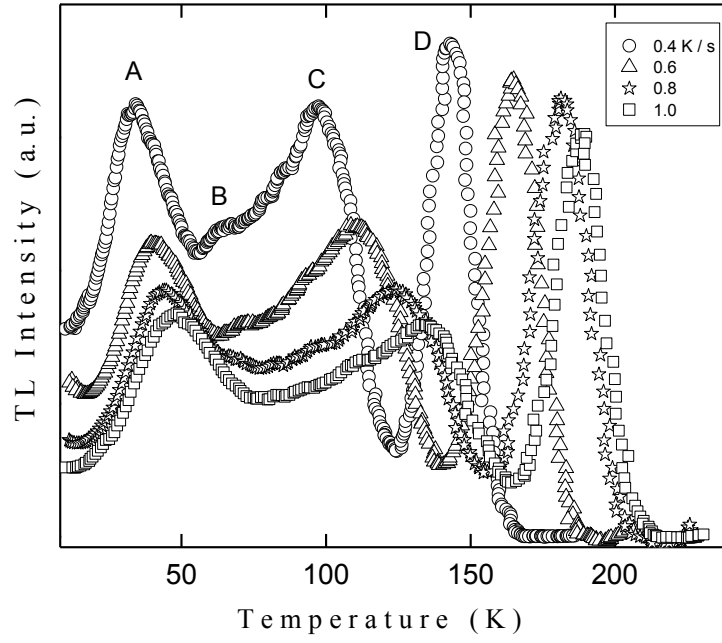
Figure 4.41. Experimentally detected TL curves of GaSe:Mn crystal with varied β values.
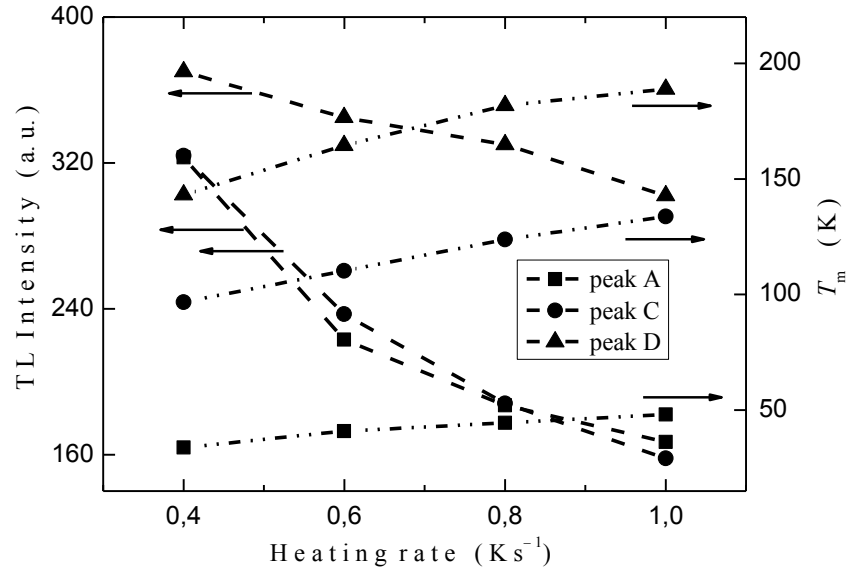
Figure 4.42. TL intensity and T_m dependencies on heating rate for GaSe:Mn crystal (peaks A, C and D).

Figure 4.42 illustrates the heating rate dependencies of TL intensity and T_m values of TL curves. Increase of heating rate resulted with increase of T_m value from 34 to 48 K, from 97 to 134 K and from 143 to 189 K for peaks A, C and D, respectively. In addition, increase of the heating rate led to decrease of the TL intensities from 323 to 167, from 324 to 158 and from 370 to 302 (a.u.) as can be seen in the Fig. 4.42 [121].

4.5.3. Distribution of trap levels in GaS, Ga₂SSe, Ga₄Se₃S, and GaSe:Mn crystals

In order to understand the nature of the traps associated with our observed glow peaks of GaS crystal, we applied thermally cleaning technique for T_{stop} values ranging from 10 to 70 K. Figures 4.43a and 4.43b show the recorded TL curves obtained after illuminating the GaS sample at these temperatures. Through elevating T_{stop} value, peak C in the TL curve appeared more distinctive since the contribution of charge carriers coming from shallower traps related to peaks A and B were absent. As the concentration of trapped charge carriers diminishes gradually, the intensity of the TL curve exhibits a tendency to decrease and the T_m shifts towards higher temperatures with increasing stopping temperature. This behavior can be explained on the assumption of a quasi-continuous trap distribution [105-107]. The activation energies of released charge carriers were found by using a curve-fitting method (see inset of Fig. 4.43a and insets of Fig. 4.43b). The increase of the activation energies from 52 to 90 meV (peak A), from 200 to 268 meV (peak B) and from 304 to 469 meV (peak C) with rising stopping temperature from 10 to 30 K, from 10 to 50 K and from 30 to 70 K, respectively, showed the contribution of charge carriers released form deeper levels for the responsible trap levels [118]. Similar outcomes for distribution of traps were also reported in Refs. [115-117].

By the assumption for the density of revealed traps to be proportional to E_t, we utilized the well-known approach under the light of Eq. (4.3). Plots of ln (S_0) versus the E_t were straight lines with slopes of $\alpha = 0.063$, 0.058 and 0.013 meV^{-1} for peaks A, B and C, respectively (see inset of Fig. 4.43a and insets of Fig. 4.43b). These

determined values imply a variation of one order of magnitude in the density of traps for depths of 36, 39 and 166 meV associated with peaks A, B and C, respectively.
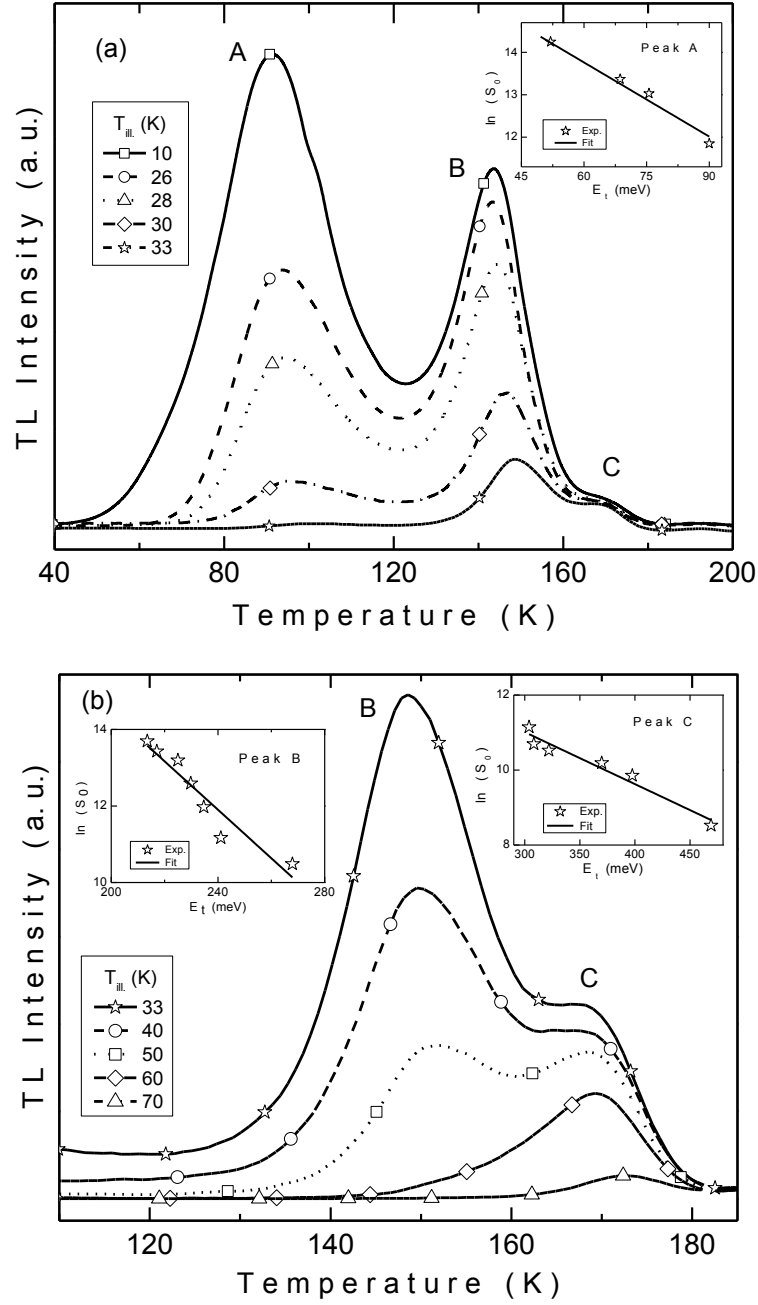
Figure 4.43(a) and (b). Experimentally detected TL curves of GaS crystal with different T_{stop} values at $\beta = 1.0$ K/s. Insets: Logarithmic plot of S_0 as a function of E_t.

Table 4.13. The obtained T_m, S_0, E_t and s values for GaS crystal at different T_{stop}.

Curve	1	2	3	4	5	6	7	8	9
T_{stop} (K)	10.0	26.0	28.0	30.0	33.0	40.0	50.0	60.0	70.0
T_{mA} (K)	91	93	94	95	--	--	--	--	--
T_{mB} (K)	146	146	146	148	150	151	153	--	--
T_{mC} (K)	169	169	169	169	169	169	170	171	172
E_{tA} (meV)	52	69	76	90	--	--	--	--	--
E_{tB} (meV)	200	217	225	230	235	241	268	--	--
E_{tC} (meV)	--	--	--	304	308	322	367	398	469
s_A (s^{-1})	55.3	508.0	1.2×10^3	6.9×10^3	--	--	--	--	--
s_B (s^{-1})	8.7×10^5	3.7×10^6	7.2×10^6	8.3×10^6	9.5×10^6	1.4×10^7	9.0×10^7	--	--
s_C (s^{-1})	--	--	--	1.3×10^8	1.9×10^8	5.2×10^8	1.1×10^{10}	8.5×10^{10}	1.0×10^{13}

Fig. 4.44 depicts the TL curves of Ga_2SSe crystals obtained after applying the T_{stop} method for different values between 10 and 52 K at a rate of 0.4 K/s. The activation energy of the shallowest level in each TL glow curve was calculated using IR method. Although, a traps distribution case are considered as the contribution of released charge carriers remaining after cleaning process, only one value for activation energy is obtained by IR method. Hornyak and Chen reported the found energy from initial rise method as centered energy value of continuous distribution of activation energies in an energy range [124]. Therefore, the previously obtained energies from curve fitting method are attributed to the centered energy value (or mean energy of distribution) of three discrete trapping centers. Inset 1 of Fig. 4.44 represents the ln (I_{TL}) vs 1/T plots of the experimental data (stars) and their linear fits (solid lines) for three measurements. Inset 2 of Fig. 4.44 shows the T_{stop} dependencies of activation energies. The increase of activation energy from 6 to 14 meV can be

associated to the traps distribution of shallowest level (peak A). The remaining increasing energies from 33 to 136 meV are related to the distribution of peak B and C [119]. Since these peaks are closely overlapped, we assume that excitation of trapped charge carriers can occur from both of the centers for some T_{stop} values. Therefore, we avoid giving specific energy ranges of distribution of traps for these centers.
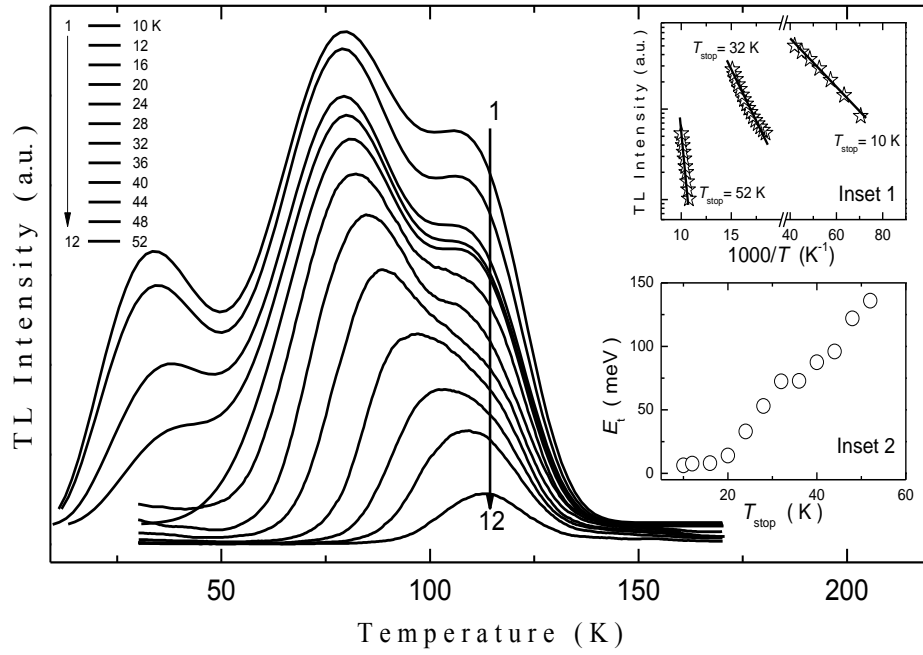
Figure 4.44. Experimentally detected TL curves of Ga$_2$SSe crystal with different T_{stop} values at β = 0.4 K/s. Inset 1: TL intensity versus 1000/T. The stars and the lines exemplify the experimental data and theoretical fits, respectively. Inset 2: E_t vs. T_{stop} plot.

Traps distribution study was also accomplished for the trap level in Ga$_4$Se$_3$S crystals using T_{stop} method. Figure 4.45 presents the TL curves obtained for different T_{stop} values between 15 and 36 K employing the heating rate of 0.4 K/s. The activation energies of the centers corresponding to these curves were calculated using curve fitting method. Activation energies increase from 27 to 40 meV as T_{stop} is increased from 15 to 36 K (see Inset 1 of Fig. 4.45) [120]. The E_t values were evaluated using

IR method. The obtained TL curves in Fig. 45 can also be analyzed to get information about the energy parameter (α) characterizing the traps distribution by the help of the Eq. (4.3). Inset 2 of Fig. 4.45 illustrates the $\ln(S_o)$ plotted as a function of the energy E_t. The linearly fitted plot gave a slope as $\alpha = 0.151$ meV^{-1} corresponding to 15 meV/decade, an order of magnitude variation in the trap density for every 15 meV.

Table 4.14. The obtained T_m, S_0, E_t and s values for Ga$_4$Se$_3$S crystal at different T_{stop}.

Curve	1	2	3	4	5	6
T_{stop} (K)	15	24	27	30	33	36
T_m (K)	74	76	76	78	80	82
S_0 (a.u.)	5162	4590	3362	1907	1446	877
E_t (meV)	27	30	32	34	36	40
s (s^{-1})	1.6	2.4	3.4	4.1	4.8	6.6
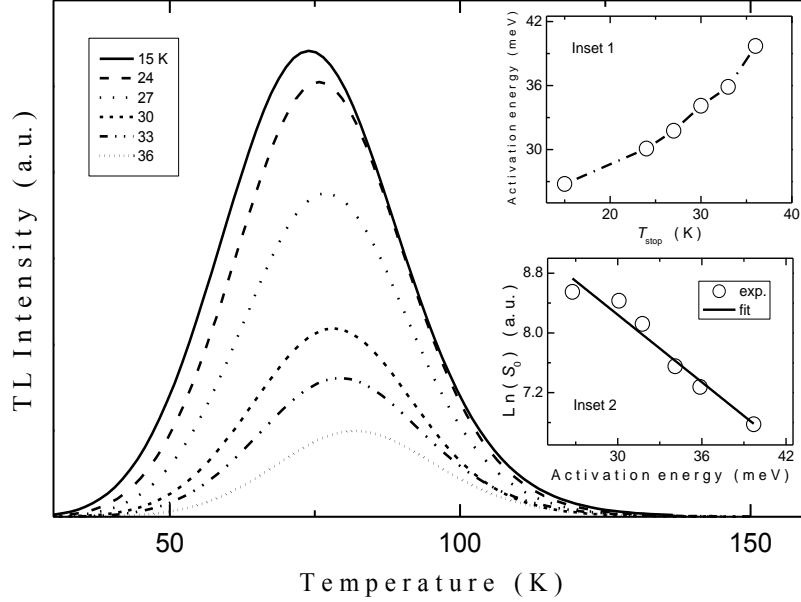
Figure 4.45. Experimentally detected TL curves of Ga$_4$Se$_3$S crystal with different T_{stop} values at $\beta = 0.4$ K/s. Inset 1: E_t vs. T_{stop} plot. Inset 2: Logarithmic plot of S_0 as a function of E_t.

TL properties of the trap levels in GaSe:Mn crystals were studied in detail achieving the thermally cleaning of the shallowest levels of the traps by varying the stopping temperature between 15 and 65 K. In literature, there are many examples explaining the characteristics of traps center. As we mentioned before, some trap states exhibit the properties of continuous distribution of traps especially in highly defective materials while the others consist of single trap level. In continuous traps which reveal the existence of many overlapping peaks, increase of the T_{stop} values leads to shift of initial tail and T_m value of each glow curves to higher temperatures distinguishably while the high temperature side of the curves is not affected [90,110,115,125]. However, in the single trap case, T_m of the curves remains unchanged and low and high temperature sides of the curves tends to decrease symmetrically as the T_{stop} value is increased [90]. The only alteration is the number of charge carriers releasing from trap level.
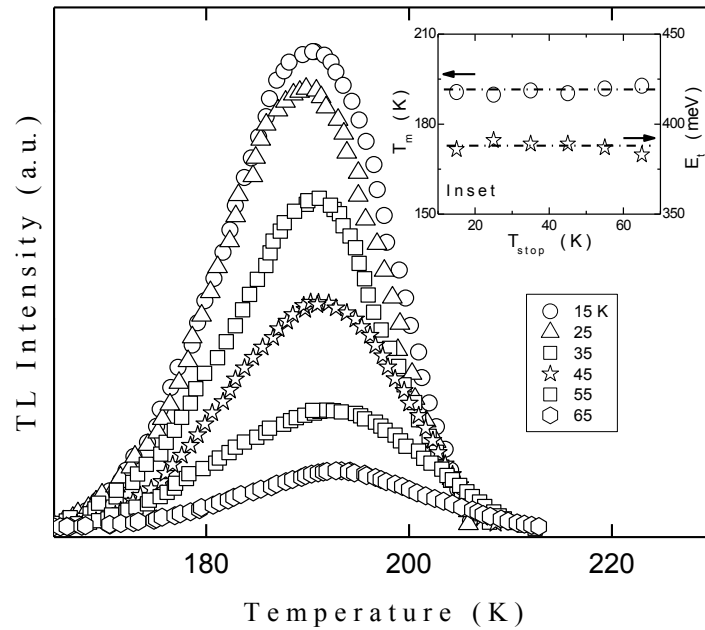
Figure 4.46. Experimentally detected TL peaks (peak D) of GaSe:Mn crystal with different T_{stop} values at $\beta = 1.0$ K/s. Inset: T_m and E_t dependencies on T_{stop} values.

Figure 4.46 depicts the TL peak D of GaSe:Mn crystal detected with different T_{stop} values between 15 and 65 K. Since the peaks observed at low temperatures (peaks A, B and C) were overlapping, we only characterized the trap level corresponding to peak labeled as D. As can be seen from the Fig. 4.46, T_m values of the curves can be considered as nearly same with negligible variation of ~2 K (difference between the maximum temperature of first and last peaks). The TL intensity of the curves decreased in both of the temperature sides symmetrically as the stopping temperature was increased. Inset of Figure 4.46 shows the T_{stop} variation of T_m and E_t values of each glow curves. Activation energies were calculated using the IR method and all of the values were found very close each other. This was another evidence for the trap to be attributed to discrete, single level. The average activation energy of the single trap level was calculated as 388 meV utilizing the energy values of each glow curves (Table 4.15) [121]. This value was in good agreement with the values evaluated by previous analysis technique for GaSe:Mn crystals.

Table 4.15. The obtained T_m, S_0, E_t and s values for GaSe:Mn crystal at different T_{stop}.

Curve	1	2	3	4	5	6
T_{stop} (K)	15	25	35	45	55	65
T_m (K)	191	190	191	190	192	193
S_0 (a.u.)	4503	4072	3015	2202	1294	562
E_t (meV)	386	391	387	388	389	385
s ($\times 10^9$ s^{-1})	1.9	2.9	2.0	2.4	2.0	1.4

CHAPTER 5

CONCLUSION

In the present thesis, defect characterizations of binary, ternary and quaternary layered structured single crystals were studied through low temperature TL measurements. Those of layered crystals are semiconducting materials that are used or have possibility of usage in technologic devices. Ternary compounds of the semiconductors possess remarkable properties attracting great interest. They have highly anisotropic properties, non-linear effects in *I-V* characteristic, photoconductivity properties, switching and memory effects and potential applications for optoelectronic devices. The quaternary compounds of these types of crystals permit to adjust band gap energy which covers wide ranges in the visible spectrum. Thus, they can be considered as possible materials for production of optoelectronic devices. Defects existing in the crystals are dominating factors for the performance of the devices. Therefore, knowing the characteristics of defects is crucial for high quality devices. TL is very sensitive experimental method to determine the defect centers in the studied crystals. In the thesis, TL properties of the crystals have been reported. Also, structural properties of Ga_4S_3Se, Ga_2SSe and Ga_4Se_3S crystals have been investigated by means of EDSA measurements and the results have been reported.

Thermoluminescence investigations of $Tl_2Ga_2S_3Se$ single crystal achieved under room temperature (10−100 K) established one trap level that corresponds to

being successively observed one TL glow peak reaching its maximum intensity at 47 K with a heating rate of 1.0 K/s. The recorded TL peak was examined under a variety of analysis methods (CF, IR and PS methods) known from the TL theory to compute the activation energy, frequency factor and capture cross section. An energy state that has 16 meV was revealed with the agreement of applied analysis methods. s and S_t values were evaluated as 2.9 s^{-1} and 1.6 × 10^{-4} cm^2 under the light of found activation energy. Analysis also implied that the general order kinetics governed the trapping process of the defect level. Heating rate dependency of demonstrated level was studied with various heating rates ranging from 0.4 to 1.2 K/s. Thermal quenching was attributed to the level by the strong evidence showing decrease in the area and intensity of the TL peak with rising heating rate. Distribution of energy levels from 16 to 58 meV corresponding to each successive peaks detected for T_{stop} values between 10 and 25 K was attributed to quasi-continuous distribution. This trap level are thought as a native defect arising from stacking faults that have great possibility to be formed between layers.

The TL studies on TlGaSSe crystals realized with various heating rates between 0.5 and 1.0 K/s at low temperatures (10−180 K) culminated in observing two distinctive TL peaks with temperature maxima of 39 and 131 K as the $\beta = 1.0$ K/s is employed. The TL peaks were analyzed with CF, IR and PS methods and E_{tA} = 16 and E_{tB} = 97 meV were found for the associated trap levels. Analysis result of peak shape method offered for the trap levels corresponding to peaks A and B, respectively, that second and mixed order of kinetics managed the TL trapping process. Frequency factors and capture cross sections were obtained as $s_A = 14.3$ and $s_B = 353.8$ s^{-1}, and $S_{tA} = 6.6 \times 10^{-24}$ and $S_{tB} = 1.4 \times 10^{-23}$ cm^2. The decreasing TL intensity and increasing T_m values despite the constant area under the peaks indicated the normal heating rate behavior of trap levels which are quite consistent with the TL theory. Traps' distribution was also investigated by thermally cleaning procedure and energy increments from 16 to 27 meV and 97 to 147 meV were ascribed to quasi-continuous distribution for trap levels related to peaks A and B, respectively.

Defect characterization of $Tl_2Ga_2Se_3S$ single crystals was accomplished by TL experiments carried out in the temperatures 10−80 K using various heating rates of 0.6−1.0 K/s. The TL spectra recorded for β = 1.0 K/s provided one TL peak with T_m = 36 K. Application of CF, IR and PS methods revealed the presence of the trap level with agreed activation energy value of 13 meV. Mixed order of kinetics was denoted to trap level with the strong evidences obtained with the applied methods. The temperature lag effect corrections for the TL peaks observed with different heating rates were utilized to calculate the activation energy with heating rate method. Frequency factor and capture cross section were calculated as 8.7 s^{-1} and 4.3×10^{-24} using the found activation energy. The increasing T_m values and decreasing TL intensity were observed as the heating rate increased regularly. Increasing energy from 13 to 18 meV as the T_{stop} was varied from 10 to 15 K implied the quasi-continuous distribution of traps.

Low-temperature thermoluminescence measurements for $Tl_4Ga_3InS_8$ crystals were performed using various heating rates between 0.2 and 1.2 K/s. The TL spectra shown in the temperature ranges of 10-200 K exhibited three TL peaks at T_m values of 58, 103 and 166 K. Application of different analysis methods indicated the existence of trapping levels associated with these peaks with activation energies of 13, 44 and 208 meV. These analysis methods indicate also that the properties of the first order kinetics were exhibited by the traps. Frequency factors and capture cross sections of the revealed traps were computed as s_A = 0.5, s_B = 8.4 and s_C = 2.0×10^5 s^{-1} and S_{tA} = 2.9×10^{-25}, S_{tB} = 9.4×10^{-25} and S_{tC} = 9.6×10^{-21} cm^2. Normal heating rate behavior of trap level related to peak A was established by observing the increase in T_m value and decrease in TL intensity. The distribution of trap level related to peak A was also investigated and increase of energy from 13 to 41 meV was attributed to quasi-continuous distribution.

Analysis on detected TL spectra of Tl_2GaInS_4 single crystals with various heating rate ranging from 0.2 to 1.2 K/s at low temperature indicated the presence of two trapping levels correlated to apparent TL peaks that have T_m values of 34 and 55 K. The resulted TL analysis methods were in good compliance with each other on

account of obtaining activation energies of 12 and 26 meV. The trapping processes of the levels were determined by CF and PS analyses and it was found that the first and general order kinetics were responsible for the traps with the parameters $b_A = 1.0$ and $b_B = 1.6$. The strongly dependencies of frequency factors and capture cross sections to the found activation energies and T_m values brought out the small values of 7.2 and 24.1 s^{-1}, and 1.0×10^{-23} and 1.3×10^{-23} cm^2 for the demonstrated traps. The peak appearing at $T_m = 55$ K was also analyzed in terms of heating rate dependency and traps distribution after removal of the initial tail of the TL spectra which are bounded to neighboring TL peak. Measurements with varying heating rate allow to observation of TL peaks with increasing intensity, area and shift of T_m values. Such an alterations of the TL parameters were referred to the anomalous heating rate behavior and can be explained with the semi-localized transition model that suggests the behavior is due to the competition between radiative and non-radiative transitions. Increase in energy value of the traps from 27 to 67 meV deduced the validity of quasi-continuous distribution.

TL properties of $Tl_4In_3GaS_8$ crystals were investigated in the temperature range 10−240 K. The TL spectra presented two separate glow peaks in the temperature regions of 15−80 K and 165−240 K as the TL measurement was performed with $\beta = 1.0$ K/s. The T_m values of the successive peaks were 36 and 213 K. The characterization of observed related trap levels was achieved by analyzing the glow peaks separately and it was shown that the peak at lower temperature side consists of numerous overlapping peaks that means the existence of distributed many energy levels. The analysis for obtaining the activation energies of the distribution indicated the increment from 12 meV to 125 meV for the trap level with increasing T_{stop} from 10 to 36 K. The s and S_t of the continuum traps were found to be shifted from 3.0 to 1.3×10^9 s^{-1} and form 5.3×10^{-24} to 5.8×10^{-16} cm^2, respectively. However, the relatively high temperature peak was suitable for implementation of TL analysis methods which are successful to calculate the activation energy of single levels. CF, IR and PS methods were applied to this peak and 293 meV was found for the activation energy. The s and S_t values were found to be 6.1×10^5 s^{-1} and $2.6 \times$

10^{-20} cm^2. Moreover, curve fitting and peak shape method were in good agreement for the result that first order of kinetics dominates the trapping levels. Heating rate dependency of low temperature peak was also investigated using the rates between 0.2 and 1.0 K/s. It was found the TL intensity had a loss in magnitude while the T_m had tendency for shifting to higher values as expected.

TL characteristics of defect centers in GaS single crystals were investigated under room temperature (10−225 K) using various β values of 0.2−1.0 K/s. TL emission from the defects exhibited a curve consisting of three peaks labeled as peaks A, B and C nearly appearing at 91, 146 and 170 K. The intensities of the peaks A and B were too strong so that the existence of peak C was faint. The activation energies of these peaks were found using the analysis methods as 52, 200 and 304 meV. Mixed order of kinetics was assigned for the trap levels correlated to peaks A and B with the help of the parameter $b = 1.6$ and $b = 1.2$, respectively, found by CF method. s and S_t values were found to be 55.3, 8.7×10^5 and 1.3×10^8 s^{-1}, and 4.4×10^{-24}, 2.7×10^{-20} and 2.9×10^{-18} cm^2, respectively. Heating rate method showed the coexistence of the normal and anomalous behavior of trap levels. Increasing heating rate leads to decrease in TL intensity of peak A and shift of the T_m value to higher temperatures while it increased the TL intensity of peak B with shifting T_m. The SLT model explained the anomalous behavior by assuming the radiative and non-radiative transitions take place competitively. Quasi-continuous distribution was dedicated to the traps thorough the analysis of TL curves obtained with different T_{stop} values between 10 and 30 K (peak A), 10 and 50 K (peak B), and 30 and 70 K (peak C) with increasing activation energies from 52 to 90 K, from 200 to 268 K, and from 304 to 469 K, respectively.

Thermoluminescence spectra for Ga$_4$S$_3$Se crystal detected in the 10−300 K utilizing varying heating rates from 0.4 to 0.8 K/s revealed one TL glow peak around $T_m = 168$ K. The properties of trap level donated to this peak were investigated by TL analysis methods to obtain the activation energy and to comprehend the TL mechanism. Application of analysis techniques gave the E_t value as 495 meV. The CF and PS method revealed the s and S_t values of trap level to be 5.8×10^{13} s^{-1} and

1.5×10^{-12} cm^2, respectively. The parameter $b = 1.5$ implied that the mixed order of kinetic was dominant for the trapping process. Normal heating rate behavior that is the diminishing in TL intensity and increasing T_m value of the TL peak was observed.

Ga$_2$SSe single crystals were studied in virtue of TL experiments performed in 10−300 K temperature region employing various heating rates of 0.4−1.0 K/s. Recorded TL spectra possess three distinctive peaks with T_m values of 34, 79 and 108 K. It was found that charge carriers occupying the associated trapping levels need activation energies of 6, 30 and 72 meV to be stimulated into delocalized states. The frequency factors and capture cross sections of the traps were found as with 1.2, 2.8 and 65.6 s^{-1}, and 1.3×10^{-25}, 2.2×10^{-25} and 4.2×10^{-24} cm^2, respectively. CF analysis revealed the trapping mechanism is governed by first order of kinetic. Heating rate dependencies of the successive peaks were investigating by increasing the heating rate. The best-known and expected result that is the diminution of TL intensity and rising T_m value was observed for each TL peak. Due to overlapping of trapping levels with each other, distribution of traps was taken under consideration without separating each peak to individual one. Consequently, energy shift from 6 to 136 meV was observed with increasing T_{stop} from 10 to 52 K.

TL investigation was continued to get knowledge about the defect center in Ga$_4$Se$_3$S single crystal under room temperature (10−300 K). TL spectra obtained with heating the sample at a rate of 0.4 K/s presented one glow peak at $T_m = 74$ K. Analyses brought out the existence of one trap level correlated to exhibited peak possessing activation energy of 27 meV. Moreover, using the E_t of trap level, we found the s and S_t values as 1.6 s^{-1} and 2.4×10^{-25}. The glow peak was fitted with the parameter $b = 1.2$ that implies the trap levels is dominated by mixed order of kinetic. Normal heating rate behavior was shown for the trap level by varying the rate between 0.4 and 1.2 K/s. Distribution of traps was demonstrated by illuminating the sample with rising T_{stop} value from 15 to 36 K and increasing energy value from 27 to 40 meV was assigned to quasi-continuous distribution.

Thermoluminescence measurements for GaSe:Mn single crystals were carried out in the temperature range of 10−225 K for different heating rates of 0.4 and 1.0

K/s. The TL curve possessed four peaks with T_m values of 47,102,139 and 191 K. Four trapping levels were dedicated to these peaks by the help of the analysis methods. The peak observed at highest temperature region (peak D) was analyzed separately. As a result, the E_t values of the traps were obtained as 8, 34, 130 and 388 meV. The trap levels related to first three peaks were found to carry the characteristics of first order kinetics. Also, the properties of mixed order of kinetics are exhibited by the trapping center associated with peak D. The s and S_t values were obtained by using activation energy and peak maximum temperature values and they were calculated as 0.3, 1.8, 4.1×10^3 and 4.6×10^9 s^{-1}, and 2.6×10^{-26}, 4.4×10^{-26}, 6.8×10^{-23} and 2.2×10^{-17} cm^2, respectively. The energy levels of 130 and 388 meV were ascribed to defects and defect complexes which were also presented in GaSe crystals. On the other hand, the 8 and 34 meV energy levels were observed merely in Mn doped GaSe crystals. Therefore, it was thought these levels originated from the Mn atoms. Heating rate dependencies of the trapping levels were studied and decrease in TL intensity and shift of the T_m values were established through the analyses. Traps distribution analysis revealed the presence of single trap level for peak D unlike the traps having distributed energy levels.

REFERENCES

[1] Yee K. A., Albright A., 1991, J. Am. Chem. Soc., 113, 6474

[2] Panich A.M., 2008, J. Phys.: Condens. Matter., 20, 293202

[3] Allakhverdiev K.R., Mamedov T.G., Akinoglu B.G., EllialtiogluS., 1994, Turk. J. Phys., 18, 1

[4] Micocci G., Serra A., Tepore A., 1997, J. Appl. Phys., 82, 2365

[5] Cingolani A., Minafra A., Tantalo P., Paorici C., 1971, Phys. Status Solidi A, 4, K83

[6] Somogyi M., 1971, Phys. Status Solidi A, 7, 263

[7] Gamal G.A., Azad M.I., 2005, J. Phys. Chem. Sol., 66, 5

[8] Ho C.H., Lin S.L., 2006, J. Appl. Phys., 100, 083508

[9] Ho C.H., Huang K.W., 2005, Solid State Commun., 136, 591

[10] Ashraf I.M., Abdel-Rahman M.M., Badr A.M., 2003, J. Phys. D: Appl. Phys., 36, 109

[11] Grivickas V., Bikbajevas V., Grivickas P., 2006, Phys. Status Solidi B, 243, R31

[12] Allakhverdiev K.R., 1999, Solid State Commun., 111, 253

[13] Duman S., Gurbulak B., 2005, Physica Scripta, 72, 82

[14] Shim Y., Okada W., Wakita K., Mamedov N., 2007, J. Appl. Phys., 102, 083537

[15] Hanias M., Anagnostopoulos A., Kambas K., Spiridelis J., 1992, Mater. Res. Bull., 27, 25

[16] Kato A., Nishigaki M., Mamedov N., Yamazaki M., Abdullaeva S., Kerimova E., Uchiki H., Iida S., 2003, J. Phys. Chem. Solids., 64, 1713

[17] El Nahass M.M., Sallam M.M., Rahman S.A., Ibrahim E.M., 2008, Solid State Sci., 8, 488

[18] Gasanly N.M., 2010, J. Korean Phys. Soc., 57, 164

[19] Muller D., Hahn H., 1978, Z. Anorg. Allg. Chem., 438, 258

[20] Isik M., Gasanly N.M., 2012, Physica B, 407, 2229

[21] Guler I., Gasanly N.M., 2007, J. Korean Phys. Soc., 51, 2031

[22] Gasanly N.M., 2012, Physica Scripta, 85, 065701

[23] Ibragimov T.D., Aslanov I.I., 2002, Solid State Commun., 123, 339

[24] Uchiki H., Kanazawa D., Mamedov N., Iida S., 2000, J. Lumin., 664, 87

[25] Samedov S.R., Baykan O., Gulubayov A., 2004, Int. J. Infrared Millimet. Waves, 25, 735

[26] Akmedov A.M., Bakhshov A.E., Lebedov A.A., Yakobson M.A., 1978, Sov. Phys. Semicond., 12, 299

[27] Hanias M., Anagnostopulos A., Kambas K., Spyridelis J., 1989, Physica B, 160, 154

[28] Goksen K., Gasanly N.M., Ozkan H., 2007, Acta Phys. Pol. A, 112, 93

[29] Goksen K., Gasanly N.M., Ozkan H., 2007, J. Phys.: Cond. Matter, 19, 256210

[30] Goksen K., Gasanly N.M., 2008, J. Phys. Chem. Sol. 69, 2385

[31] Balkanski M., Wallis R.F., 2000, Semiconductor Physics and Applications, Oxford University Press, Oxford

[32] Wu C.C., Ho C.H., Shen W.T., Cheng Z.H., Huang Y.S., Tiong K.K., 2004, Mat. Chem. Phys., 88, 313

[33] Auclich E., Brebner J.L., Mooser E., 1969, Phys. Status Solidi B, 31, 129

[34] Aono T., Kase K., Kinoshita A., 1993, J. Appl. Phys., 74, 2818

[35] Manjon F.J., Segura A., Munoz V., 1997, J. Appl. Phys., 81, 6651

[36] Akhundov G., Aksyanov I.G., Gasumov G.M., 1969, Sov. Phys. Semicond., 3, 767

[37] Karaman M.I., Mushinskii V.P., 1970, Sov. Phys. Semicond., 4, 662

[38] Shigetomi S., Ikari T., Nakashima H., 1993, J. Appl. Phys., 74, 4125

[39] Kyazym-zade A.G., Mekhtieve R.N., Akhmedov A.A., 1991, Sov. Phys. Semicond., 25, 840

[40] Singh N.B., Suhre D.R., Balakrishna V., Marable M., Meyer R., Fernelius N., Hopkins F.K., Zelmon D., 1998, Prog. Cryst. Growth Charact. Mater., 37, 47

[41] Shi W., Ding Y.J., Fernelius N., Vodopyanov K., 2002, Opt. Lett., 27, 1454

[42] Zhang H.Z., Kang Z.H., Jiang Y., Gao J.Y., Wu F.G., Feng Z.S., Andreev Y.M., Lanskii G.V., Morozov A.N., Sachkova E.I., Sarkisov S.Y., 2008, Opt. Express, 16, 9951

[43] Allakverdiev K.R., Yetis M.O., Ozbek S., Baykara T.K., Salaev E.Yu., 2009, Lazer Phys., 19, 1092

[44] Nazarov M.M., Kosobutsky A.V., Sarkisov S.Y., Brudnyi V.N., Tolbanov O.P., Shkurinov A.P., 2011, Proc. SPIE, 7993, 799326

[45] Masui A., Onari S., Allakhverdiev K.R., Gashimzade F., Mamedov T., 2001, Phys. Status Solidi B, 223, 139

[46] Osman M.A., 2000, Physica B, 275, 351

[47] Allakhverdiev K.R., Akhmedov N., Ibragimov Z., Ellialtioglu S., Lothar K., Haarer D., 1995, Solid State Commun., 93, 147

[48] Qasrawi A., Gasanly N.M., 2007, Solid State Commun., 142, 566

[49] Isik M., Gasanly N.M., 2015, Mod. Phys. Lett. B, 29, 1550088.

[50] Delice S., Isik M., Gasanly N.M., 2015, Mater. Res. Bull., 70, 236

[51] Yildirim T., Nasser H.A., Gasanly N.M., 2010, Int. J. Mod. Phys. B, 24, 2149

[52] Yildirim T., Gasanly N.M., 2009, Solid State Sci., 11, 1562

[53] Gasanly N.M., 2012, Physica B, 407, 4318

[54] Yildirim T., Gasanly N.M., 2009, Cur. Appl. Phys., 9, 1278

[55] Gasanly N.M., 2011, J. All. Comp., 509, 4205

[56] Qasrawi A.F., Gasanly N.M., 2013, J. Appl. Phys., 113, 023712

[57] Isik M., Gasanly N.M., 2009, J. Phys. Chem. Solids, 70, 1048

[58] Gasanly N.M., 2013, Acta Physica Pol. A, 124, 128

[59] Goksen K., Gasanly N.M., 2007, J. Phys.: Condens. Matter, 19, 456221

[60] Mogaddam N.A.P., Yuksek N.S., Gasanly N.M., Ozkan H., 2006, J. Alloys Compd., 417, 23

[61] Goksen K., Gasanly N.M., Aydinli A., Ozkan H., 2005, J. Korean Phys. Soc., 47, 267

[62] Qasrawi A.F., Gasanly N.M., 2007, Solid State Commun., 141, 117

[63] Gasanly N.M., Ozkan H., Mogaddam N.A.P., 2006, Semicond. Sci. Technol., 21, 1250

[64] Goksen K., Gasanly N.M., 2008, Cryst. Res. Technol., 43, 514

[65] Gasanly N.M., Aydinli A., Yuksek N.S., Salihoglu O., 2003, Appl. Phys. A, 77, 603

[66] Aydinli A., Gasanly N.M., Goksen K., 2000, J. Appl. Phys., 88, 7144

[67] Aytekin S., Yuksek N.S., Goktepe M., Gasanly N.M., Aydinli A., 2004, Phys. Status Solidi A, 201, 2980

[68] Gasanly N.M., Goksen K., Ozkan H., 2002, Cryst. Res. Technol., 37, 581

[69] Karabulut O, Parlak M., Yılmaz K., Gasanly N.M., 2005, Cryst. Res. Technol., 3, 253

[70] Aydinli A, Gasanly N.M., Aytekin S, 2004, Solid State Commun., 132, 857

[71] Aydinli A., Gasanly N.M., Goksen K., 2001, Mater. Res. Bull. 36, 1823

[72] Qasrawi A.F., Gasanly N.M., 2002, Phys. Status Solidi A, 1, 81

[73] Goksen K., Gasanly N.M., 2009, Phil. Mag., 89, 435

[74] Goksen K., Gasanly N.M., Seyhan A., Turan R., 2006, Mater. Sci. Engineering B, 127, 41

[75] Qasrawi A.F., Gasanly N.M., 2008, J. Phys. Chem. Solids, 69, 2719

[76] Gasanly N.M., Aydinli A., Salihoglu O., 2001, Cryst. Res. Technol., 36, 295

[77] Aydinli A., Gasanly N.M., Goksen K., 2001, Phil. Mag. Letters, 81, 859

[78] Isik M., Hadibrata W., Gasanly N.M., 2014, J. Lumin., 154, 131

[79] Hsu Yu-Kuei, Chang Chen-Shiung, 2004, J. Appl. Phys., 96, 1563

[80] Shigetomi S., Ikari T., 2004, J. Appl. Phys., 95, 6480

[81] Shigetomi S., Ikari T., 2005, Phys. Status Solidi B, 242, 3123

[82] Turton R., 2000, The Physics of Solids, Oxford University Press, Oxford

[83] Hummel R.E., 1993, Electronic Properties of Materials, Springer-Verlag, New York

[84] Kittel C., 1971, Introduction to Solid State Physics, Wiley, New York.

[85] McKeever S.W.S., 1985 Thermoluminescence of Solids, Cambridge Uni. Press, Cambridge (1985).

[86] Chen R., Kirsh Y., 1981, Analysis of Thermally Stimulated Processes, Pergamon Press, Oxford.

[87] Randall J.T., Wilkins M.H.F., 1945, Proc. R. Soc Lon. Ser.-A, 184, 366

[88] Garlick G.F.J., Gibson A.F., 1948, P. R. Soc. London, 60, 574

[89] May C.E., Partridge J.A., 1964, J. Chem. Phys., 40, 1401

[90] Chen R., McKeever S.W.S., 1997, Theory of Thermoluminescence and Related Phenomena, World Scientific, Singapore

[91] Delice S., Isik M., Bulur E., Gasanly N.M., 2013, J. Appl. Phys., 113, 193510.

[92] Delice S., Gasanly N.M., 2014, Mod. Phys. Lett. B, 28, 1450133

[93] Delice S., Gasanly N.M., 2014, Cryst. Res. Technol., 49, 845

[94] Yuksek N.S., Gasanly N.M. Ozkan H., 2005, In: Focus on Semiconductor Research, Ed.: B. Elliot, Nova Science Publishers, New York,

[95] Aybek A.S., Baysal N., Zor M., Turan E., Kul M., 2011, J. Alloy Compd., 509, 2530

[96] Betts D.S., Couturier L., Khayrat A.H., Luff B.J., Townsend P.D., 1993, J. Phys. D: Appl. Phys., 26, 843

[97] Betts D.S., Townsend P.D., 1993, J. Phys. D: Appl. Phys., 26, 849

[98] Piters T.M., Bos A.J.J., 1994, J. Phys. D: Appl. Phys., 27, 1747

[99] Kitis G., Tuyn J.W.N., 1998, J. Phys. D: Appl. Phys., 31, 2065

[100] Kitis G., Furetta C., Prokic M., Prokic V., 2000, J. Phys. D: Appl. Phys., 33, 1252

[101] Kitis G., Spiropulu M., Papadopoulos J., Charalambous S., 1993, Nucl. Instrum. Methods Phys. Res., 73, 367

[102] Ege A., Ekdal E., Karali T., Can N., Prokic M., 2007, Meas. Sci. Technol., 18, 889

[103] Anishia S.R., Jose M.T., Annalakshmi O., Ramasamy V., 2011, J. Lumin., 131, 2492

[104] Bube R.H., 1992, Photoelectronic Properties of Semiconductors, Cambridge University Press, Cambridge

[105] Serpi A., 1976, J.Phys. D: Appl. Phys., 9, 1881

[106] Anedda A., Casu M.B., Serpi A, Burlakov I.I., Tiginyanu I.M., Ursaki V.V., 1997, J. Phys. Chem. Solids, 58, 325

[107] Ricci P.C., Anedda A., Corpino R., Tiginyanu I.M., Ursaki V.V., 2003, J. Phys. Chem. Solids, 64, 1941

[108] Delice S., Isik M., Bulur E., Gasanly N.M., 2015, Indian J. Phys., 89, 571

[109] Delice S., Bulur E., Gasanly N.M., 2014, J. Mater. Sci., 49, 8294

[110] Delice S., Isik M., Gasanly N.M., 2014, Phil. Mag., 94,141

[111] Bos A.J.J., Poltoon N.R.J., Wallinga J., Bessiere A., Dorenbos P., 2010, Radiat. Meas., 45, 343

[112] Chen R., Lawless J.L., Pagonis V., 2012, Radiat. Meas., 47, 809

[113] Mandowski A., Bos A.J.J., 2011, Radiat. Meas., 46, 1376

[114] Pagonis V., Blohm L., Brengle M., Mayonado G., Woglam P., 2013, Radiat. Meas., 51-52, 40

[115] Correcher V., Gomez-Ros J.M., Garcia-Ginea J., Lis M., Sanchez-Munoz L., 2008, Radiat. Meas., 43, 269

[116] Gomez-Ros J.M., Correcher V., Garcia-Ginea J., Delgado A., 2006, Radiat. Prot. Dosim., 119, 93

[117] Gomez-Ros J.M., Furetta C., Cruz-Zaragoza E., Lis M., Torres A., Monsivais G., 2006, Nuclear Instr. Methods Res. A, 566, 727

[118] Delice S., Bulur E., Gasanly N.M., 2015, Phil. Mag., 95, 998

[119] Isik M., Delice S., Gasanly N.M., 2015, J. Lumin., 168, 236

[120] Isik M., Delice S., Gasanly N.M., 2016, Pramana-J. Phys., 86, 893

[121] Delice S., Gasanly N.M., 2016, Phil. Mag., 96, 112

[122] Shigetomi S., Ikari T., Nakashima H., 1996, J. Appl. Phys., 80, 4779

[123] Cui Y., Dupere R., Burger A., Johnstone D., Mandal K.C., Payne S.A., 2008, J. Appl. Phys., 103, 01370

[124] Hornyak W.F., Chen R., 1989, J. Lumin., 44, 73

[125] Schafferhans J., Deibel C., Dyakonov V., 2011, Adv. Energy Mater., 1, 655

CURRICULUM VITAE

PERSONAL INFORMATION

Surname, Name: Delice, Serdar

Nationality: Turkish (TC)

Date and Place of Birth: 30 July 1987, Mamak/ANKARA

Marital Status: Single

Phone: +90 312 210 5059

e-mail: srdrdelice@gmail.com

EDUCATION

Degree	Area	Institution	Year
BS	Physics	Anadolu University	2010

WORK EXPERIENCE

Year	Institution	Position
2010-2012	Hitit University	Research Assistant
2012-2016	Middle East Technical University	Research Assistant

PUBLICATIONS

1. **S. Delice**, M. Isik, E. Bulur and N. M. Gasanly, Thermoluminescence properties of $Tl_2Ga_2S_3Se$ layered single crystals, *J. Appl. Phys.* **113**, 193510 (2013).

2. **S. Delice**, M. Isik and N. M. Gasanly, Thermoluminescence characteristics of $Tl_4GaIn_3S_8$ layered single crystals, *Phil. Mag.* **94**, 141 (2014).

3. **S. Delice**, M. Isik and N. M. Gasanly, Trapping centers and their distribution in $Tl_2InGaSe_4$ single crystals by thermally stimulated luminescence, *J. Mater. Sci.* **49**, 2542 (2014).

4. **S. Delice** and N. M. Gasanly, Determination of trapping parameters in $Tl_4Ga_3InSe_8$ single crystals by thermally stimulated luminescence, *Physica B* **441**, 37 (2014).

5. **S. Delice** and N. M. Gasanly, Thermoluminescence study on TlGaSSe layered single crystals, *Modern Phys. Letters. B* **28**, 1450133 (2014).

6. M. Isik, **S. Delice** and N. M. Gasanly, Optical properties of $TlGa_xIn_{1-x}Se_2$-layered mixed crystals ($0.5 \leq x \leq 1$) by spectroscopic ellipsometry, transmission, and reflection measurements, *Phil. Mag.* **94**, 2623 (2014).

7. **S. Delice**, E. Bulur and N. M. Gasanly, Anomalous heating rate dependence of thermoluminescence in Tl_2GaInS_4 single crystals, *J. Mater. Sci.* **49**, 8204 (2014).

8. **S. Delice** and N. M. Gasanly, Characteristics of traps in $Tl_2Ga_2Se_3S$ single crystals by low-temperature thermoluminescence measurements, *Cryst. Res. Technol.* **49**, 845 (2014).

9. **S. Delice**, E. Bulur and N. M. Gasanly, Thermoluminescence in gallium sulfide crystals: an unusual heating rate dependence, *Phil. Mag.* **95**, 998 (2014).

10. M. Isik, **S. Delice** and N. M. Gasanly, Low-temperature thermoluminescence studies on $TlInS_2$ Layered Single Crystals, *Acta Physica Pol. A* **126**, 1299 (2014).

11. **S. Delice**, M. Isik, E. Bulur and N. M. Gasanly, Low temperature thermoluminescence of quaternary thallium sulfide $Tl_4InGa_3S_8$, *Indian J. Phys.* **89**, 571 (2015).

12. **S. Delice**, M. Isik and N. M. Gasanly, Transmission, reflection and thermoluminescence studies on $GaS_{0.75}Se_{0.25}$ layered single crystals, *Mater. Res. Bull.* **70**, 236 (2015).

13. M. Isik, **S. Delice** and N.M. Gasanly, Analysis of glow curve of $GaS_{0.5}Se_{0.5}$ single crystals, *J. Lumin.* **168**, 236 (2015).

14. **S. Delice** and N.M. Gasanly, Low-temperature thermoluminescence study of GaSe: Mn layered single crystals, *Phil. Mag.* **96**, 112 (2016).

15. M. Isik, **S. Delice** and N.M. Gasanly, Defect characterization of Ga_4Se_3S layered single crystals by thermoluminescence, *Pramana-J. Phys*. **86**, 893 (2016).

INTERNATIONAL CONFERENCES

1. **S. Delice**, M. Isik and N. Hasanli "Low-temperature study of thermally stimulated currents in layered-structured $Tl_4GaIn_3S_8$ crystals (FIZIKA, 2013)" International Conference Novel Semiconductor Materials and Structures, 4-6.07.2013, Baku, Azerbaijan.

2. N. Hasanli, M. Isik and **S. Delice** "Dielectric Functions and Interband Transitions in Anisotropic Layered Structured Tl_2GaInS_4 Crystals by Spectroscopic Ellipsometry" Fourth International Meeting On dielectric Materials, 29-31.05.2013, Marrakesh, Morocco.

3. **S. Delice**, M. Isik, E. Bulur and N.M. Hasanli."Characterization of defect centers in TlGaSeS layered crystals by thermoluminescence measurements" International Conference "Condensed Matter in Paris 2014", 24-29.08.2014, Paris, France, p. 126.

4. N.M. Hasanli, **S. Delice** and M. Isik "Optical constants and energy gaps of $TlGa_xIn1_{-x}Se_2$ mixed crystals by ellipsometry, transmission and reflection measurements." International Conference "Condensed Matter in Paris 2014", 24-29.08.2014, Paris, France, p. 387.

5. N. Hasanli, M. Isik, **S. Delice** and E. Bulur. "The analysis of photo-transferred low temperature thermoluminescence from BeO ceramics after β -irradiation." The Seventh Eurasian Conference "Nuclear Science and Its Application", 21-24.10.2014, Baku, Azerbaijan, p. 167.

6. **S. Delice**, M. Isik, T. Yildirim and N. Hasanli "Low- and high-temperature thermoluminescence in TlGaSSe semiconductor crystals" 28. International Conference on Defects in Semiconductors, 25-31.07.2015, Espoo, Finland.

7. M. Isik, **S. Delice** and N. Hasanli "Analysis of Thermoluminescence Glow Curves of Ga_2SeS Layered Crystals" The 4. International Conference on the Physics of Optical Materials and Devices, August 31st – September 4th 2015, Becici, Budva, Montenegro.

8. N. Hasanli, M. Isik and **S. Delice** "Photoluminescence and Thermoluminescence Study on $Tl_2Ga_2S_3Se$ Layered Crystals" The 4. International Conference on the Physics of Optical Materials and Devices, August 31st – September 4th 2015, Becici, Budva, Montenegro.

NATIONAL CONFERENCES

1. **S. Delice**, N. Hasanli, M. Işık and E. Bulur "$Tl_4Ga_3InS_8$ tek kristallerinde termoluminesans yöntemiyle tuzak merkezlerinin karakterizasyonu" 7. Ulusal Lüminesans Dozimetri Kongresi, 10-12.09.2013, Isparta.

2. M. Işık, **S. Delice**, E. Bulur, N. Hasanli "Beta Radyasyonuna Maruz Bırakılan BeO Seramiklerinde Düşük Sıcaklık Fototransfer Termolüminesans Ölçümleri" 20. Yoğun Madde Fiziği - Ankara Toplantısı, 26 Aralık 2014, Ankara, Türkiye, P 09.

3. **S. Delice**, M. Isik and N. Hasanli "$Tl_2Ga_2Se_3S$ tek kristallerinde düşük sıcaklık termolüminesans ölçümleri" 21. Yoğun Madde Fiziği - Ankara Toplantısı, 25 Aralık 2015, Ankara, Türkiye.